Experimental High Energy Physics at Colliders
Lecture 2: Reconstruction of Objects - 2

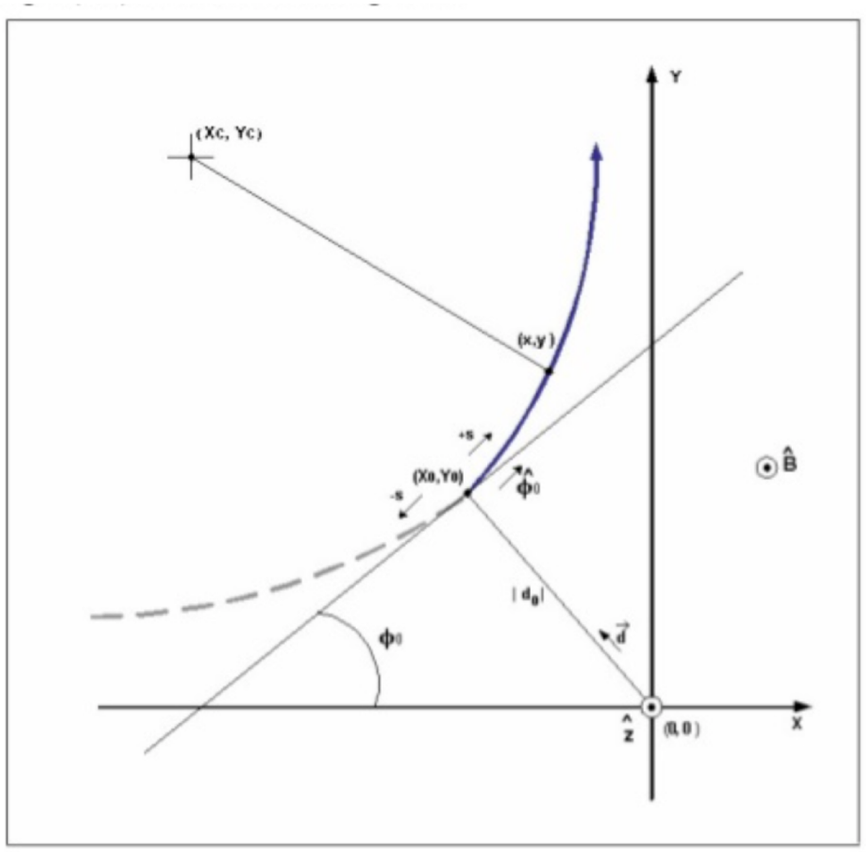

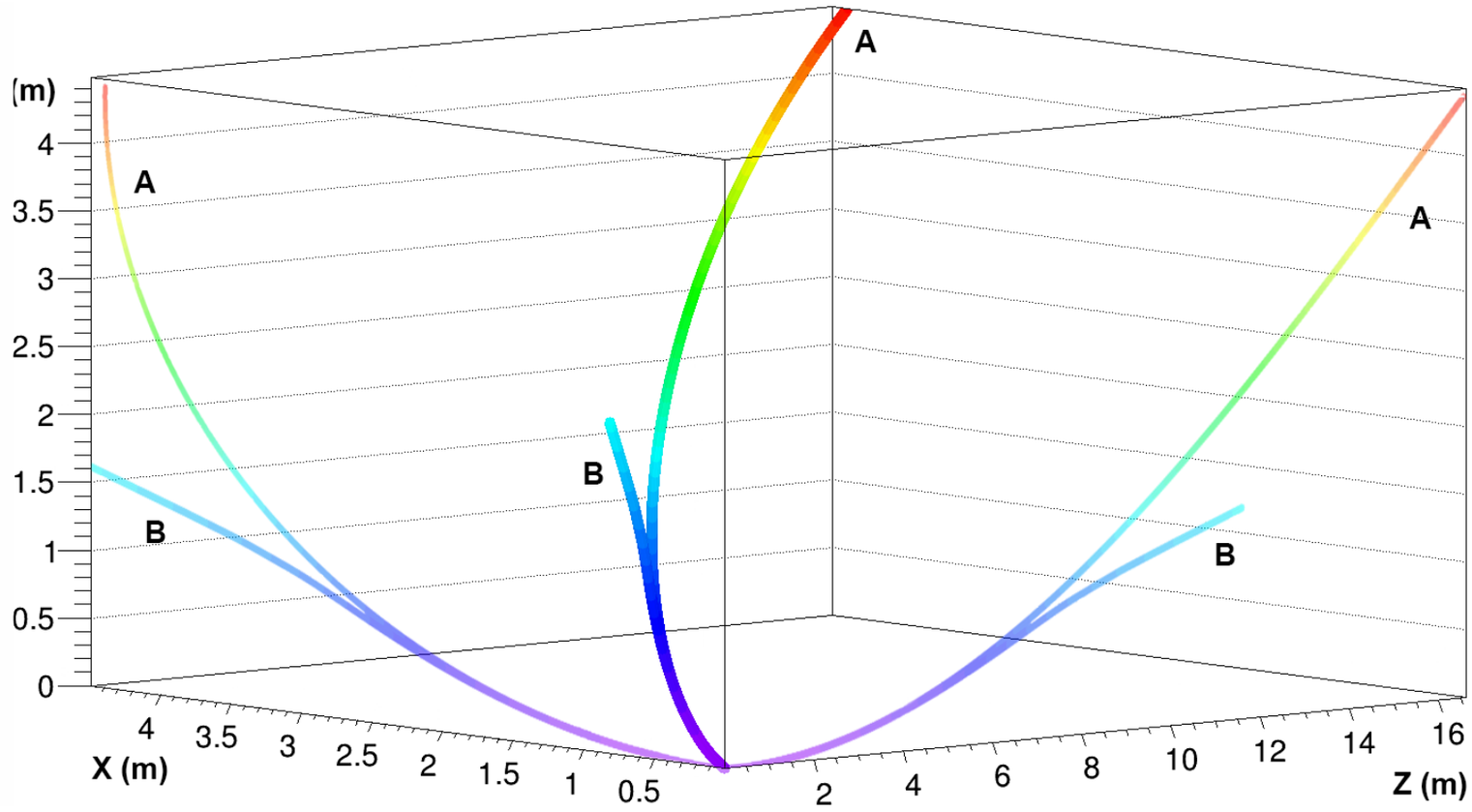

Inventory of Objects

Objects (from inside – out):

- Tracks
- Vertices
- Calorimeter clusters
- Jets (colorimeter & track)
- MET (missing transverse energy)
- Muons
- Fit of event topology (check if a given assumption fits the event topology)

Using the MC in HEP analysis

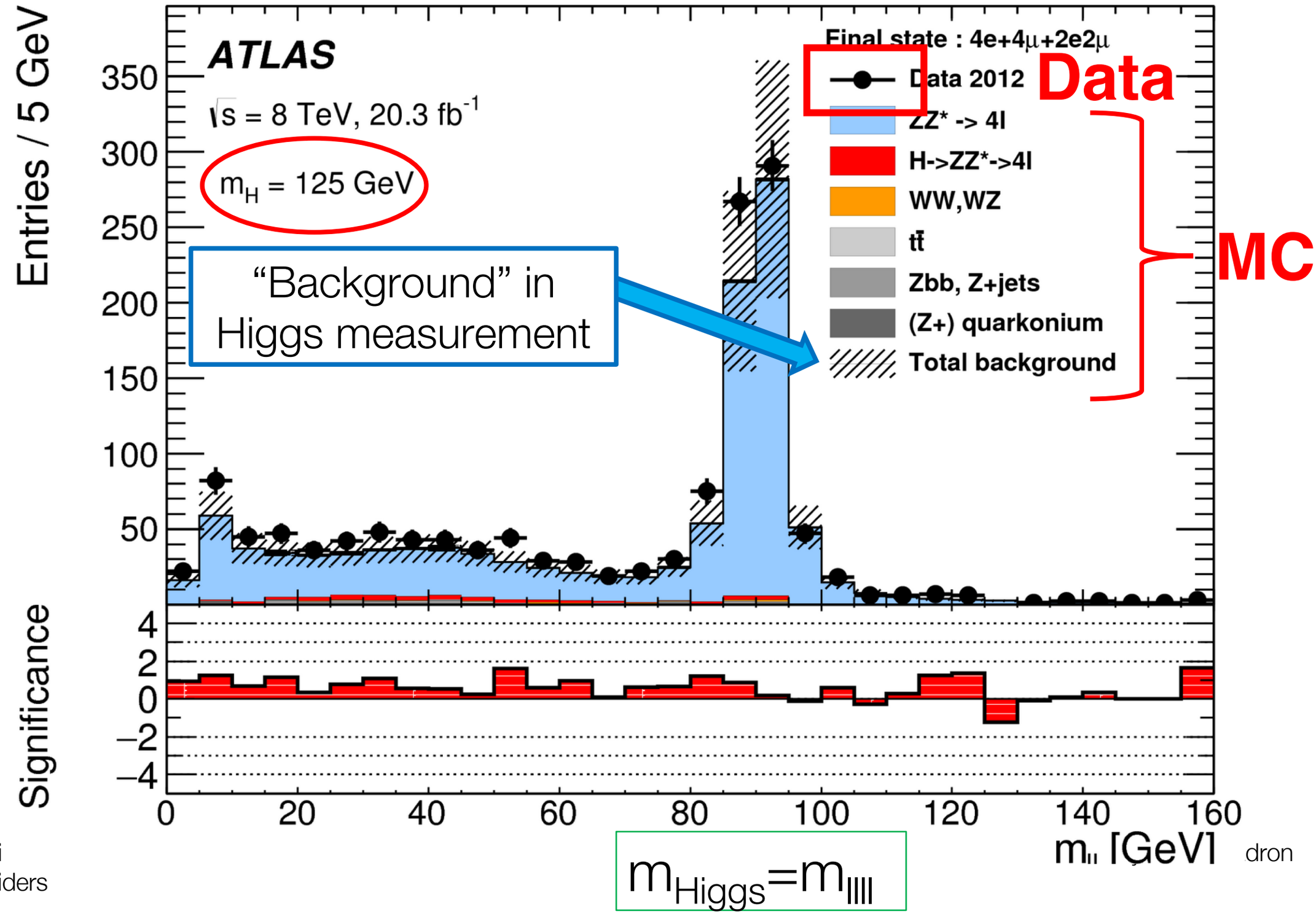

Using the MC in HEP analysis

MC is heavily used in any type of analysis:

- In measurements it is used to compute acceptances, efficiencies
- In searches it is used to derive Signal – Background

This means having an excellent knowledge of the detector performance. For this MC simulation needs to

- Include expected resolutions and efficiencies (first guess)
- be “tuned” to experimental findings. This is an iterative procedure based on comparison between data and MC

Scale factors & Control Regions

Material budget

Knowing the real structure of our detectors

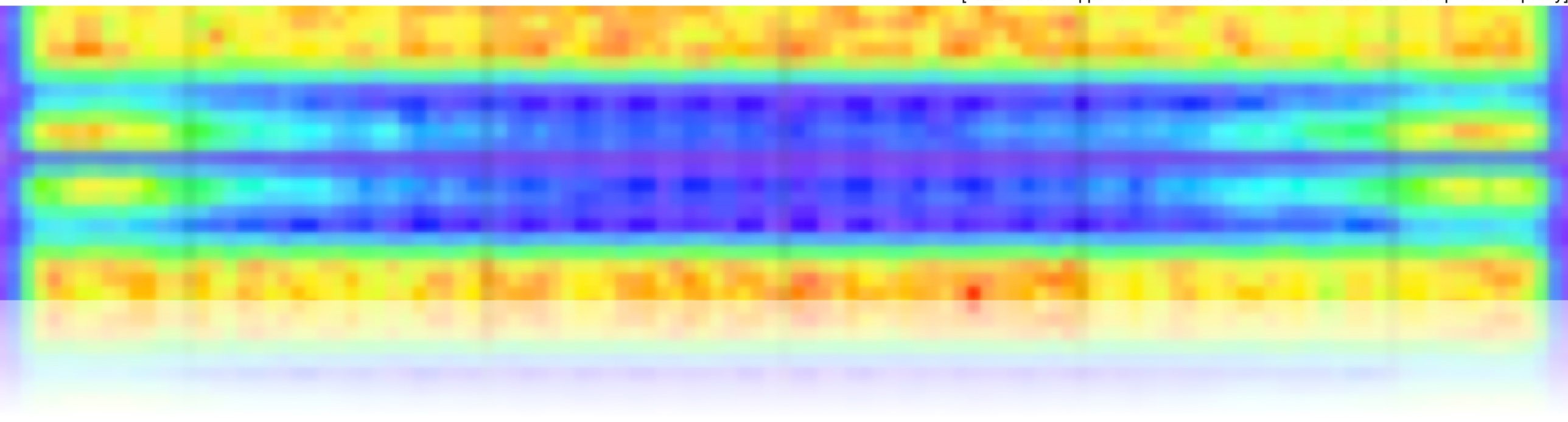

Radiation Length X_0, interaction length λ: Why?

Dead Material (cables, pipes, ducts) affects the reconstruction of tracks → important for tracking detectors, less for EM calorimeters, much less for hadronic calorimeters

Electrons:

Energy loss mainly via bremsstrahlung
Radiation length [X_0]: characteristic scale for e/γ
Electron energy down to 1/e after passing through X_0

Reminder energy loss via Bremsstrahlung:

$$-\frac{dE}{dx} = \frac{E}{X_0}$$

Goals: only little material in front of calorimeters (trackers, solenoid)
more than 20 X_0 for EM calorimeter to fully contain EM showers
Examples: X_0/ρ for water 36 cm, for lead 0.56 cm, for steel 1.76 cm

Photons:

Mean free path for e^+e^- pair production from γ: 7/9 X_0

Hadrons:

Characteristic scale: nuclear interaction length λ
Relevant for total calorimeter depth (hadronic + electromagnetic)
Examples: λ/ρ for water 83.6 cm, for lead 17.1 cm, for steel 17 cm

Dead Material

... via secondary hadronic vertices

(the more vertices you have the more material you have)

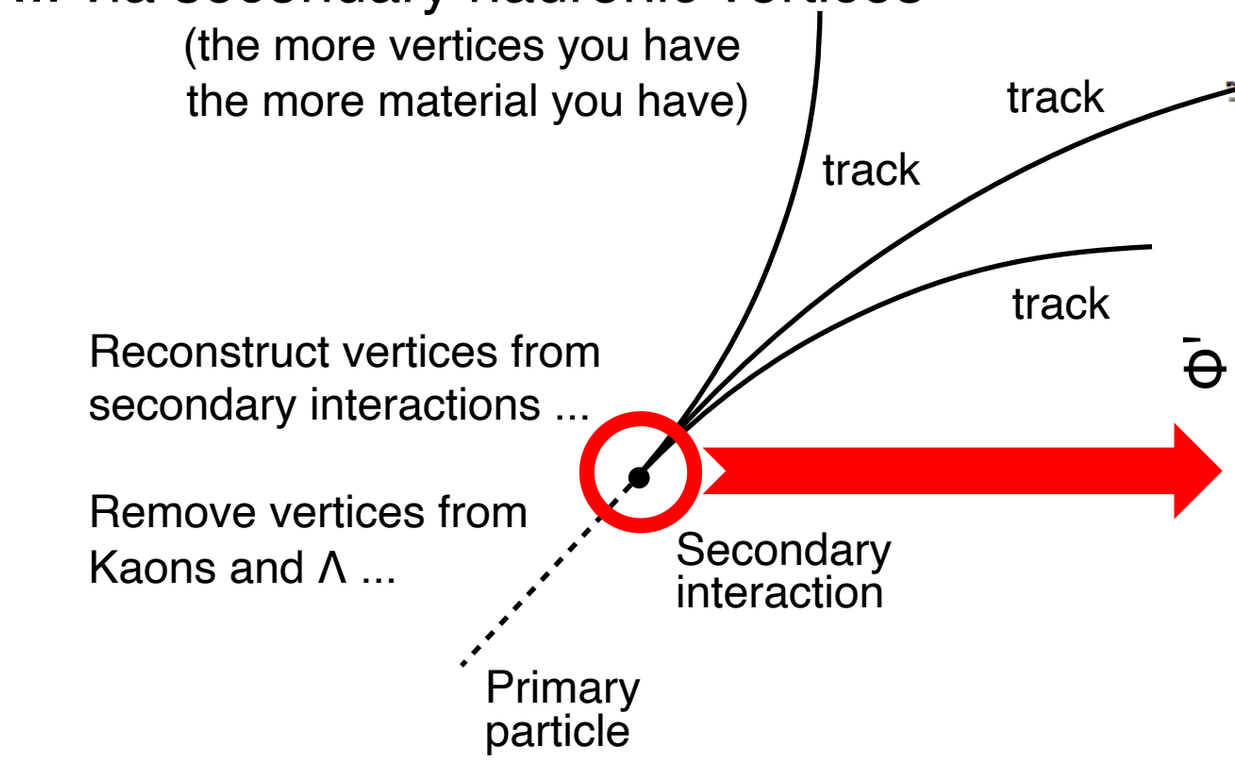

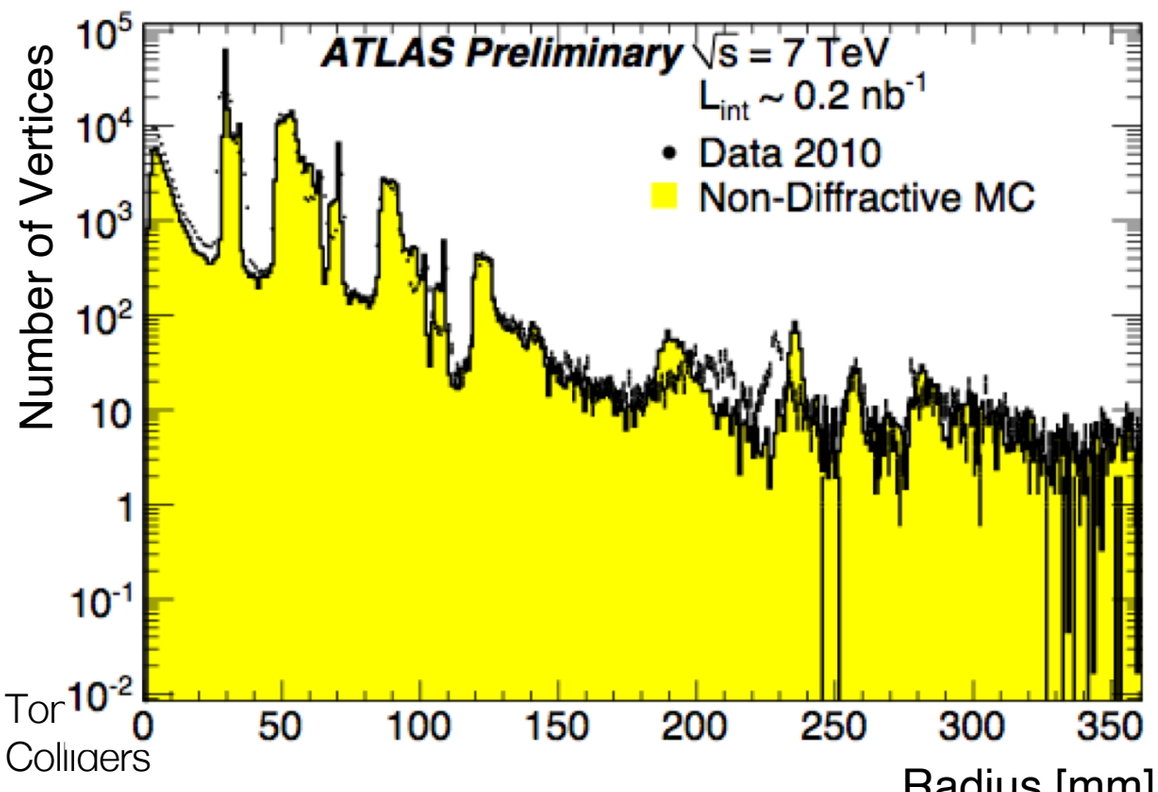

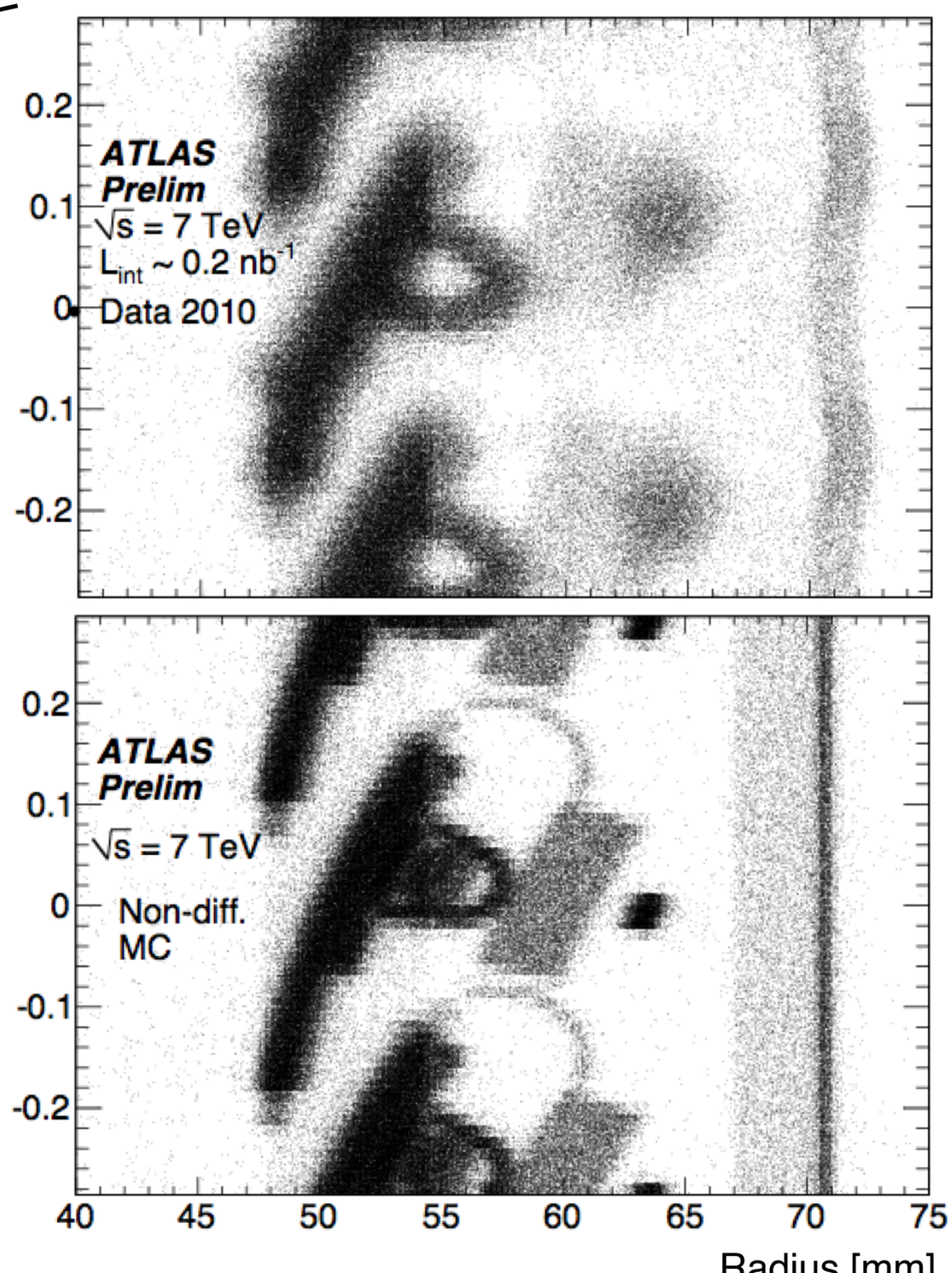

Dead Material: how to measure it?

... via photon conversion

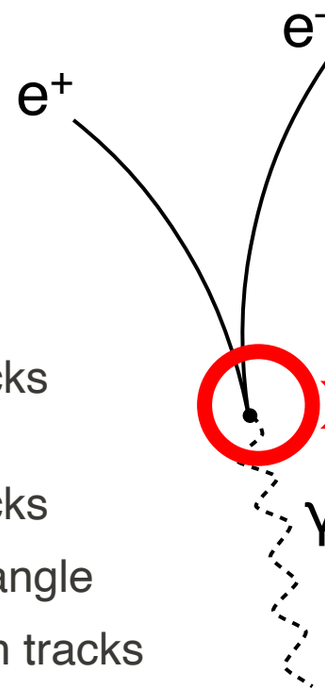

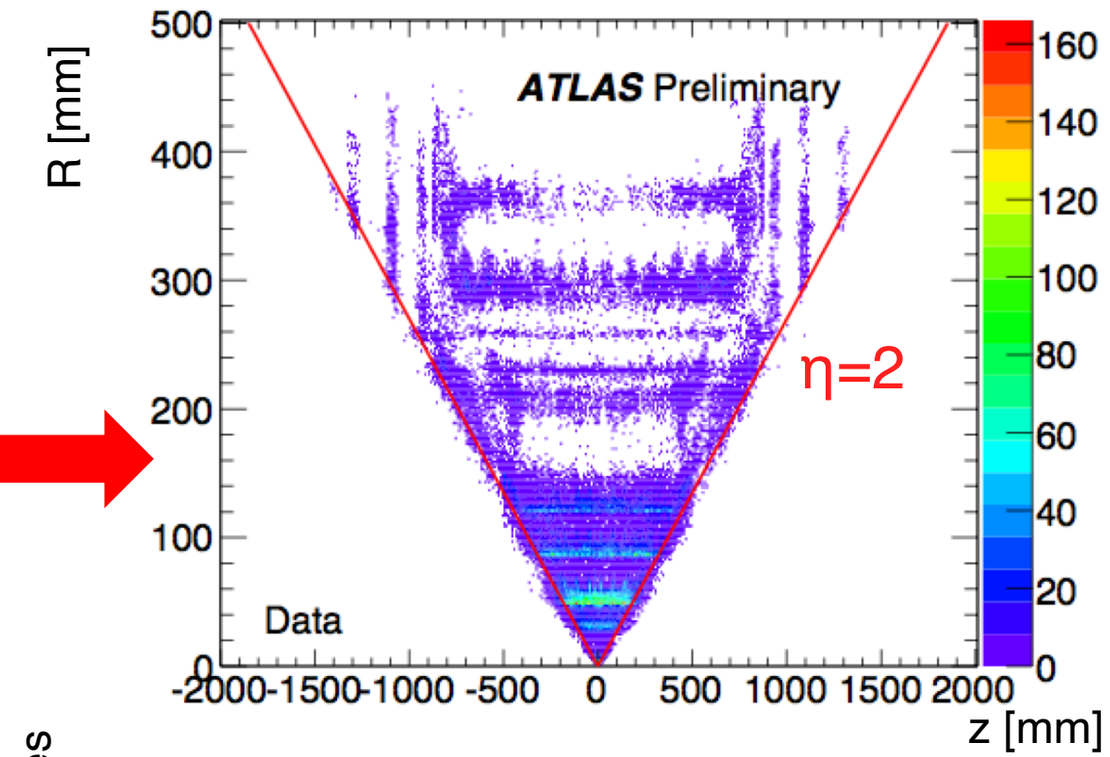

Selection:

- Two oppositely charged tracks with $p_T > 0.5$ GeV
- Small distance between tracks
- Good vertex; zero opening angle
- At least 4 silicon hits on both tracks
- More than 90 % probability for electron identification using TRT hits

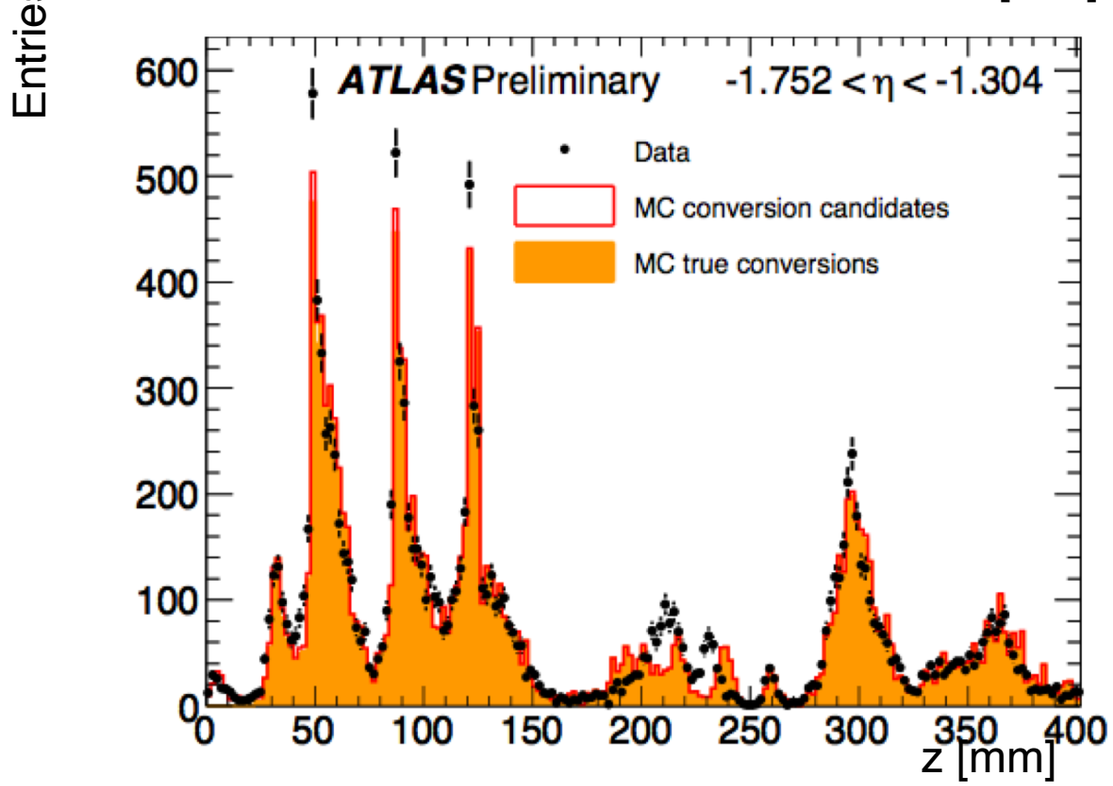

Fraction of converted photons translate into radiation length

$$\frac{X}{X_0} = -\frac{9}{7}\ln(1 - F_{\text{conv}})$$

F_{conv}: normalized conversion fraction
[Normalization according to well-known material in beam pipe]

Material Budget in ATLAS and CMS inner trackers Radiation Lenghts

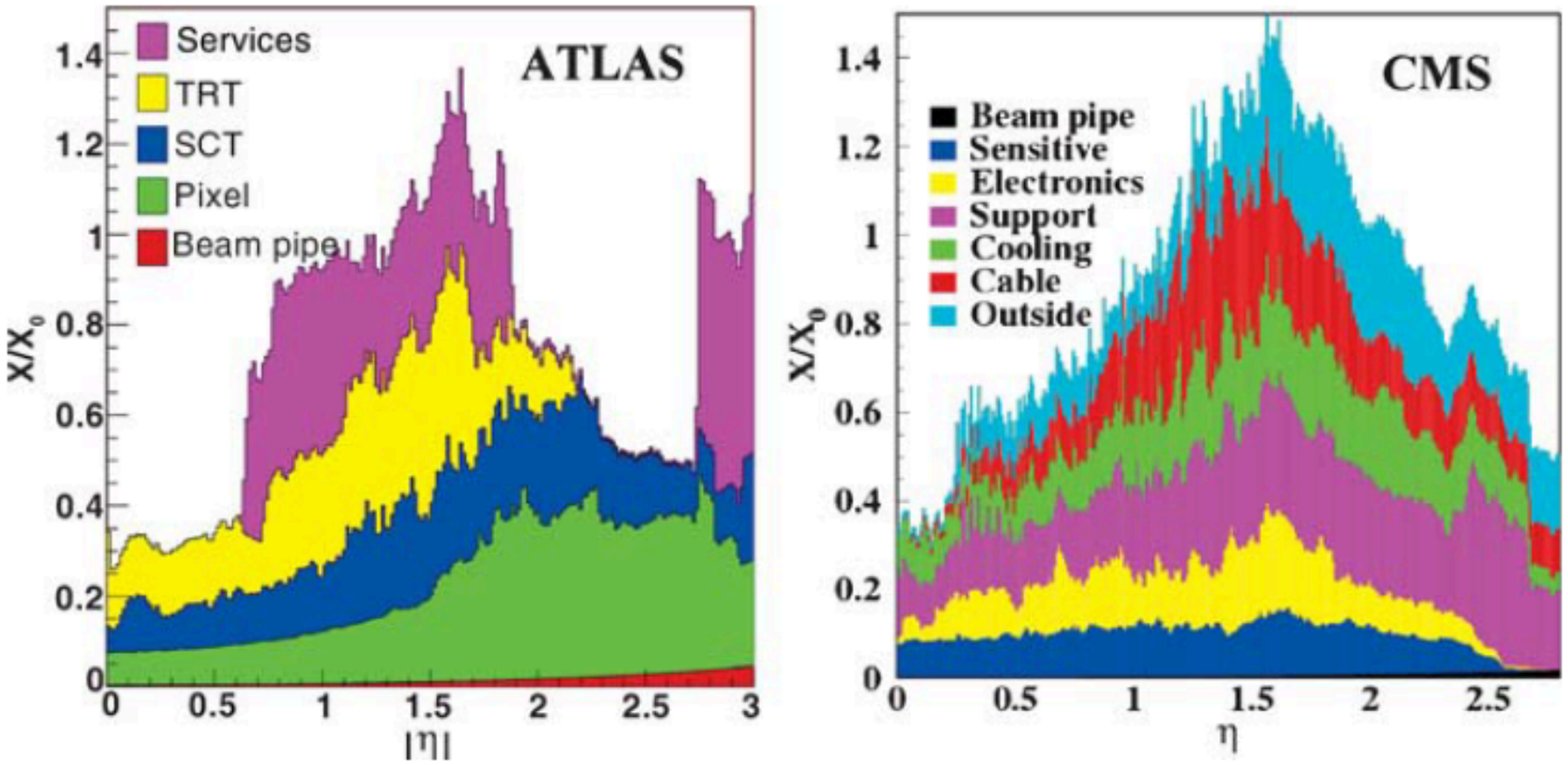

Figure 8 Distribution of amount of material in the volume of the ATLAS (*left*) and CMS (*right*) trackers, expressed as fractional radiation length X/X_0 versus pseudorapidity η. These plots do not include additional material just in front of the electromagnetic calorimeters, which is quite large in ATLAS (LAr cryostat and, for the barrel, solenoid coil) and much less in CMS (front part of crystal mechanics). For illustrative purposes, the ATLAS material has been split into its radial components from inside (beam pipe) out [Transition Radiation Tracker (TRT) and services outside the active detector volume], whereas the CMS material has been split into its various functional components.

Material Budget

TABLE 5 Evolution of the amount of material expected in the ATLAS and CMS trackers from 1994 to 2006

Date	ATLAS $\eta \approx 0$	ATLAS $\eta \approx 1.7$	CMS $\eta \approx 0$	CMS $\eta \approx 1.7$
1994 (Technical Proposals)	0.20	0.70	0.15	0.60
1997 (Technical Design Reports)	0.25	1.50	0.25	0.85
2006 (End of construction)	0.35	1.35	0.35	1.50

The numbers are given in fractions of radiation lengths (X/X_0). Note that for ATLAS, the reduction in material from 1997 to 2006 at $\eta \approx 1.7$ is due to the rerouting of pixel services from an integrated barrel tracker layout with pixel services along the barrel LAr cryostat, to an independent pixel layout with pixel services routed at much lower radius and entering a patch panel outside the acceptance of the tracker (this material appears now at $\eta \approx 3$). Note also that the numbers for CMS represent almost all the material seen by particles before entering the active part of the crystal calorimeter, whereas they do not for ATLAS, in which particles see in addition the barrel LAr cryostat and the solenoid coil (amounting to approximately 2 X_0 at $\eta = 0$), or the end-cap LAr cryostat at the larger rapidities.

[Froidevaux, Sphicas]

Evolution of dead
material expectation in ATLAS and CMS tracker

Dead Material using Hadronic Interactions

The material in the ATLAS Inner Detector (ID) is mapped by the hadronic interaction technique. Hadrons created in pp collisions traversing the detector may interact strongly with the material.

$$N_{\lambda_I}^{[C]} = \int_C \mathrm{d}s \, \frac{1}{\lambda_I(s)} \, .$$

The interaction points are reconstructed as secondary vertices (SV), by fitting vertices to the outgoing secondary tracks arising from the nuclear interactions. The vertices are reconstructed using an integrated luminosity equal to19 nb^{-1} of data collected by the ATLAS Experiment in 2010.
Secondary tracks are selected by requiring the transverse impact parameters $|\delta_0|$ of the tracks to be greater than 5 mm. These tracks need to have transverse momentum $p_T > 400$ MeV. **A second pass of tracking is run, after the standard tracking, on left over hits and effectively extend the reconstruction efficiency for secondary tracks greatly**. The hadronic interaction vertices are constructed by an inclusive vertexing algorithm, which ran over the selected tracks.

The intensity indicated by the zz-axis for all plots are equal to the amount of secondary vertices.

Secondary Hadronic Vertices in 2010 (r vs z)

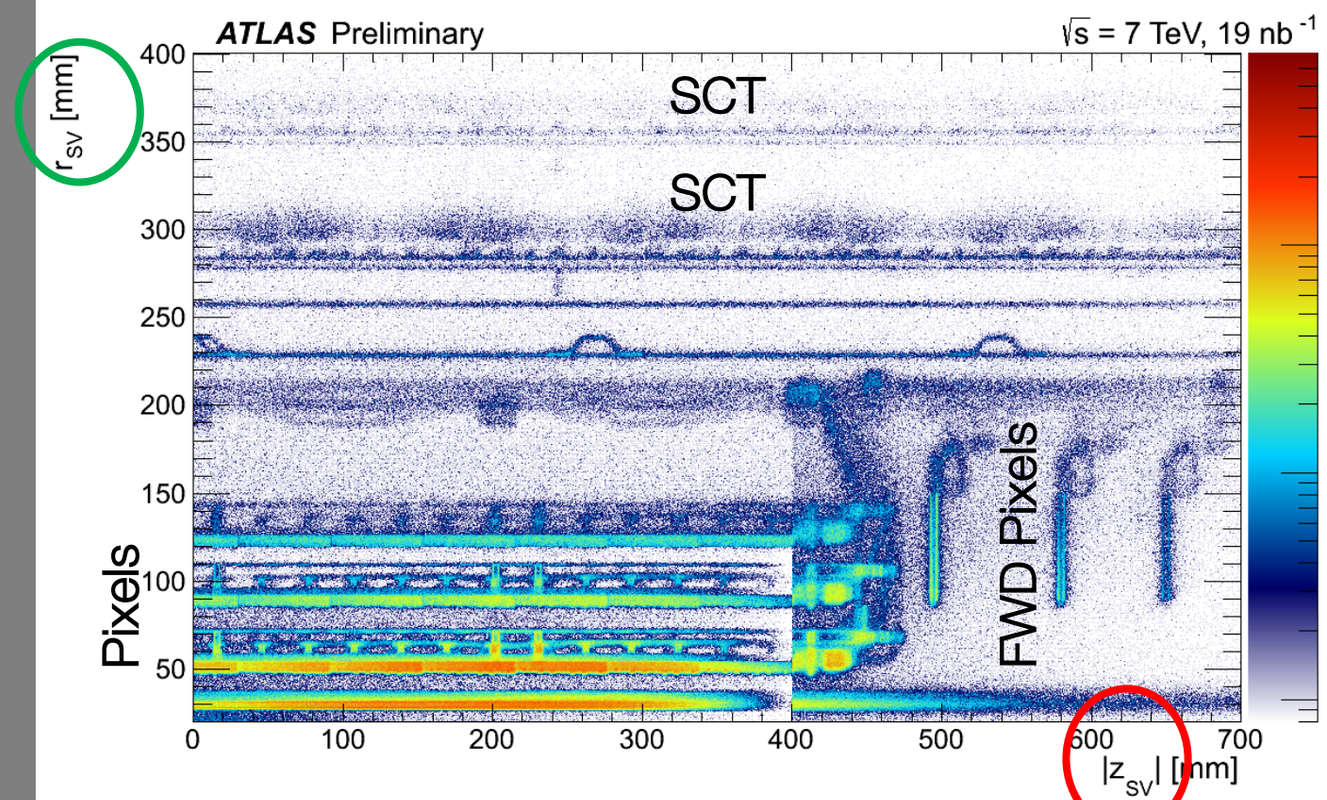

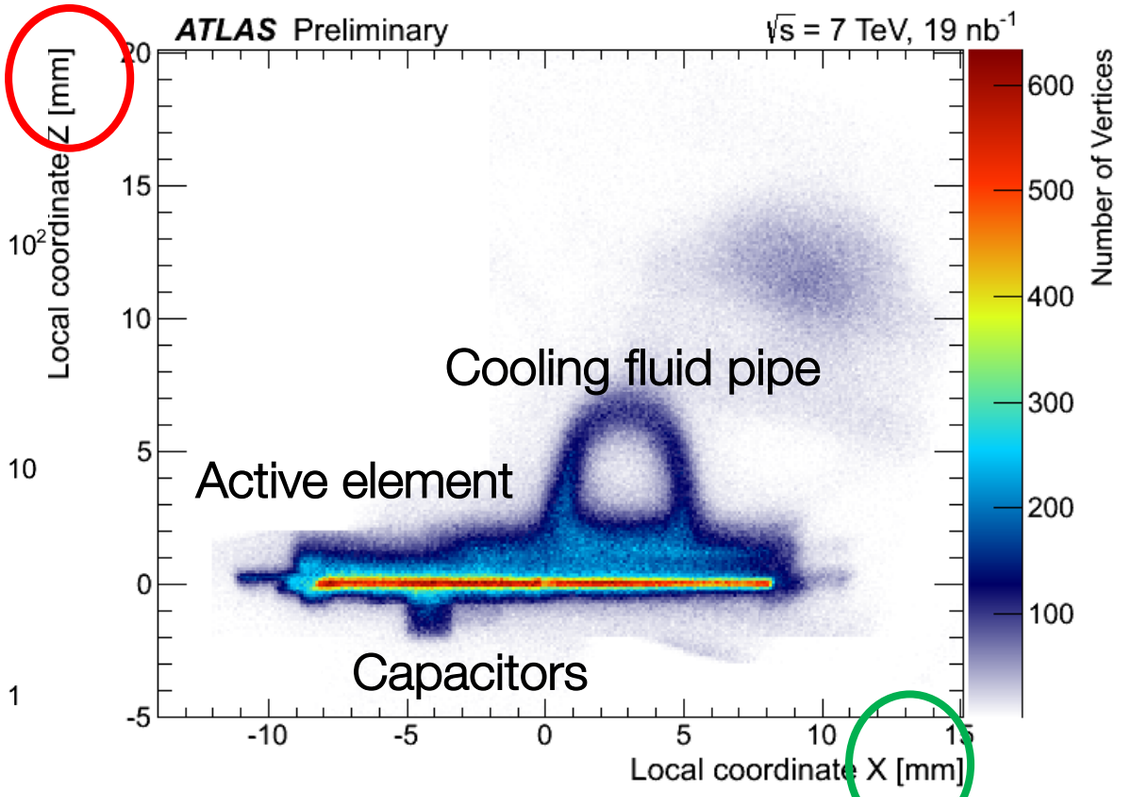

View of the material in the ATLAS Inner Detector in the rz-plane (**left**) mapped by hadronic interaction vertices (SV). The beam pipe (r_{sv} = 34.3 mm), the three pixel barrel layers (r_{sv} = 50.5, 80.5, 122.5 mm), the two first SCT barrel layers (r_{sv} = 299, 371 mm) and three disks in the pixel forward region (r_{sv} < 200 mm and |z| > 450 mm) are clearly visible.

View of the pixel modules in the first barrel layer (B-Layer) in the ATLAS Inner Detector (**right**). The high intensity object at the lower part of the module is the active Silicon-element (Z = 0 mm), the half-circle object at the top side of the modules is the cooling fluid pipe (X = 3 mm, Z = 5 mm) and in the bulk of module structures such as capacitors below the module are visible.

Secondary Vertices in 2010 (x vs y)

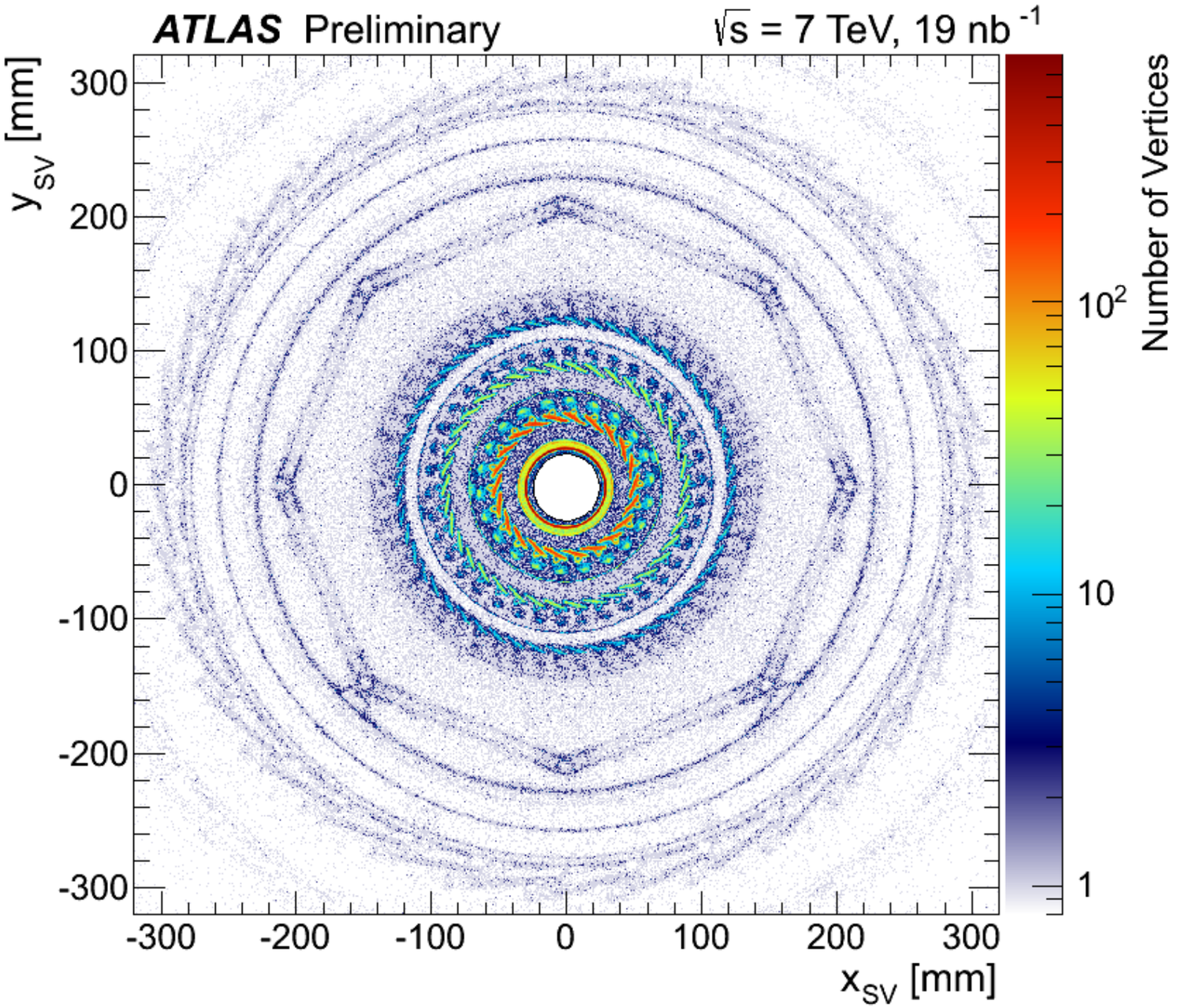

View of the material in the ATLAS Inner Detector in the xy-plane mapped by hadronic interaction vertices (SV). Only vertices found within the region $|z_{sv}| <$ 300 mm are included to provide a clear picture of the barrel region of the detector. Moving outwards in radius, the beam pipe, the three pixel barrel layers and the two first SCT barrel layers are visible.

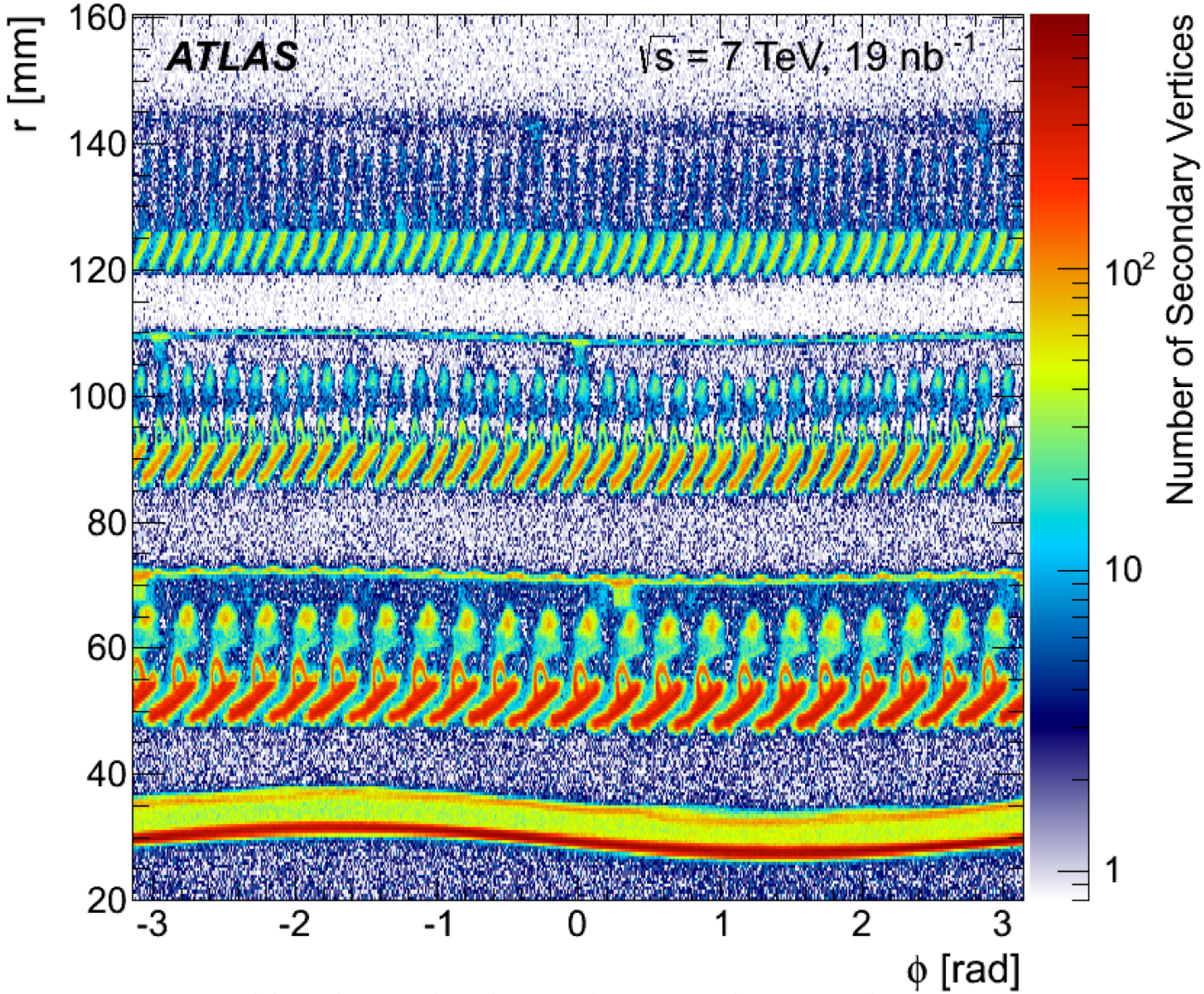

Number of selected secondary vertices in data in the r–ϕ plane of the ID

The Position of the Beam Pipe

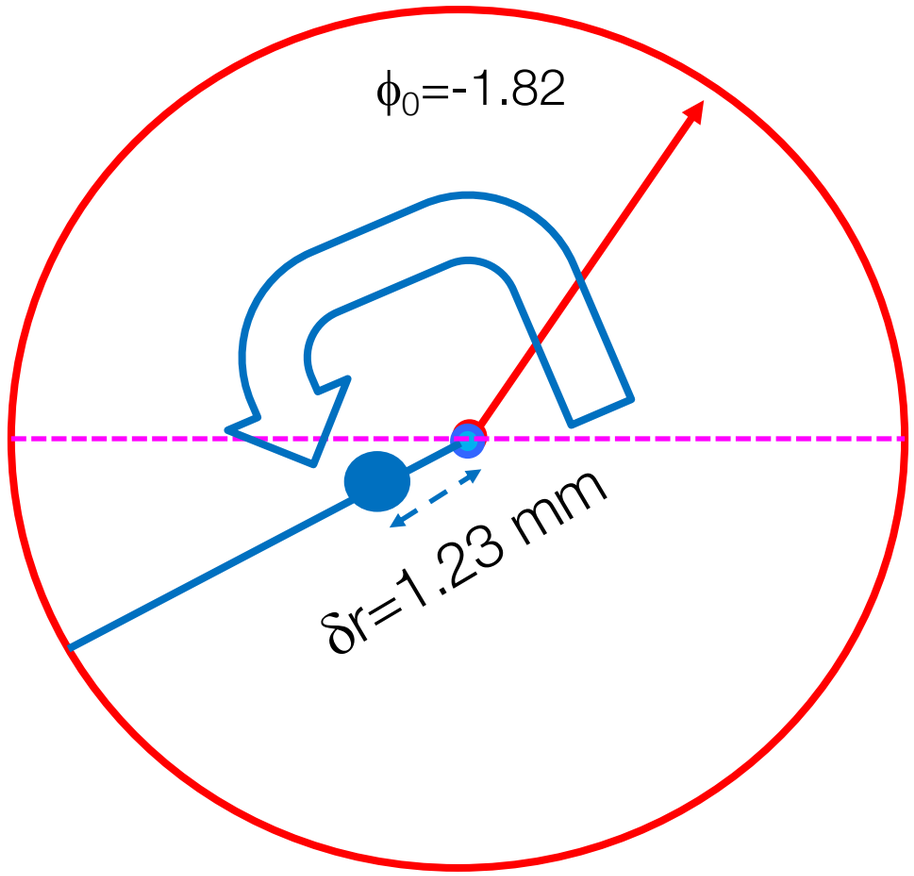

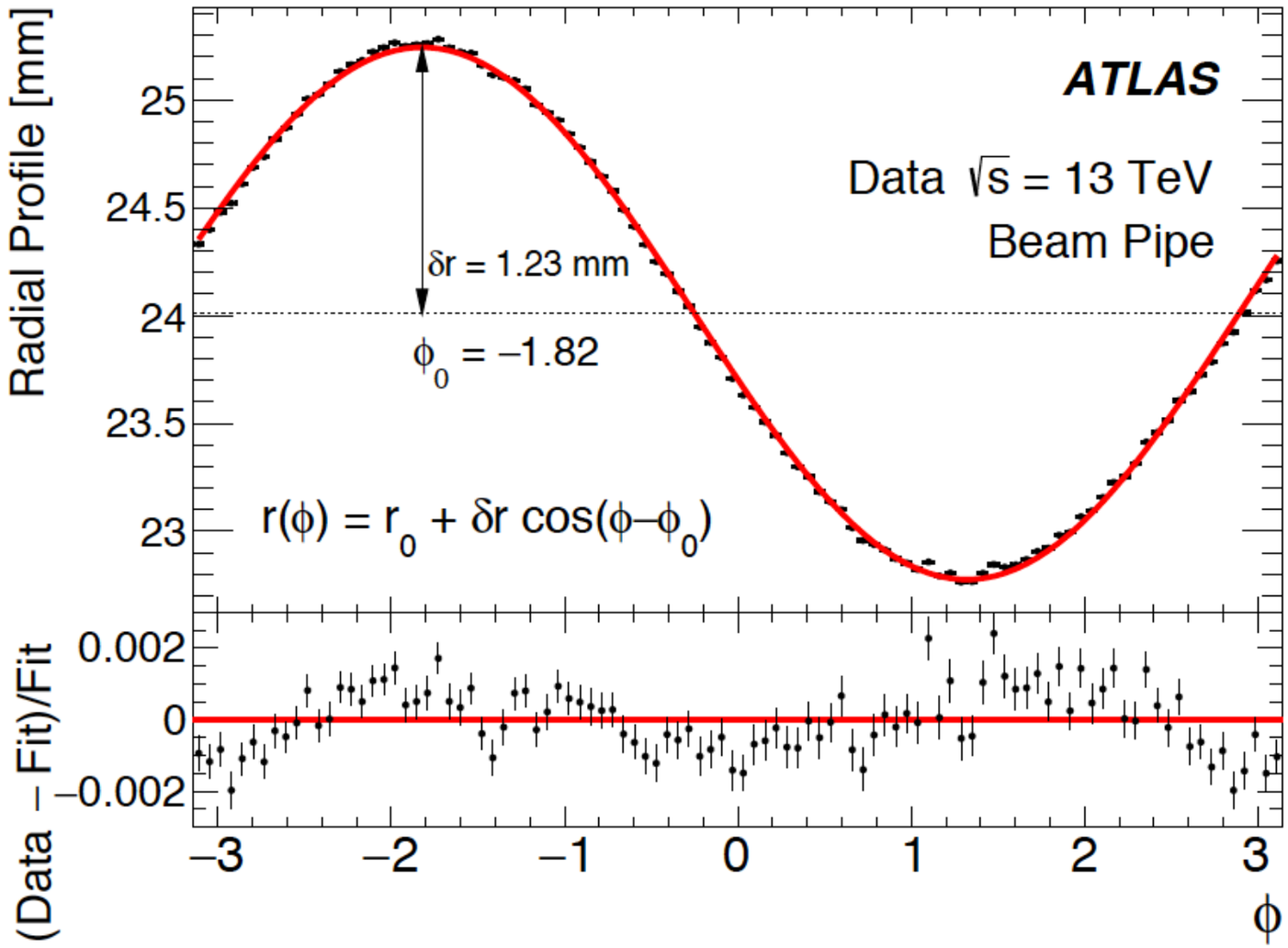

Inner Tracking

Alignment and Resolution Determination

[ATLAS: The q·pT distribution for tracks as a function of the pseudorapidity]

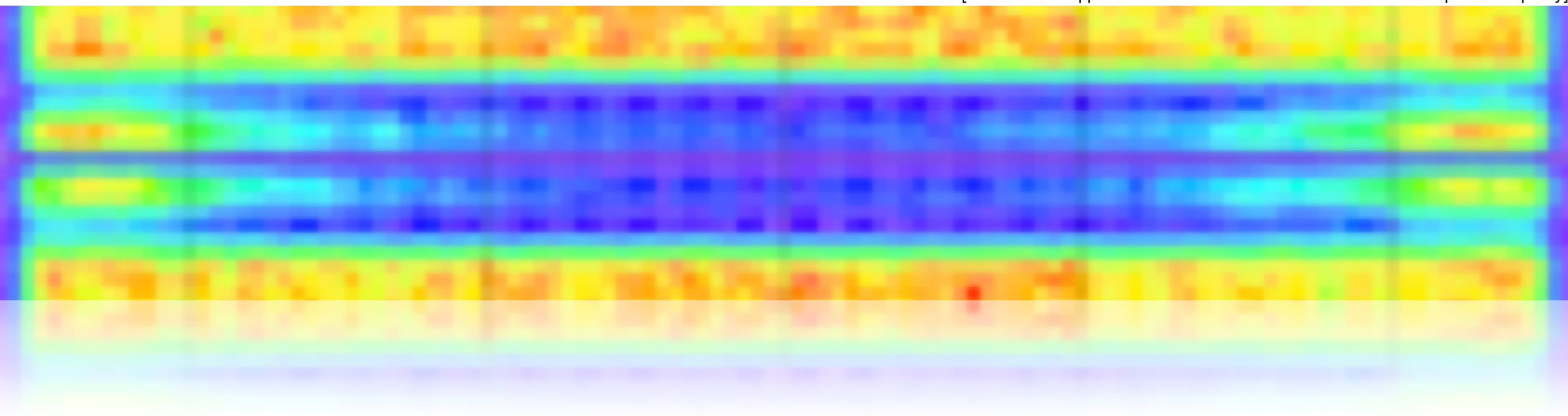

Inner Tracking – Design Goals

Track thousands of charged particles
[$p_T > 1$ GeV and $|\eta| < 2.5$]

Identify particles by signal matching
[e.g. track-cluster matching for electrons]

Identify long-lived particles e.g. B-hadrons, τ ...
[secondary vertexing]

Radiation hardness
[harsh environment close to beam pipe]

Minimum multiple scattering
[Small material budget]

CMS: pixels; silicon micro-strip detectors [200 m^2]

e.g. ATLAS: pixels; silicon micro-strip detectors & transition radiation tracker

ATLAS Inner Tracking System

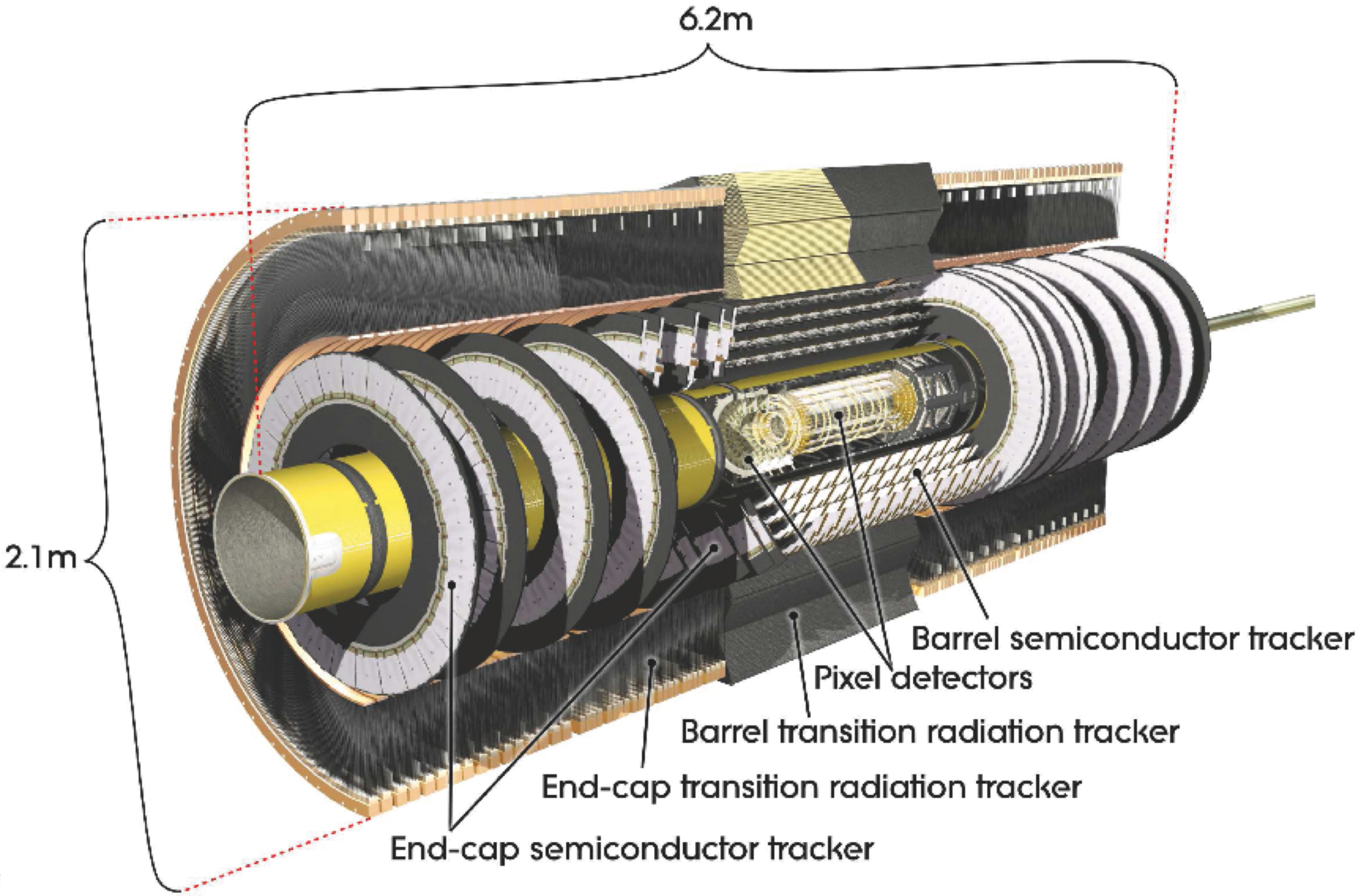

ATLAS Inner Tracking System

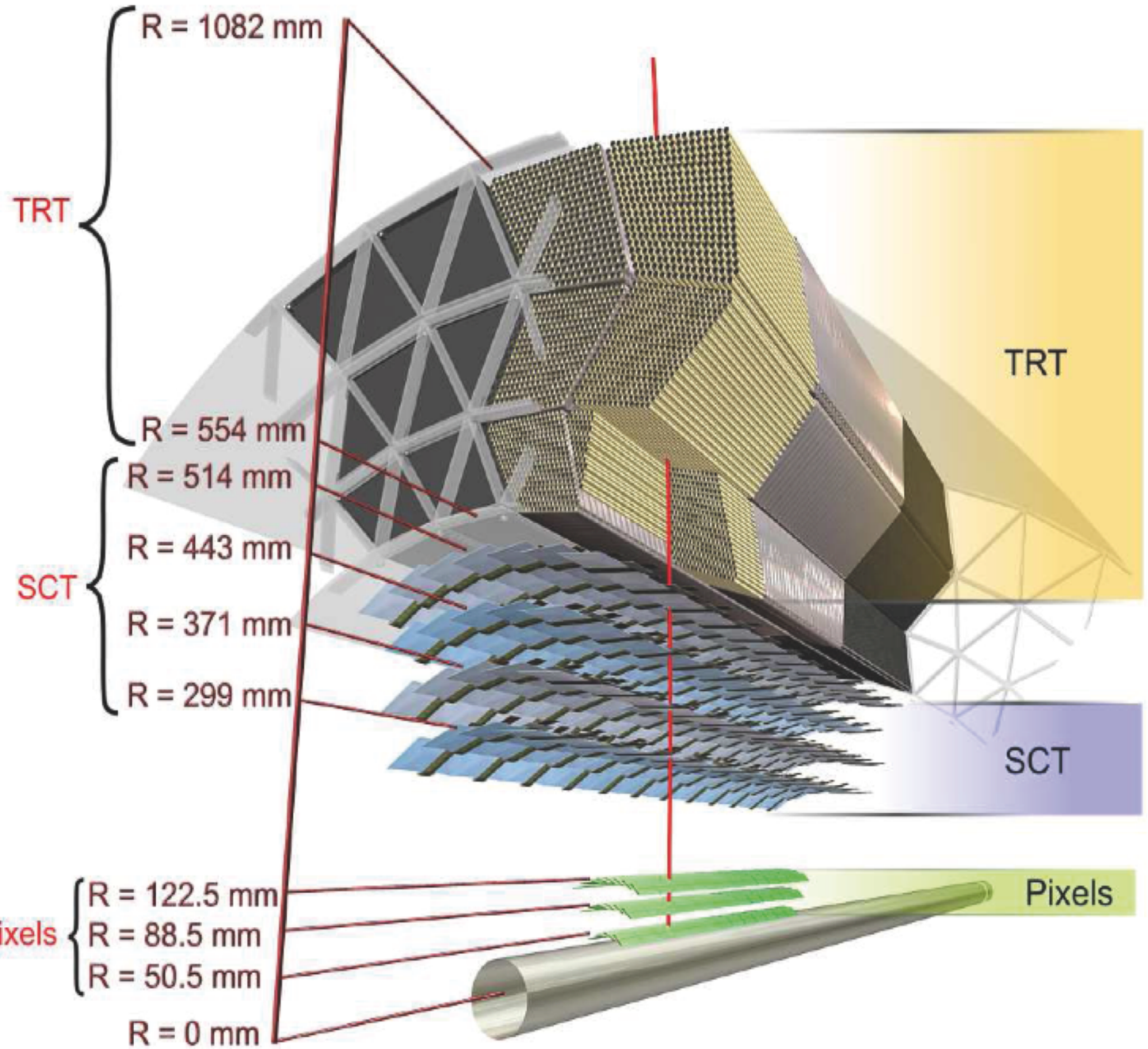

Before IBL!

Charged track
[p_T =10 GeV at η=0.3]

Passage through:

- Beryllium beam pipe
- 3 pixel layers
- 4 double SCT layers
- about 36 TRT straws

IBL (Insertable B Layer) in ATLAS inserted during LS1

- Improve performance of existing system
- Installed inside existing pixel detector together with a new smaller beam pipe
- *Tracking extended to $\eta = 2.9$*

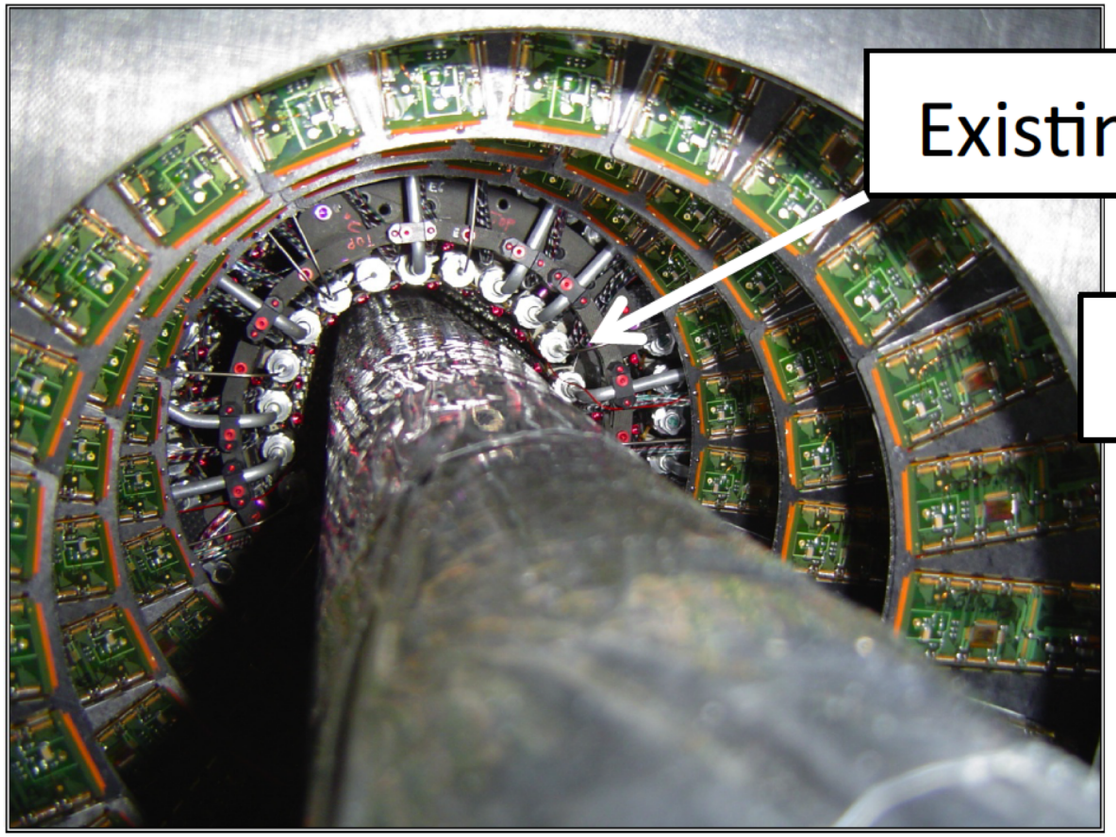

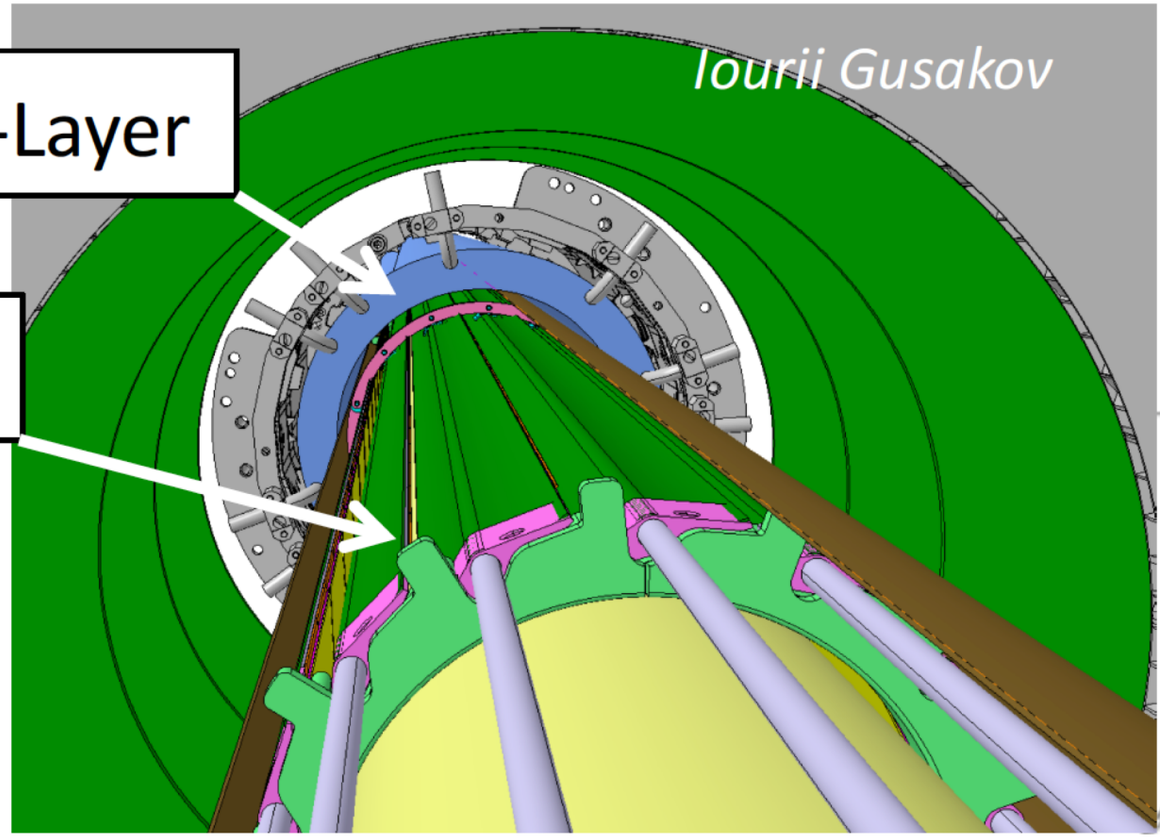

The IBL in the transverse plane

Overlap in ϕ to avoid dead zones

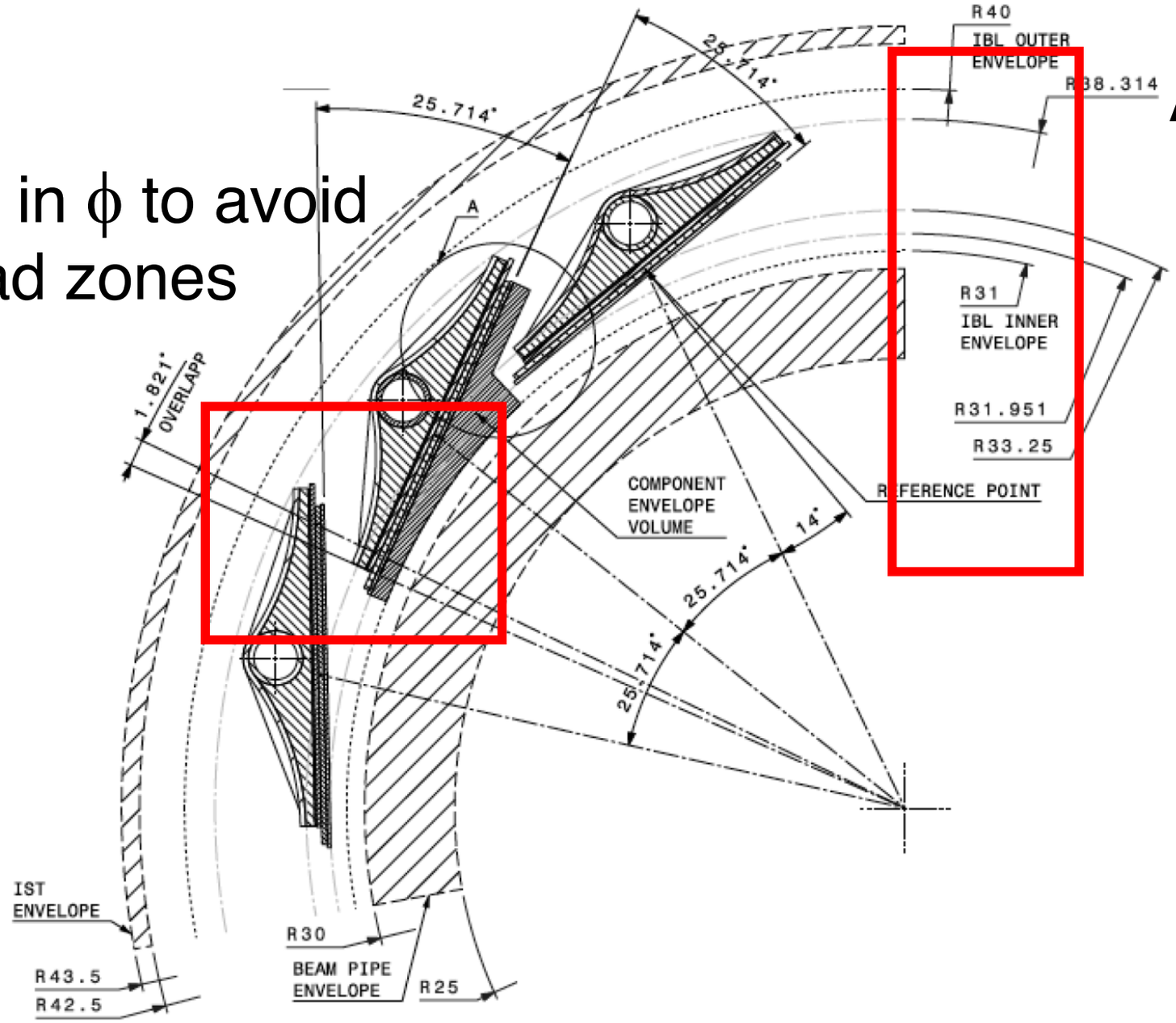

Figure 1. IBL structure in $r - \phi$ plane.

Average radius is 33.25 mm!

CMS Inner Tracking System

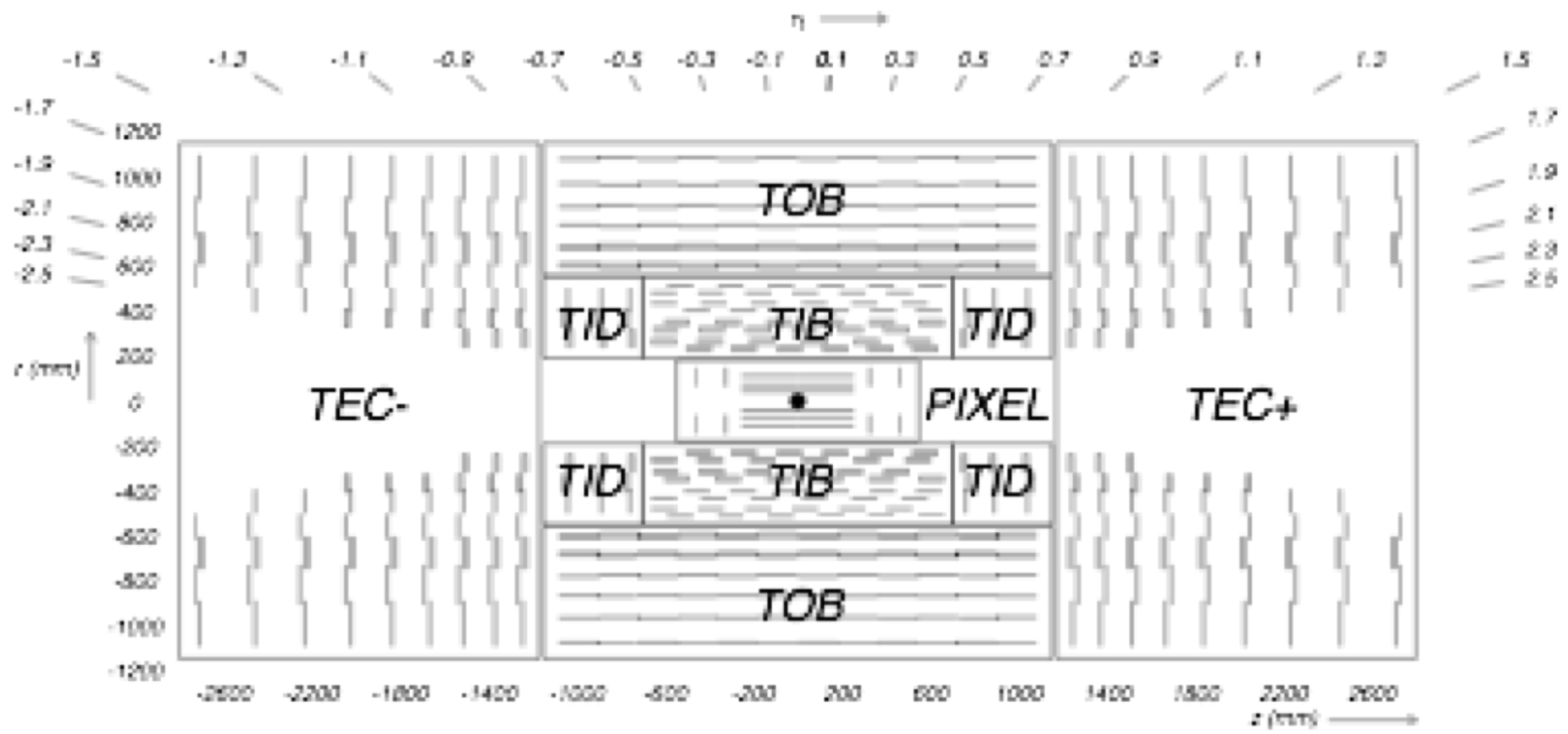

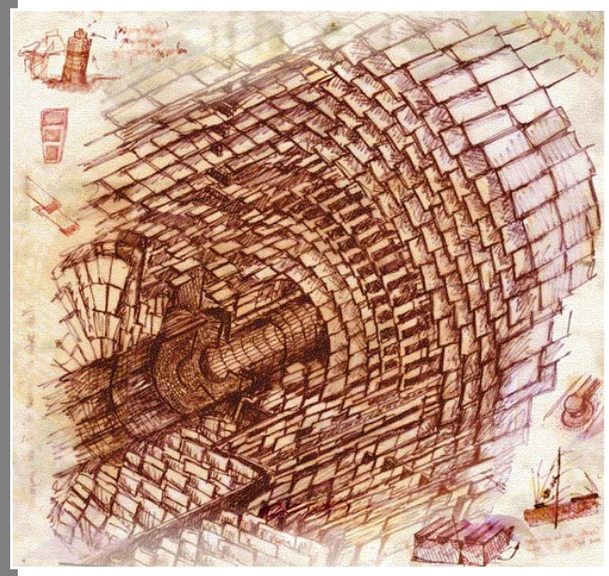

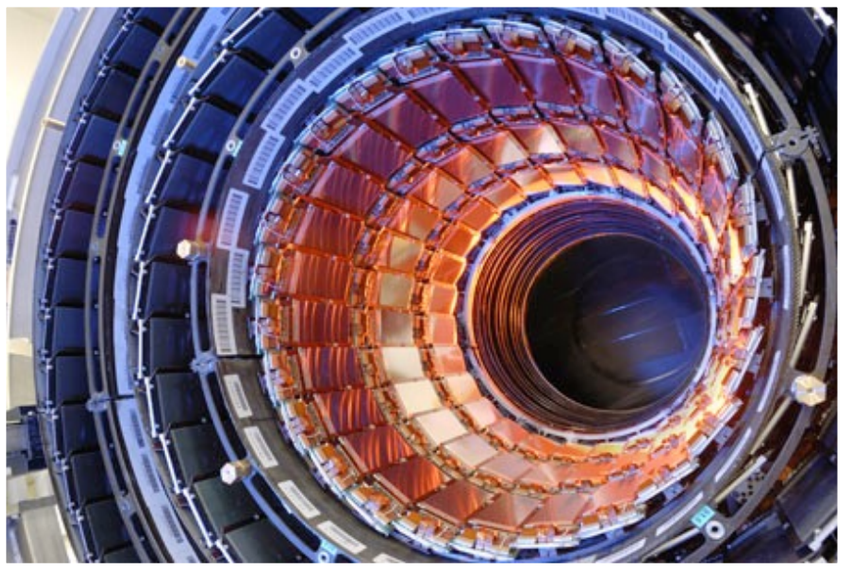

ATLAS track reconstruction

"Primary tracks", first stage

1. Start from 3-point seed in silicon detectors
2. Add hits moving away from IP using Kalman filters
3. Tracks extended to TRT
4. Tracks required to have p_T>400 MeV

Second stage, refine tracks

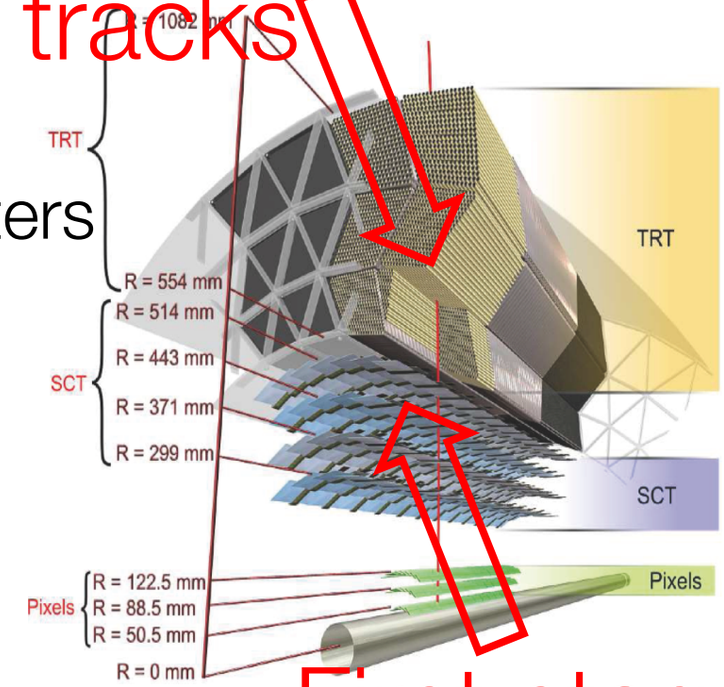

First stage

Refine tracks, second stage

1. Go back inward and add silicon hits

Mitigate effect of pile up. Robust algorithm

1. Increase of pile up induces more combinatorial fake tracks
2. Tighten track quality: 9 hits, no hole. Less fakes, less efficiency

Kalman filters

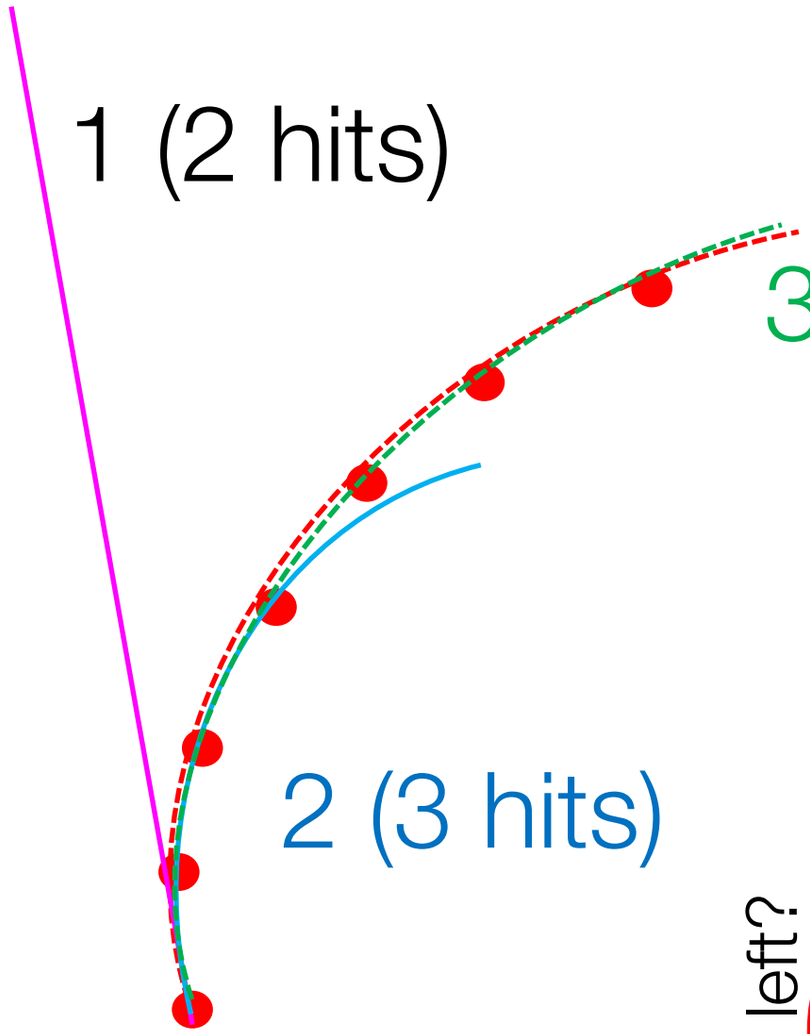

Kalman filter is an iterative procedure

- Starts from a seed (2 hits)
- Extrapolates and includes next hit; accounts for material, multiple scattering, energy loss
- Recalculates track parameters, refines extrapolation

Hits left?

Kalman filters

Combine ‘Noisy’ measurements + History + ‘Model’ (say track in a magnetic field)

Current estimation of signal

Actual measurement

K_k = Kalman gain

$$\hat{X}_k = K_k . Z_k + (1 - K_k) . \hat{X}_{k-1}$$

Previous estimation of signal

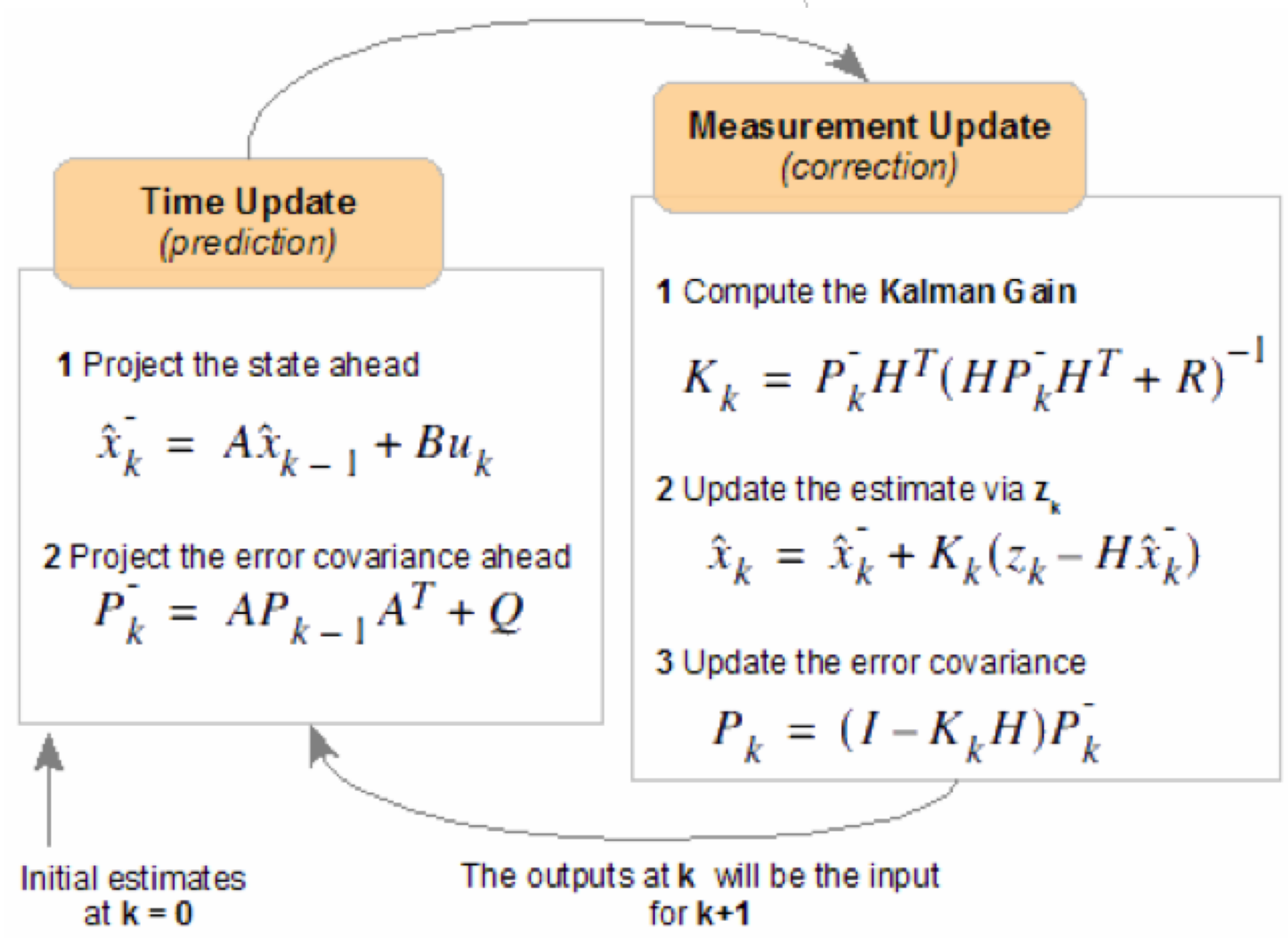

Goal: compute X, observable using a sequence of measurements (k=1,2… indicates successive measurements/states)

Computing time!

Kalman Filter

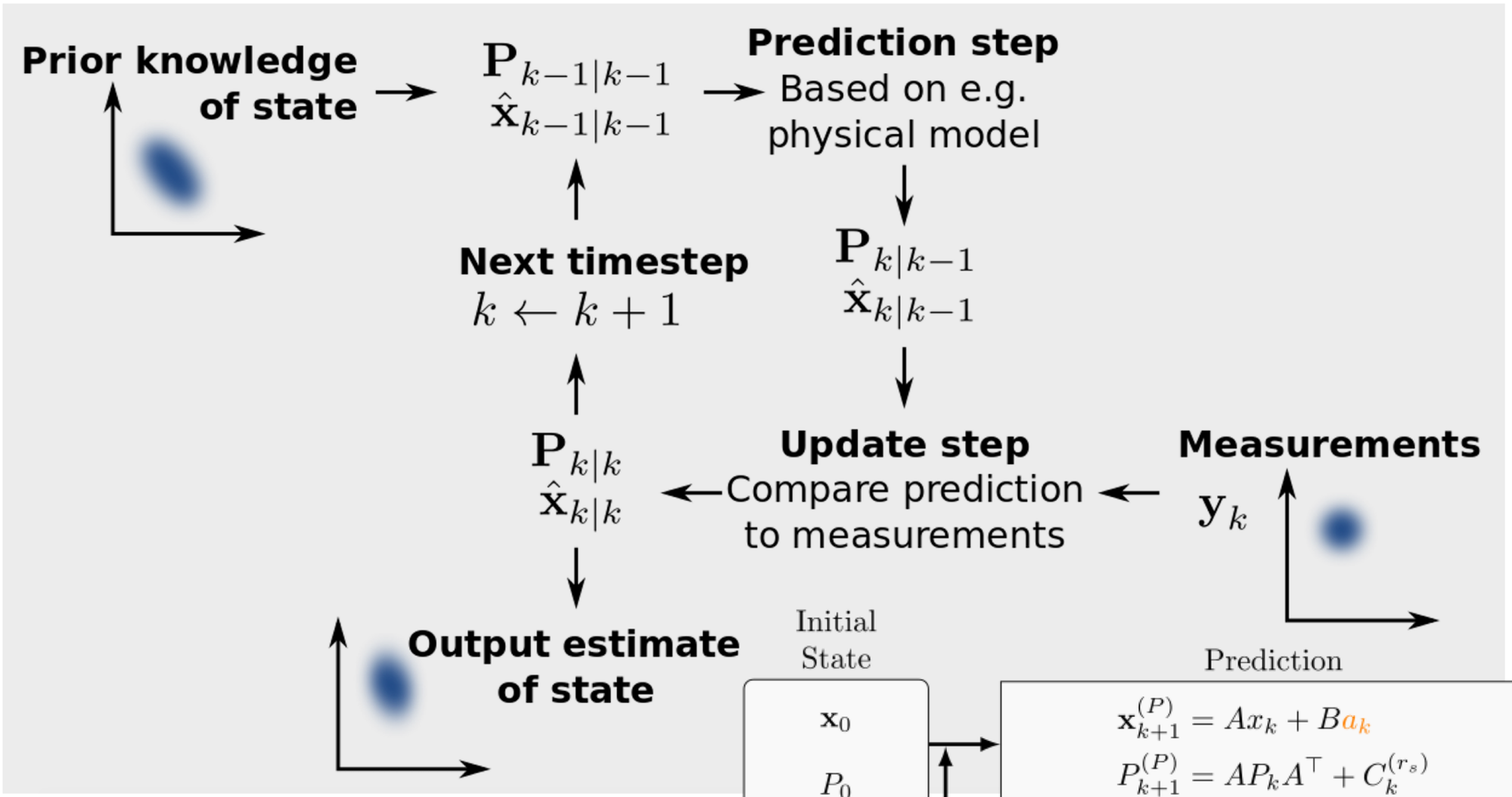

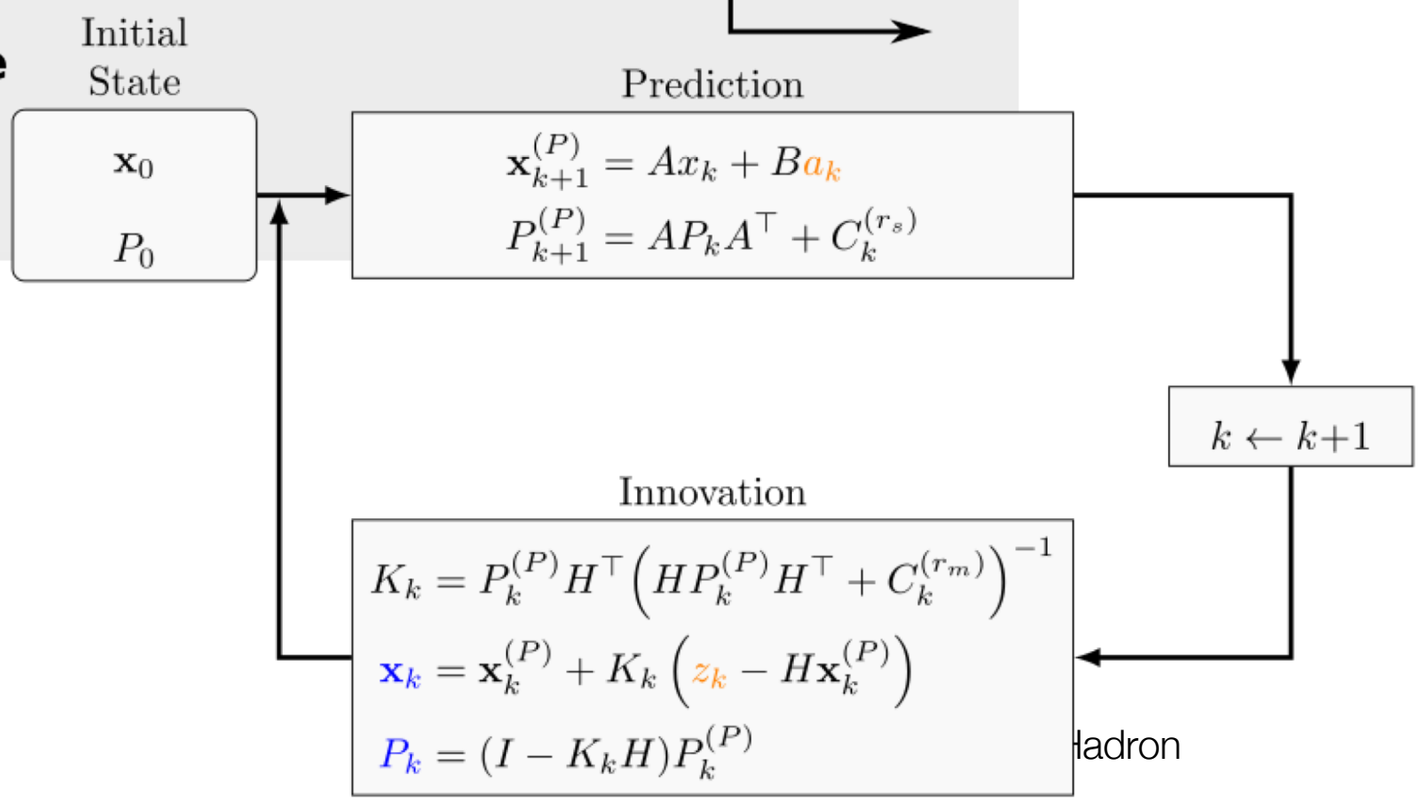

Spatial Resolution and Alignment

TRT Track Residuals

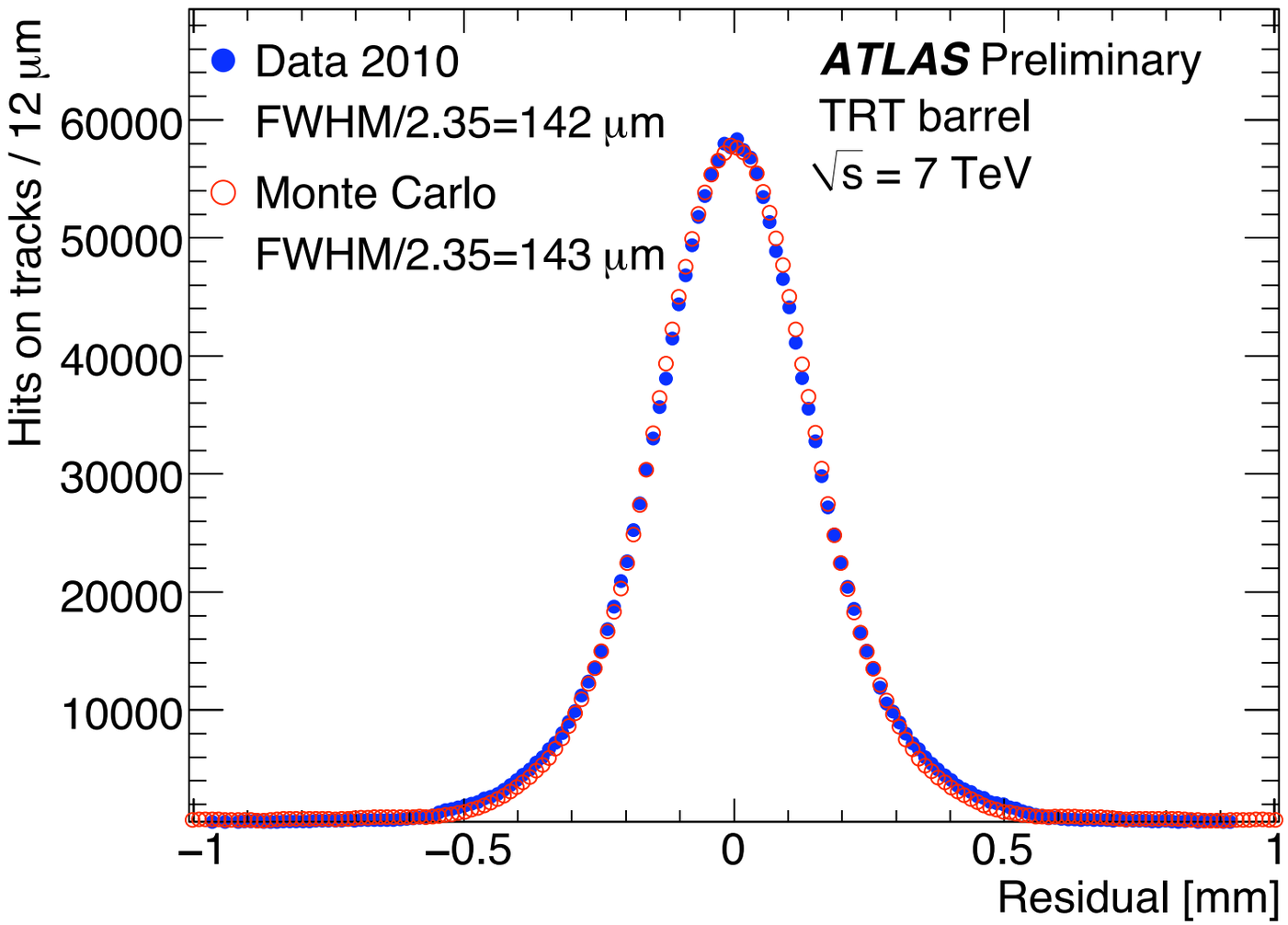

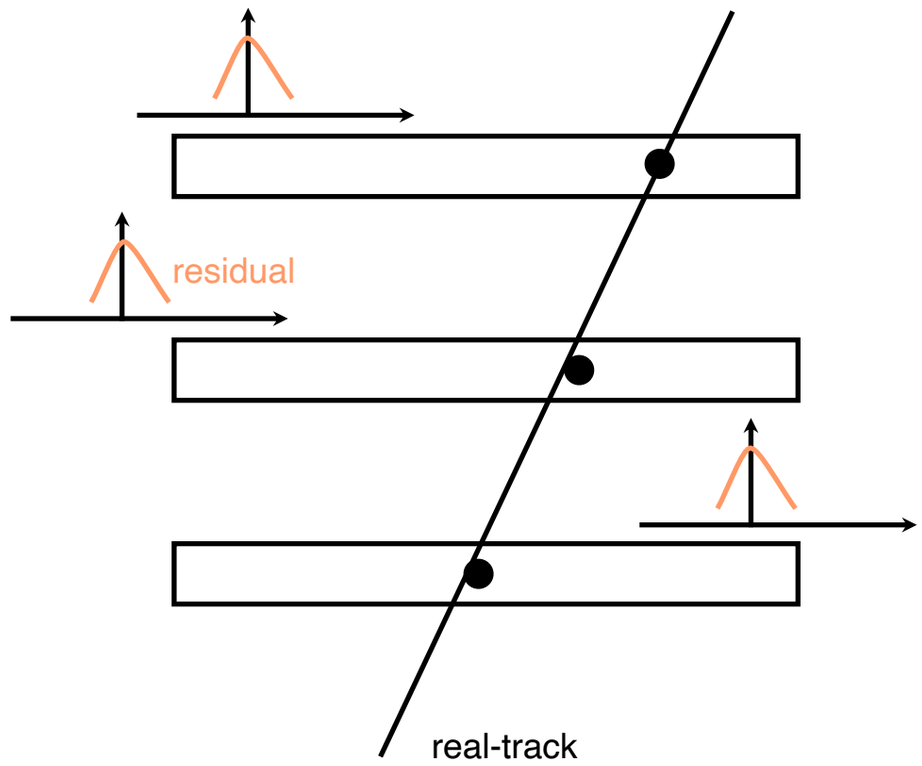

Residual distribution in TRT barrel

[TRT: Transition Radiation Tracker]

Spatial Resolution and Alignment

Alignment done using residual information

ATLAS ID detector:
more than 35000 degrees of freedom

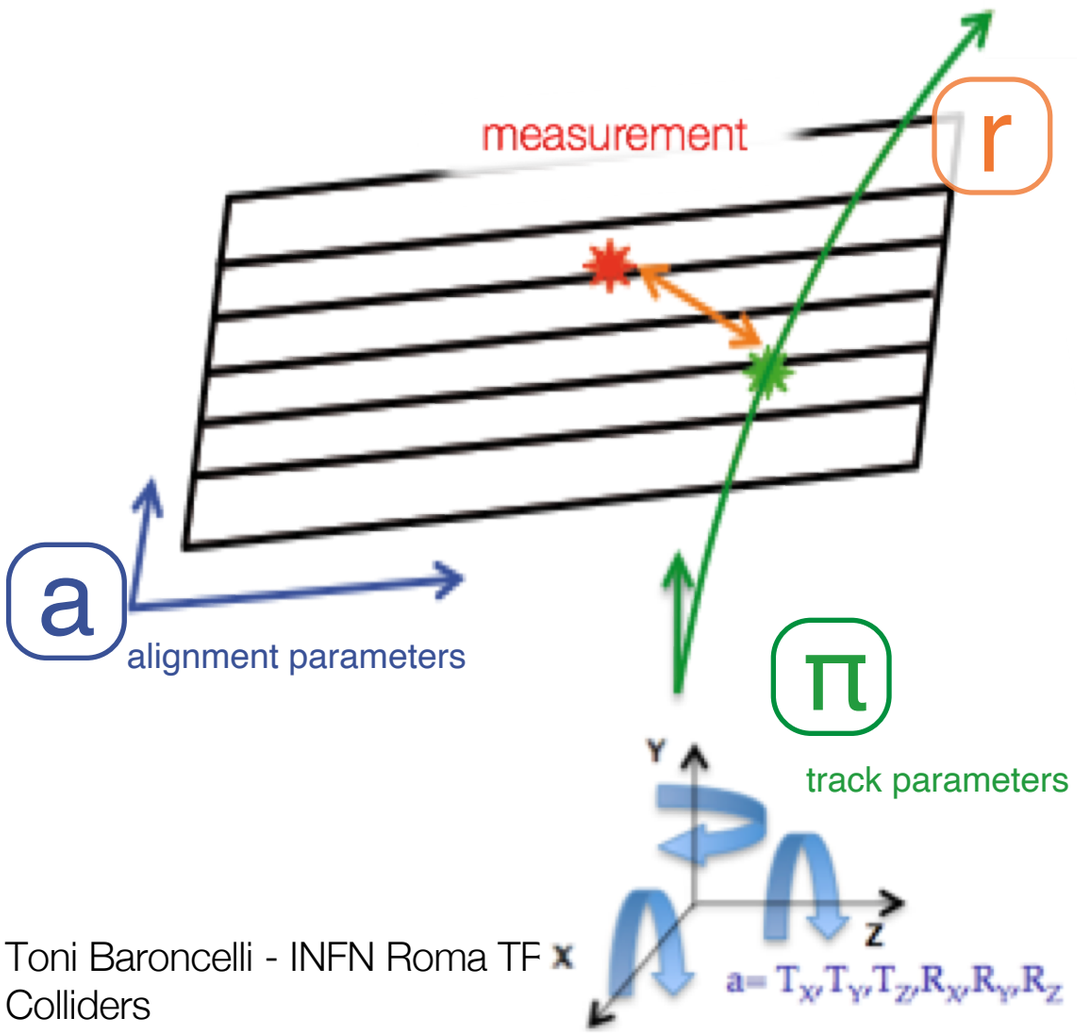

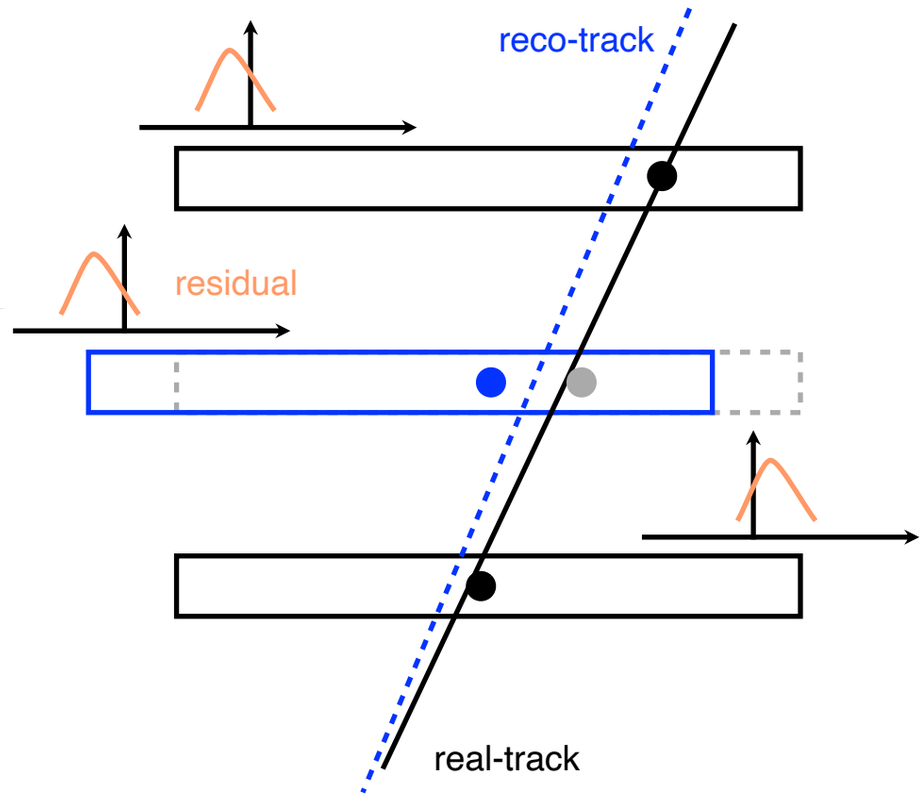

fit/extrapolation

Residual:

$$r = \text{hit}_{\text{meas.}} - \text{hit}(\pi, a)_{\text{fit}}$$

χ^2 definition:

$$\chi^2 = \sum_{\text{tracks}} r^T(\pi, a) V^{-1} r(\pi, a)$$

a: alignment parameters
π: track parameters
V: covariance matrix of hit measurements ...

Minimize χ^2

and extract alignment parameters ...

Spatial Resolution and Alignment

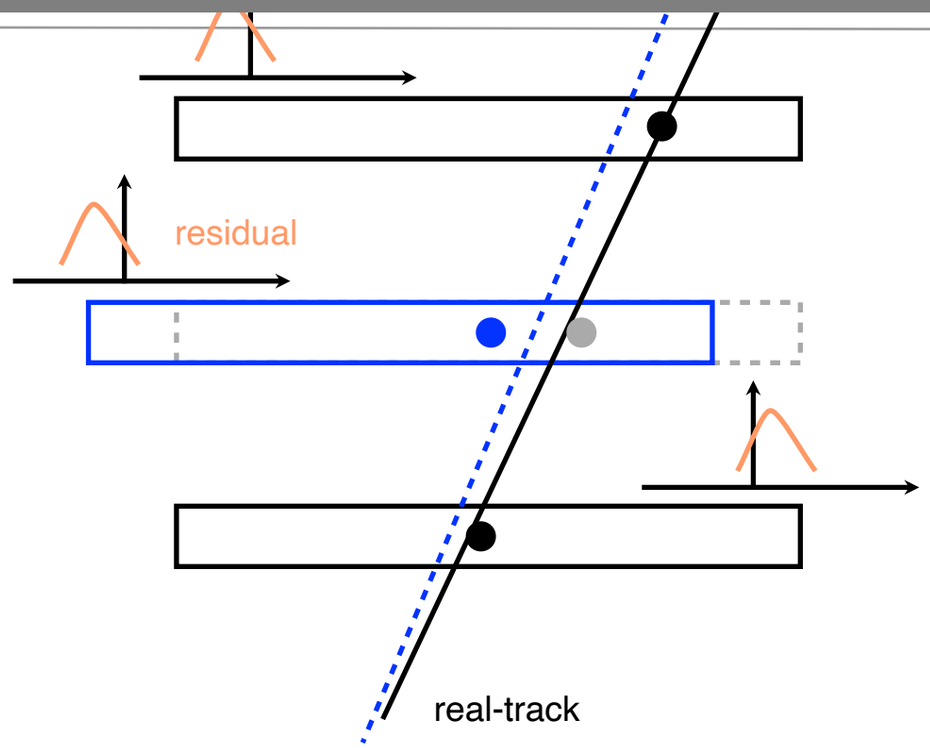

TRT Track Residuals

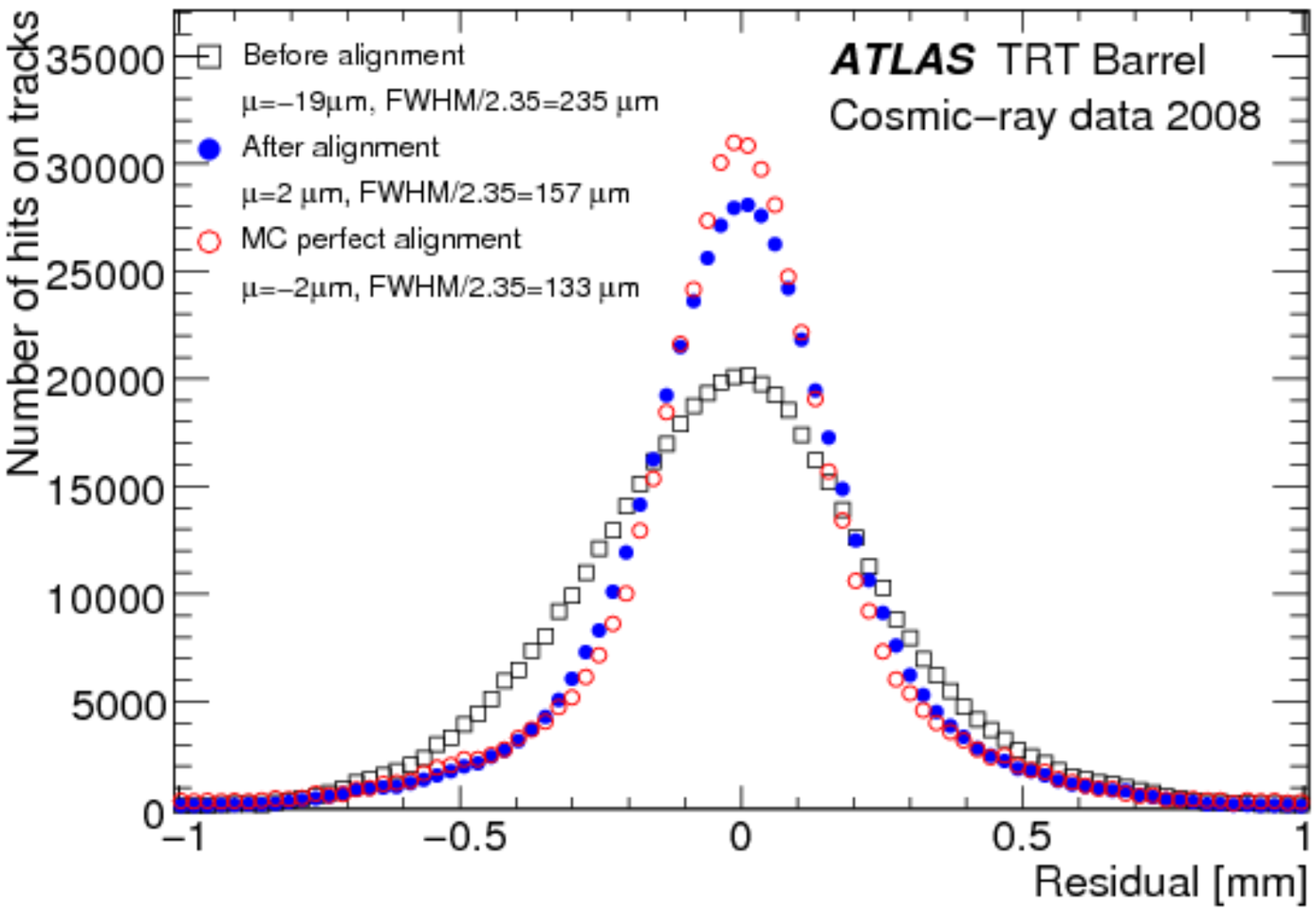

Residual distribution in TRT barrel ...

... before and after alignment

[TRT: Transition Radiation Tracker]

ATLAS alignment

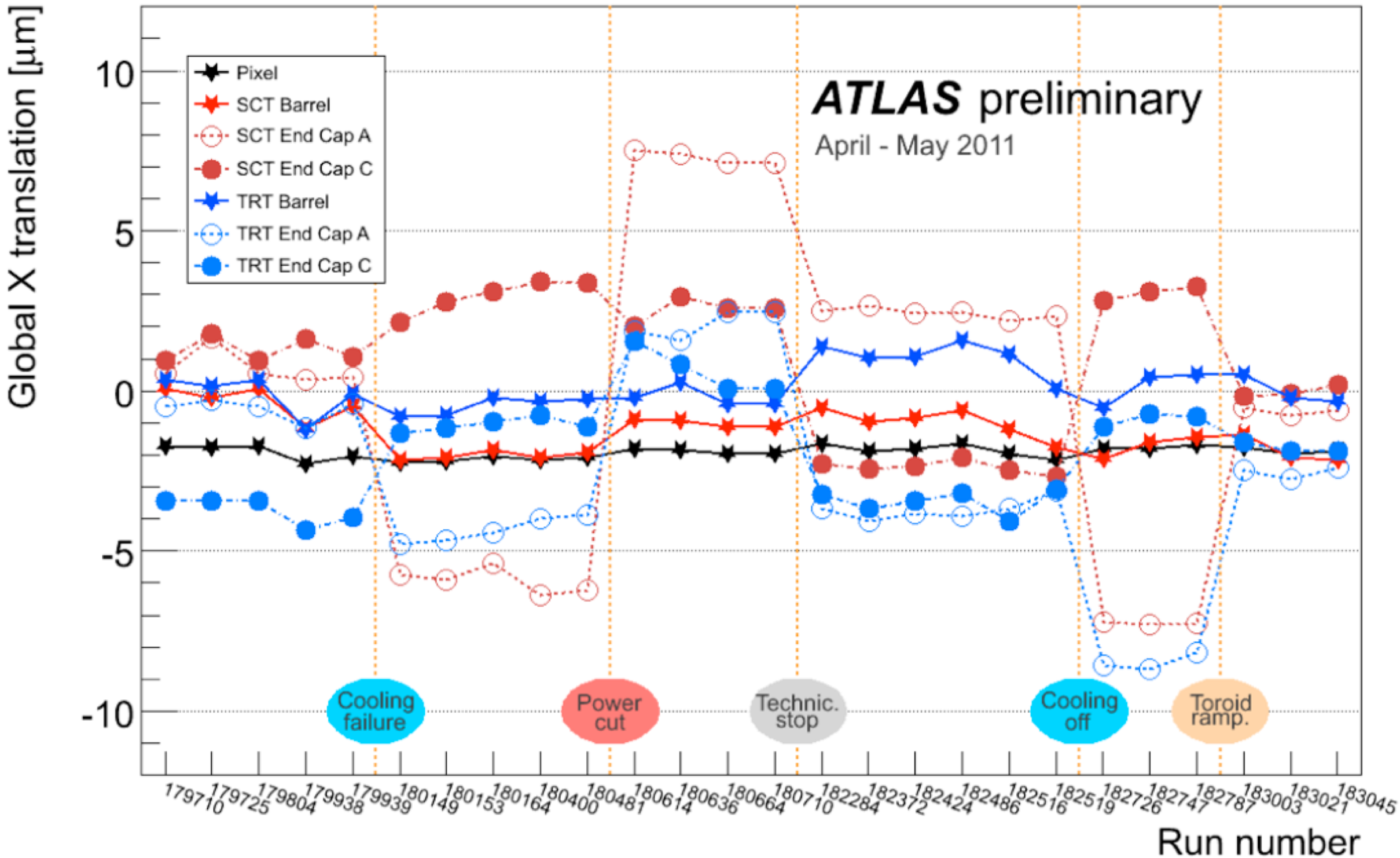

Tracker Performance

Typical track parameters:

- q/p: signed curvature (q: charge)
- d_0,z_0: impact parameters
- θ,ϕ: angles

Key performance figures:

- Reconstruction efficiency
- Momentum resolution
- Impact parameter resolution
  [e.g. transverse impact parameter]

d_0-resolution:

$$\delta_{d_0} \equiv \frac{\Delta d_0}{d_0} = \frac{|d_{0,\text{true}} - d_{0,\text{rec}}|}{d_{0,\text{true}}}$$

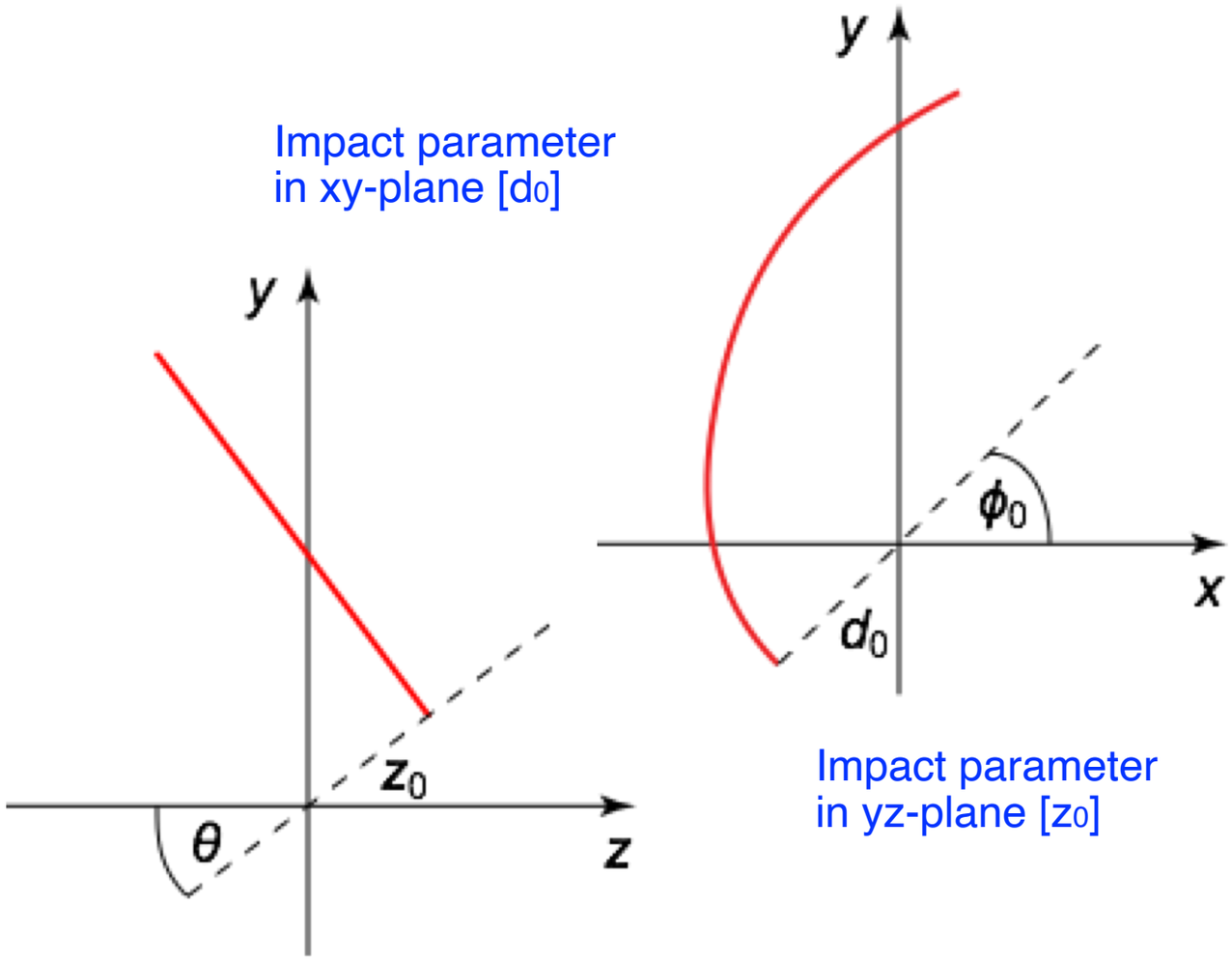

Reconstruction efficiency: $\varepsilon_{\text{rec}} \equiv \frac{N_{\text{rec}}(p_T, \eta, \dots)}{N_{\text{prod}}(p_T, \eta, \dots)}$

Momentum resolution: $\delta_p \equiv \frac{\Delta p}{p} = \frac{|p_{\text{true}} - p_{\text{rec}}|}{p_{\text{true}}}$

Tracker performance

TABLE 7 Main performance characteristics of the ATLAS and CMS trackers

	ATLAS	CMS
Reconstruction efficiency for muons with $p_T = 1$ GeV	96.8%	97.0%
Reconstruction efficiency for pions with $p_T = 1$ GeV	84.0%	80.0%
Reconstruction efficiency for electrons with $p_T = 5$ GeV	90.0%	85.0%
Momentum resolution at $p_T = 1$ GeV and $\eta \approx 0$	1.3%	0.7%
Momentum resolution at $p_T = 1$ GeV and $\eta \approx 2.5$	2.0%	2.0%
Momentum resolution at $p_T = 100$ GeV and $\eta \approx 0$	3.8%	1.5%
Momentum resolution at $p_T = 100$ GeV and $\eta \approx 2.5$	11%	7%
Transverse i.p. resolution at $p_T = 1$ GeV and $\eta \approx 0$ (μm)	75	90
Transverse i.p. resolution at $p_T = 1$ GeV and $\eta \approx 2.5$ (μm)	200	220
Transverse i.p. resolution at $p_T = 1000$ GeV and $\eta \approx 0$ (μm)	11	9
Transverse i.p. resolution at $p_T = 1000$ GeV and $\eta \approx 2.5$ (μm)	11	11
Longitudinal i.p. resolution at $p_T = 1$ GeV and $\eta \approx 0$ (μm)	150	125
Longitudinal i.p. resolution at $p_T = 1$ GeV and $\eta \approx 2.5$ (μm)	900	1060
Longitudinal i.p. resolution at $p_T = 1000$ GeV and $\eta \approx 0$ (μm)	90	22–42
Longitudinal i.p. resolution at $p_T = 1000$ GeV and $\eta \approx 2.5$ (μm)	190	70

Examples of typical reconstruction efficiencies, momentum resolutions, and transverse and longitudinal impact parameter (i.p.) resolutions are given for various particle types, transverse momenta, and pseudorapidities.

Better in CMS; higher and more uniform B field

Comparable; dominated by pixel resolutions

CMS: smaller pixels

[Froidevaux, Sphicas]

Tracking Efficiency

Example: ATLAS Pixel Detector

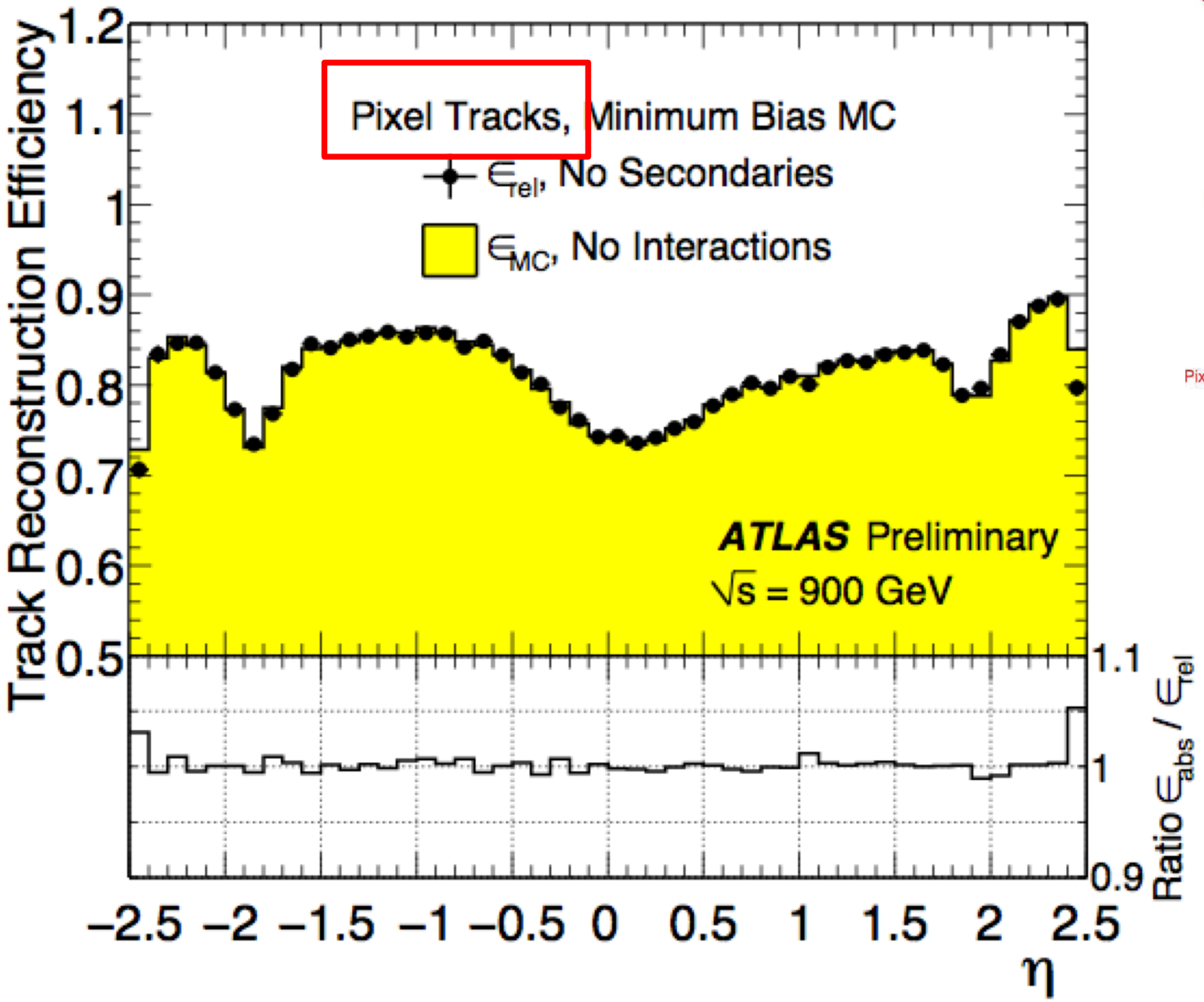

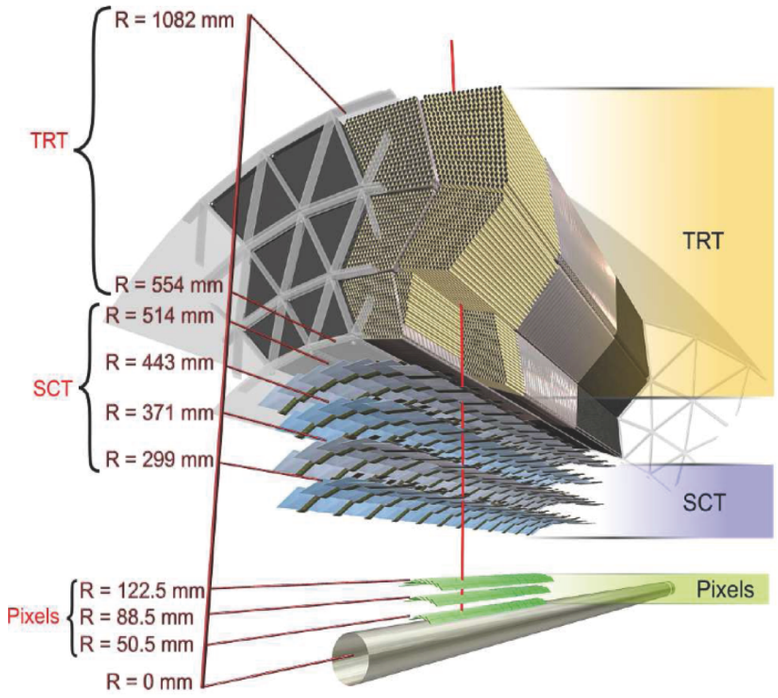

Method:

Measure tracks with SCT and TRT and check whether it is also reconstructed by Pixel detector ...

Correct for ...

Secondary particles from decays
[not seen by Pixel]

Hadronic Interactions
[not seen by SCT-TRT]

Performance

Track reconstruction efficiency is also computed from Monte Carlo (MC) simulation and compared to low-luminosity runs.

Default selection cuts are applied:

- pT > 500 MeV,
- |eta| < 2.5,
- only particles with lifetime > 10^{-10} s, B-layer hits >=1 if expected,
- SCT hits >1 .

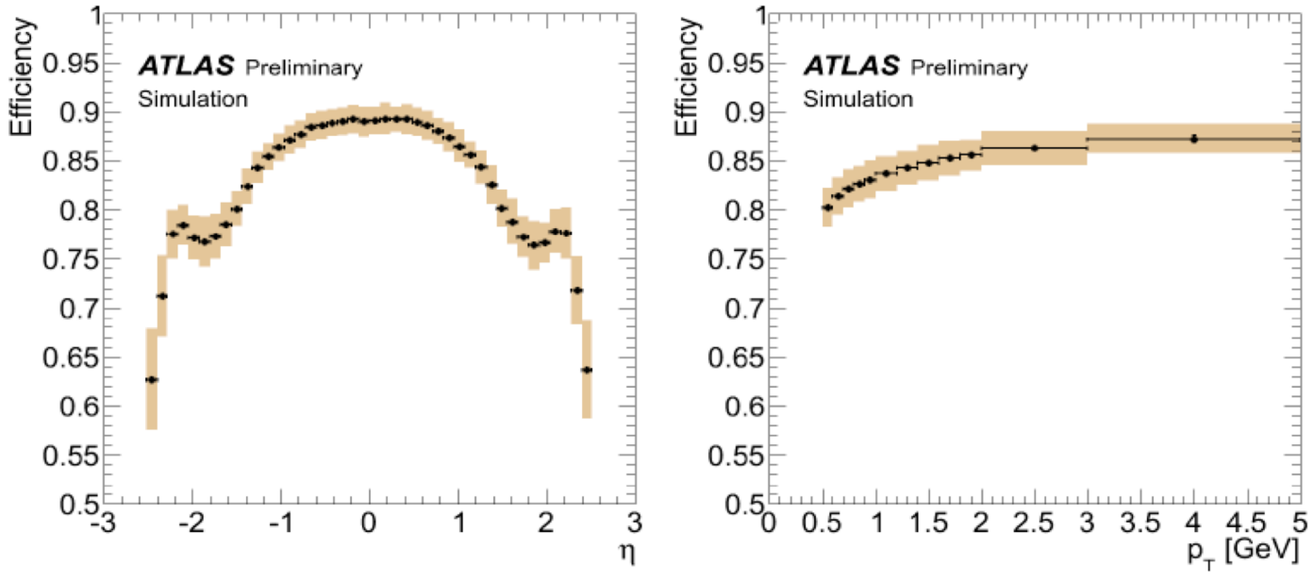

Track reconstruction efficiency as a function of pseudorapidity η (left) and transverse momentum p_T (right) [3].

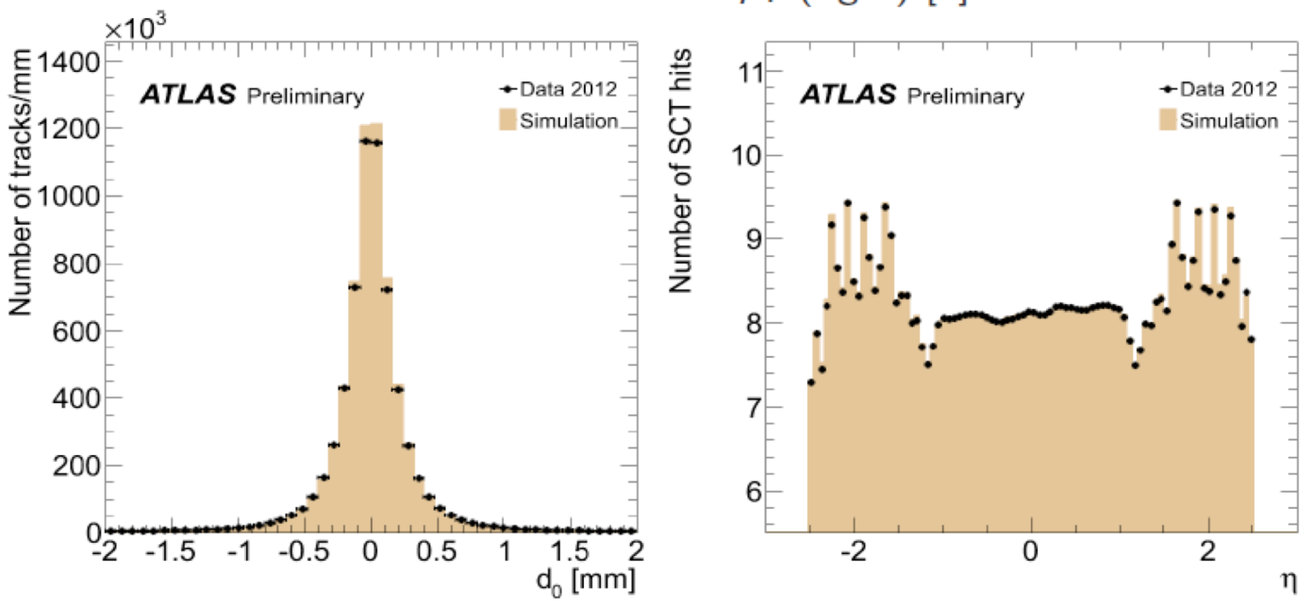

Transverse impact parameter d_0 (left) and number of SCT hits vs. η [3].

ATLAS track reconstruction efficiency

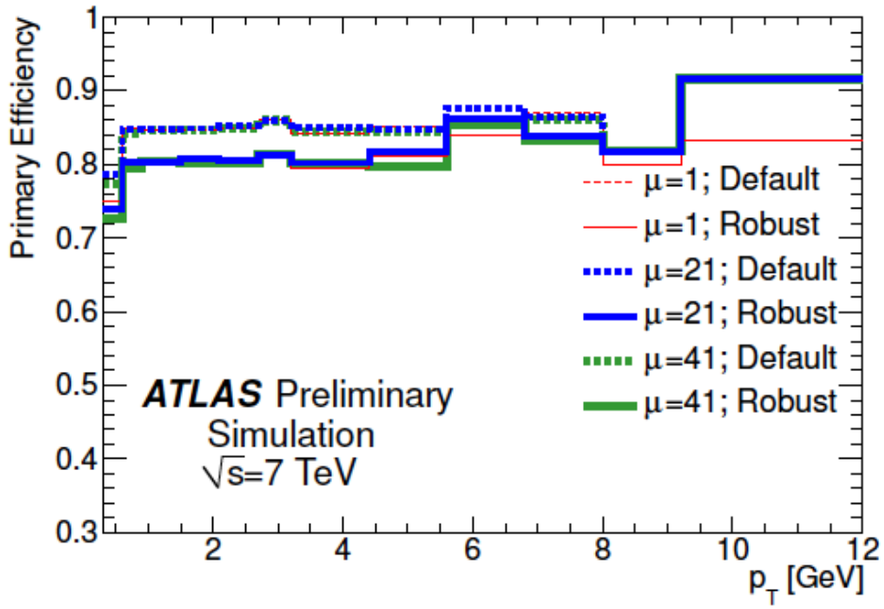

(a) Primary track reconstruction efficiency vs p_T

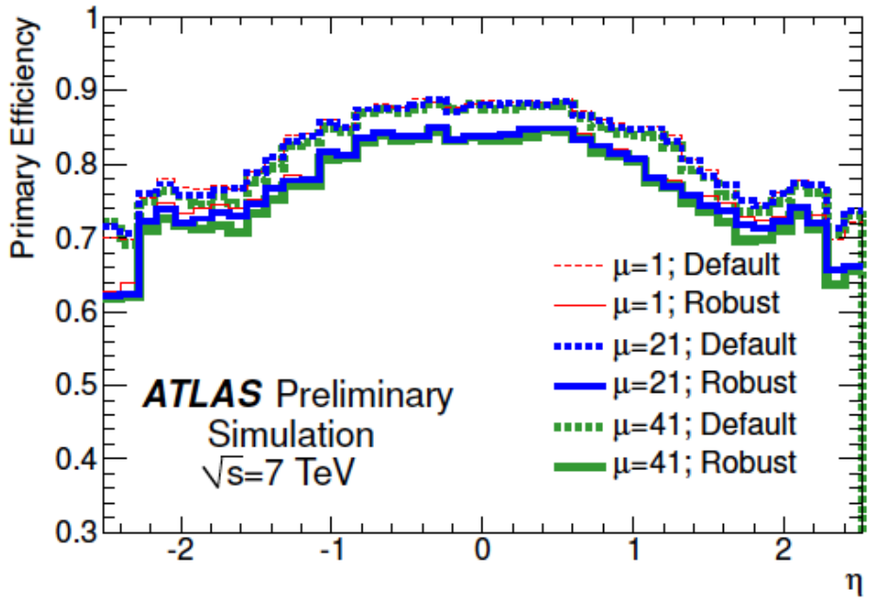

(b) Primary track reconstruction efficiency vs η

"μ" indicates pile-up
See later

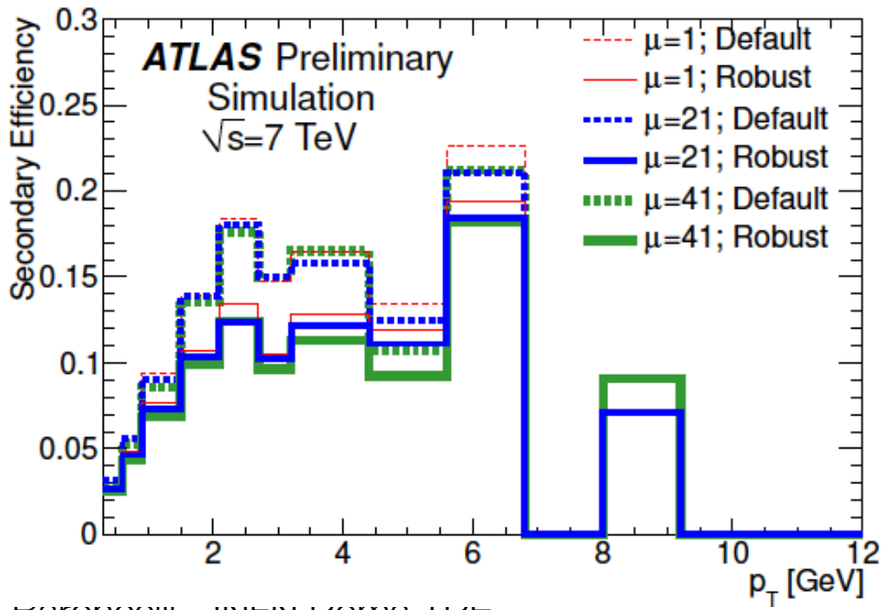

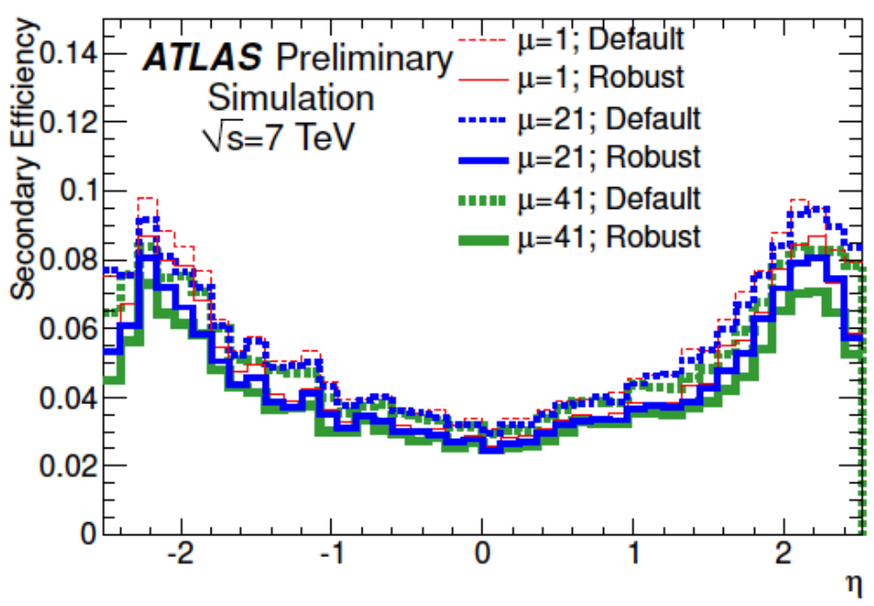

Momentum Resolution (before data taking!)

Track parameter resolution determined by comparing split-track pairs, i.e. looking at upper and lower half of cosmic muons ...

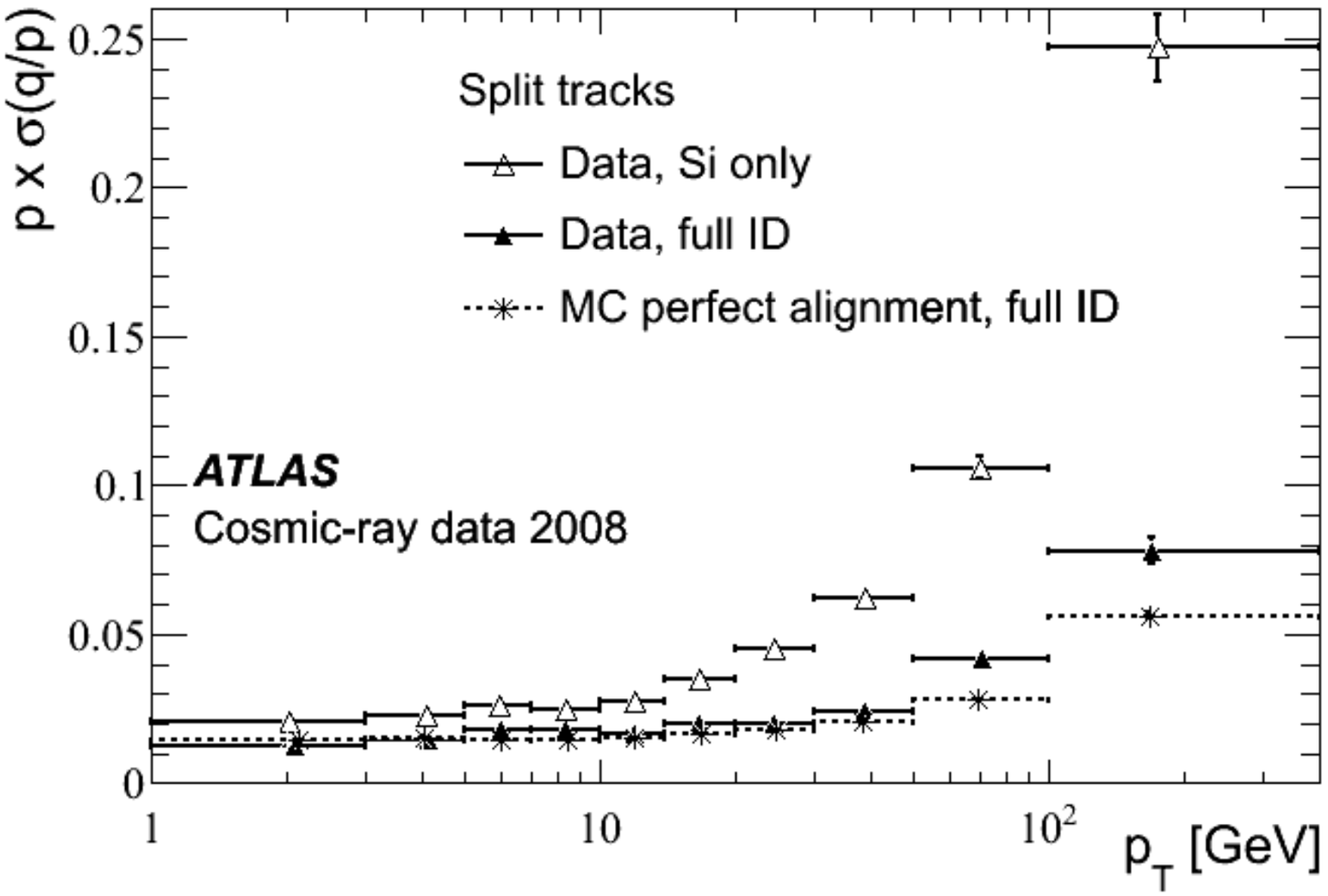

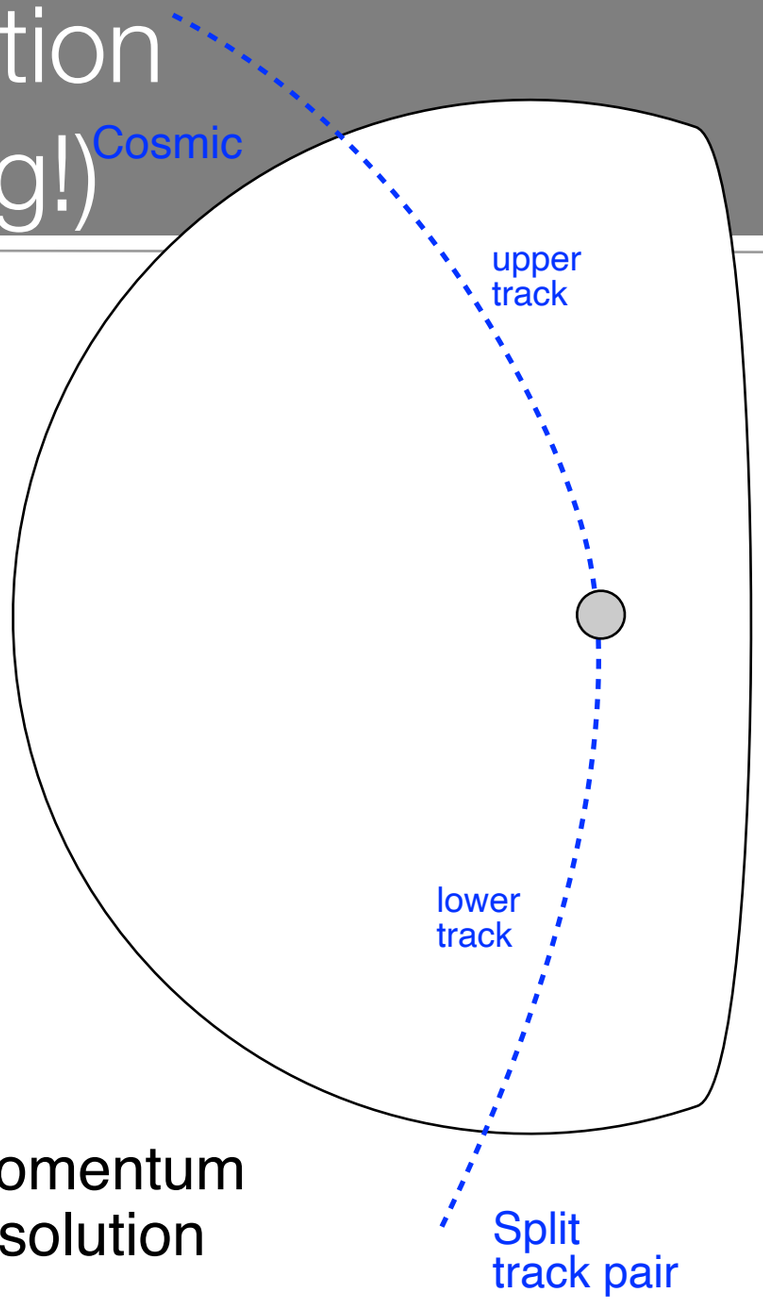

Momentum resolution

Nominal:

$$\sigma(p_T) \approx 5\cdot10^{-4}\ p_T^2 \oplus 10^{-3}\ p_T$$
$$\sigma(1/p_T) \approx 5\cdot10^{-4} \oplus 10^{-3}\ /p_T$$

Measured:

$$\sigma(1/p_T) \approx 4.83\cdot10^{-4} \oplus 10^{-3}\ /p_T\ \text{GeV}^{-1}$$

Using cosmics to prepare detectors in 2015

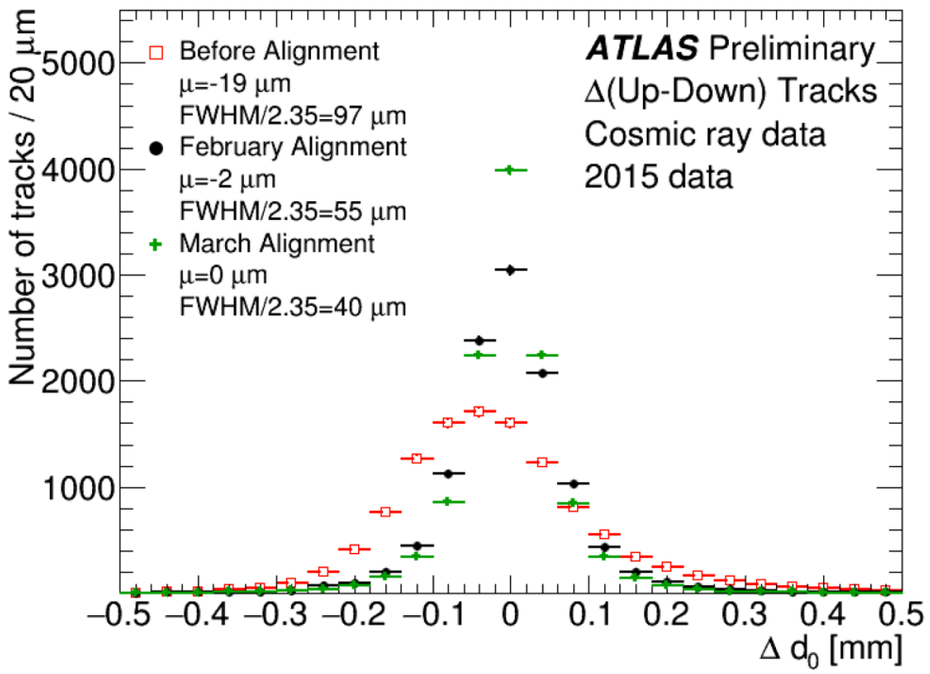

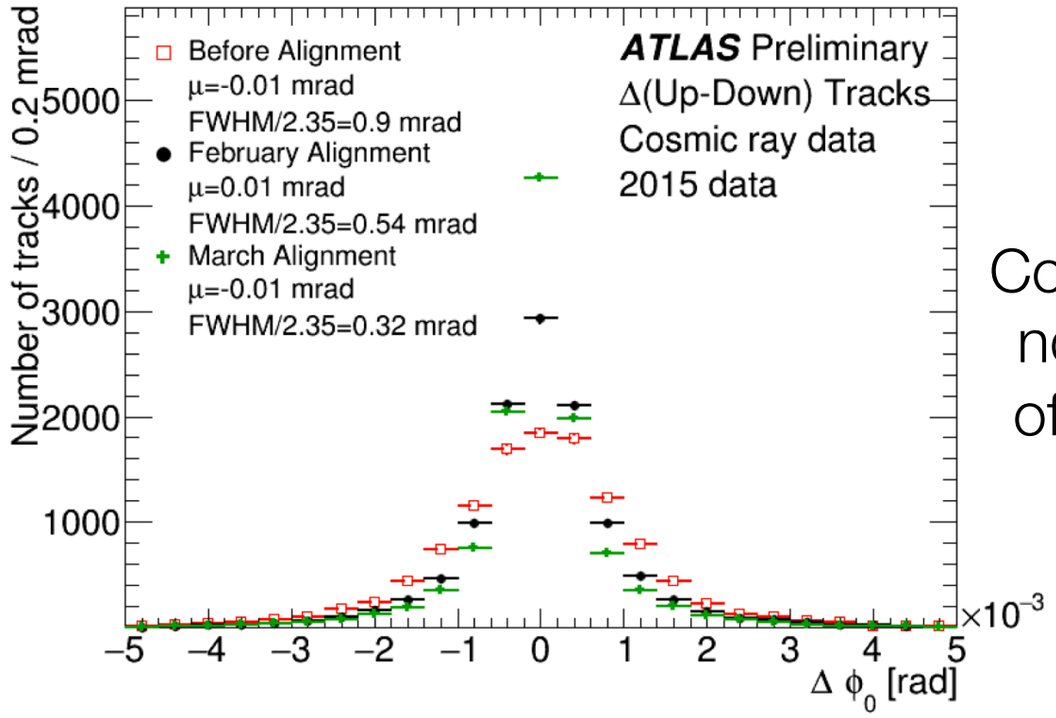

Compare upper a nd lower halves of cosmic tracks

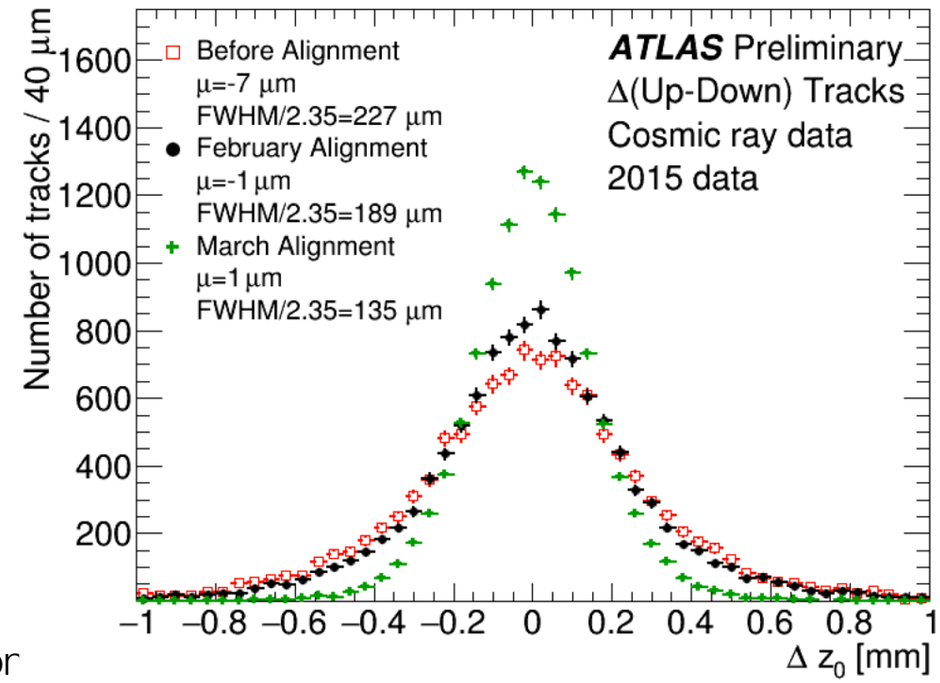

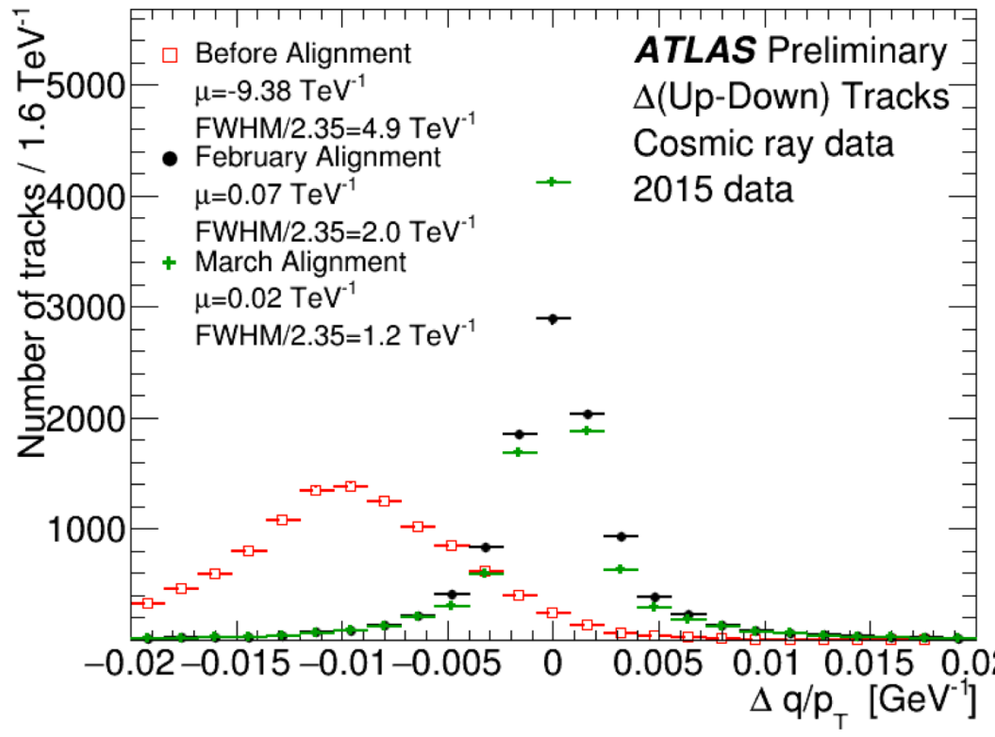

Checking the Momentum Scale

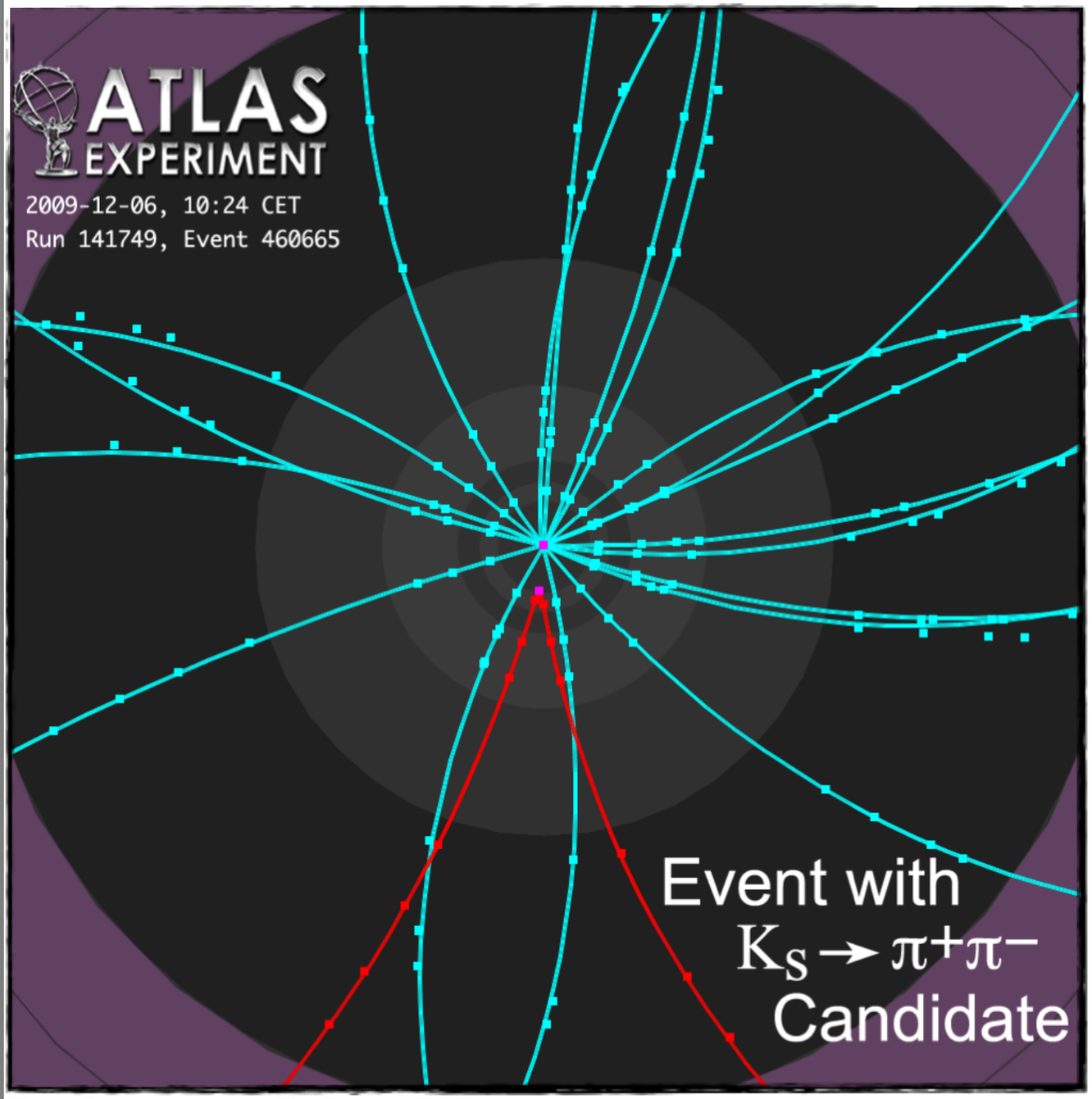

Momentum Reconstruction with Inner Tracker

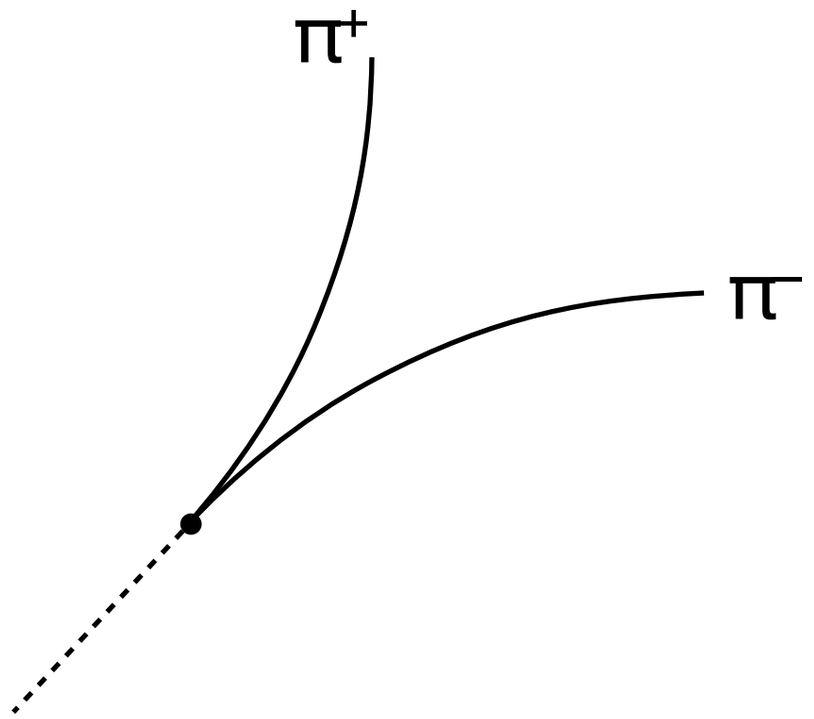

$$m_K^2 = (p_{\pi^+} + p_{\pi^-})^2$$

Checking the Momentum Scale

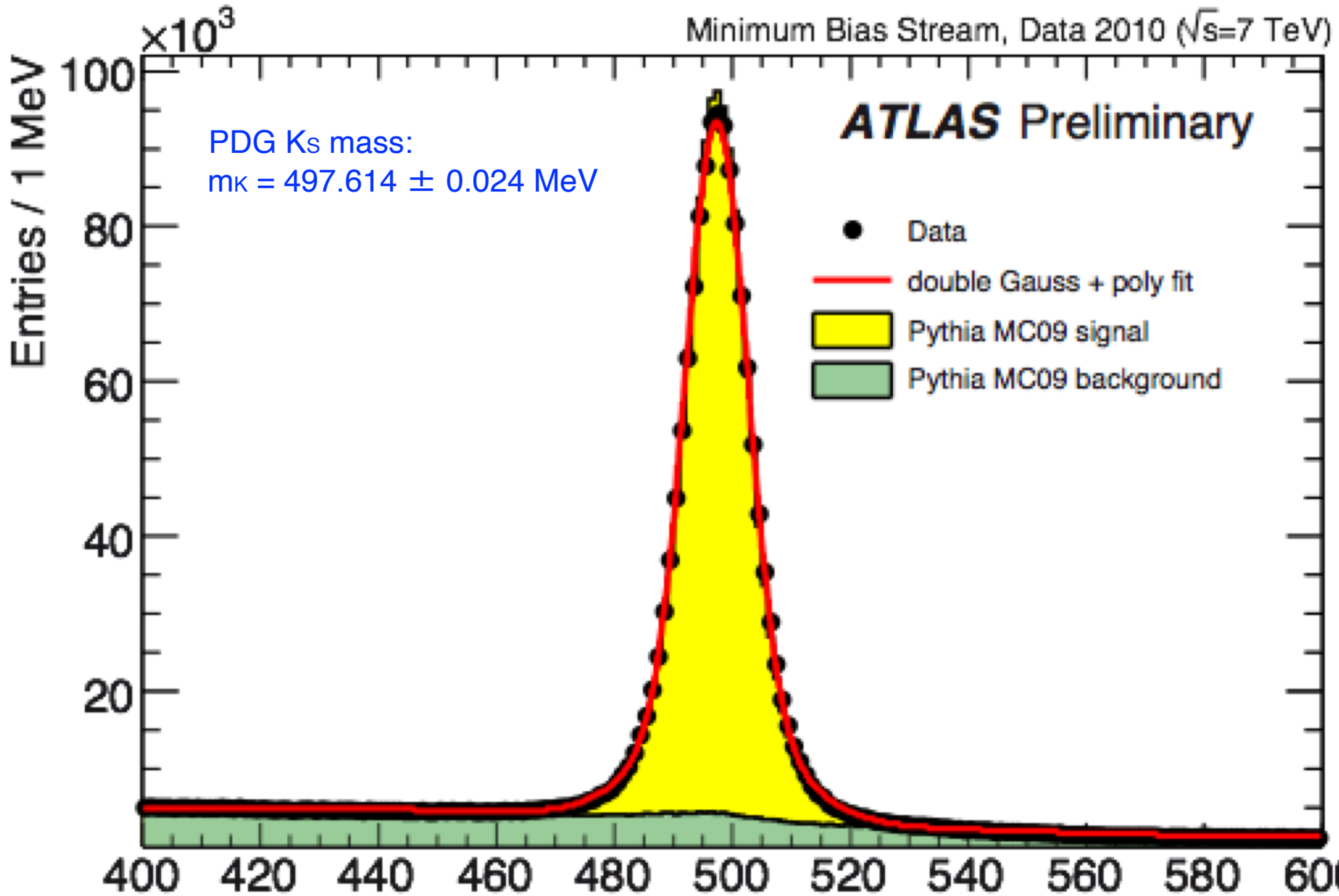

Mass resolution

Systematics on tracking and measured momentum due to misalignment have been studied using

J/Psi->μμ and Z->μμ decays.

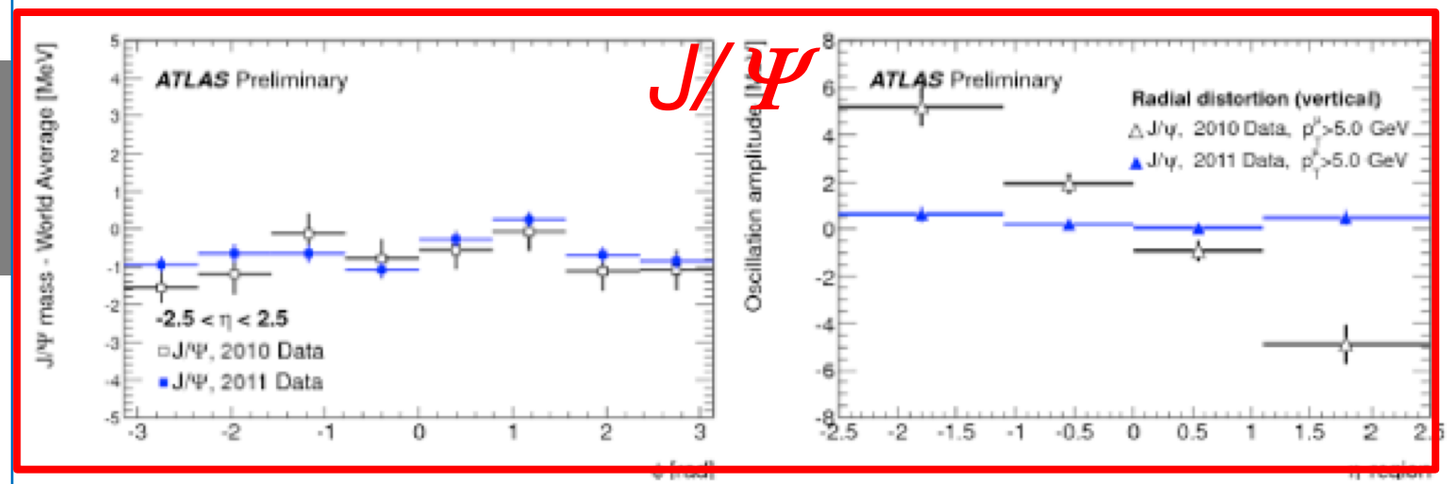

The difference between central value of the fitted mass and PDG World Average mass for J/ψ (left) and comparison of the fitted radial-deformation amplitudes in 2010 and 2011 data for the J/ψ (right) [5].

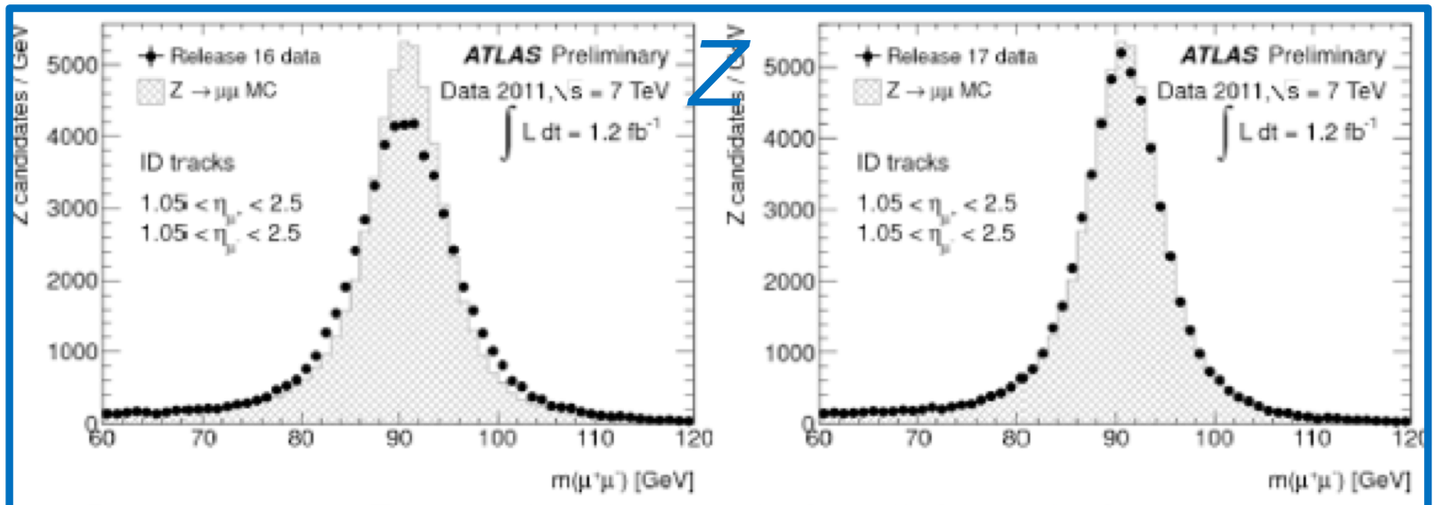

Reconstructed Z mass distributions before (left) and after alignment corrections and perfectly aligned MC (grey) for the end-cap A [5].

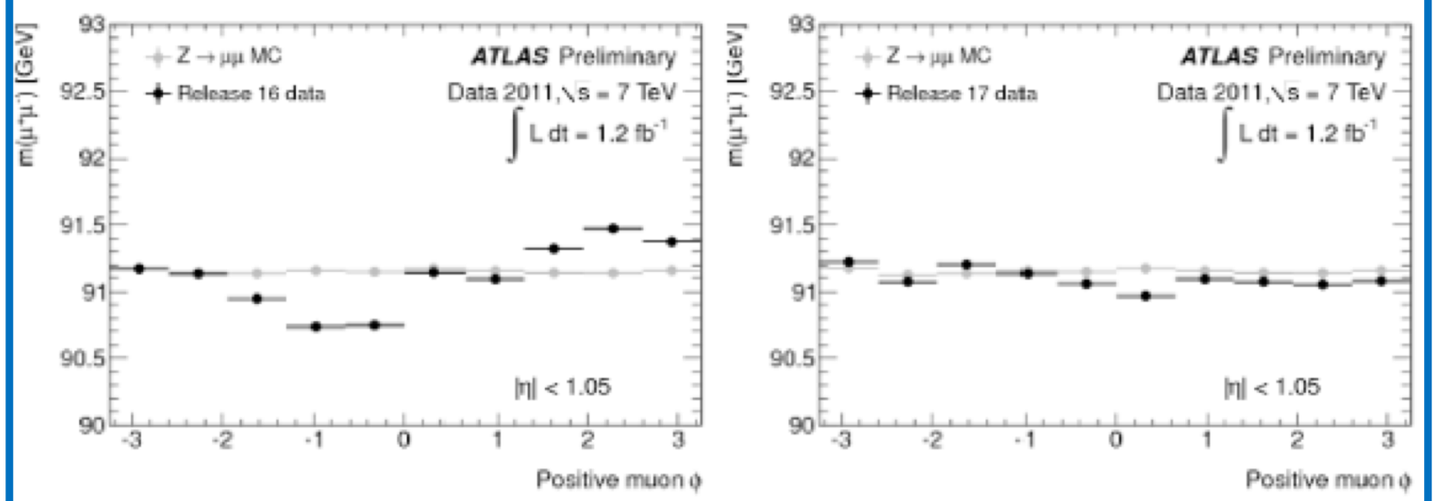

Fitted mean Z mass as a function of ϕ of the positive muon, for collision data before (left) and after charge-antisymmetric alignment corrections and compared to MC with perfect Inner Detector alignment (grey) [5].

Momentum bias (systematic differences in p_T)

Momentum bias is extracted from data for electrons and positrons from Z and W decays using

E (em calorimeter)/p (tracking detectors)

method with parametrization of momentum $q/p = q/p\,[1+qp_T\,\mathrm{delta(sagitta)}]$.

Except for a few isolated spots in very forward region, local biases stay within |delta| < 0.5 TeV^{-1}, corresponding to < 2% bias at 40 GeV.

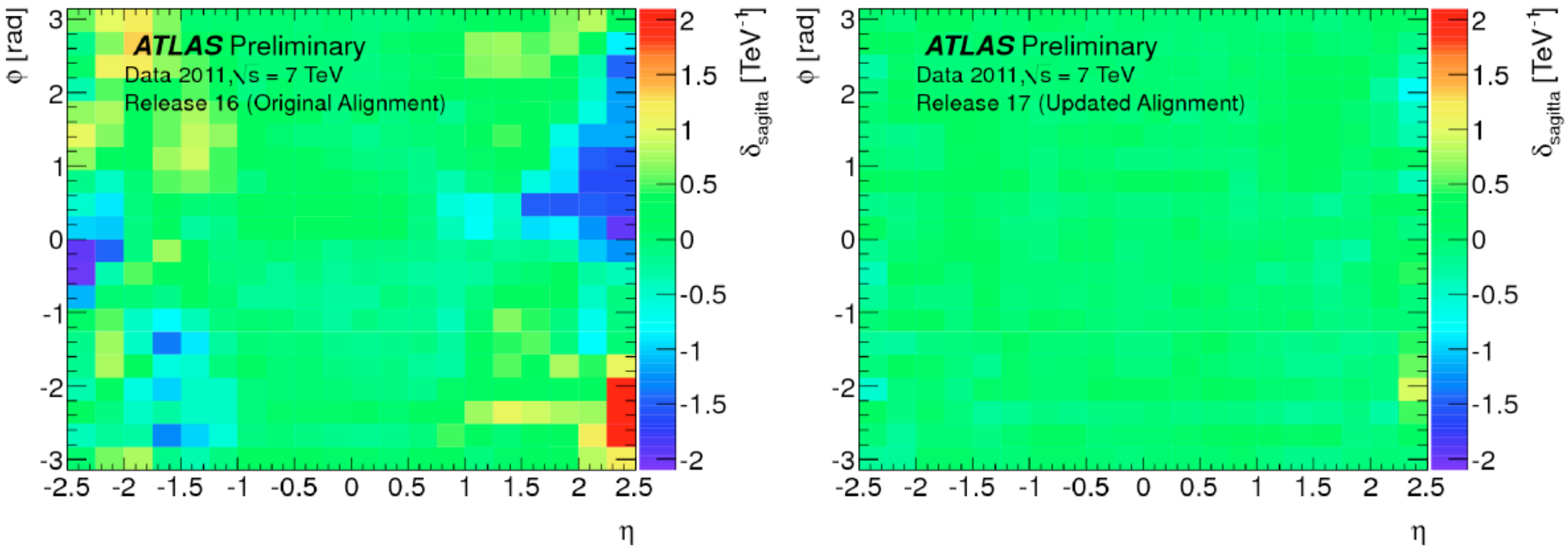

Momentum bias parameter for the charge-antisymmetric parametrization with old (left) and updated alignment (right) [5].

2 Reconstruction of primary vertices

Finding (first) Fitting (then)

The reconstruction of primary vertices is organized in two steps: a) the primary vertex finding algorithm, dedicated to associate reconstructed tracks to the vertex candidates, and b) the vertex fitting algorithm, dedicated to reconstruct the vertex position and its corresponding error matrix. It also refits the associated tracks constraining them to originate from the reconstructed interaction point. The detailed implementation of the *finding* and *fitting* algorithms is described below.

In this analysis, reconstructed tracks fulfilling the following quality requirements are used for the primary vertex reconstruction:

- $p_{\mathrm{T}} > 150$ MeV,
- $|d_0| < 4$ mm,
- $\sigma(d_0) < 5$ mm,
- $\sigma(z_0) < 10$ mm,
- at least 4 hits in the SCT detector,
- at least 6 hits in the pixel and SCT detectors.

Here d_0 and z_0 denote the transverse and longitudinal impact parameters of tracks with respect to the centre of the luminous region, and $\sigma(d_0)$ and $\sigma(z_0)$ denote the corresponding uncertainties as estimated in the track fit. The symbol p_{T} denotes the reconstructed track transverse momentum. The selection criteria based on the impact parameters are designed to remove a good fraction of the tracks originating from secondary interactions. As estimated from simulations, based on results obtained with the PYTHIA Monte Carlo program [6] and the full simulation of the ATLAS detector, in non-diffractive pp collisions

Robust vertex reconstruction

at 7 TeV, the above requirements are fulfilled by $(83.5 \pm 0.1)\%$ of reconstructed tracks corresponding to primary particles.

The luminous region in ATLAS is determined during a physics run, typically every $\approx$ 10 minutes, by applying an unbinned maximum likelihood fit to the distribution of primary vertices recorded in this period of time, where the same primary vertex reconstruction algorithm is used as described in the following, but without applying the beam-spot constraint. A detailed description of how the beam-spot is determined and on the uncertainties connected with its determination can be found in Ref. [7].

The *Iterative Vertex Finding* approach used for this study works as follows:

- Reconstructed tracks compatible with originating from the interaction region are pre-selected according to the criteria listed above.
- A vertex seed is found by looking for the global maximum in the distribution of z coordinates of the tracks, computed at the point of closest approach to the beam spot center.
- The vertex position is determined using the *adaptive vertex fitting* algorithm [8], which takes as input the seed position and the tracks around it. The adaptive vertex fitter is a robust χ^2 based fitting algorithm which deals with outlying track measurements by down-weighting their contribution to the overall vertex χ^2. The down-weighting is performed progressively, while the fit iterations proceed according to a fixed number of steps (deterministic annealing scheme [8]).
- Tracks incompatible with the vertex by more than approximately 7 σ are used to seed a new vertex. The compatibility of the track to the vertex is expressed in terms of a χ^2 with 2 degrees of freedom. The present cut is $\chi^2 > 49$. This procedure is repeated until no unassociated tracks are left in the event or no additional vertex can be found.

The very loose cut of $\chi^2 > 49$ is intended to reduce the number of single vertices which split into two due to the presence of outlying track measurements.

Vertex Reconstruction

https://arxiv.org/pdf/1611.10235.pdf

Vertex fitting - 0

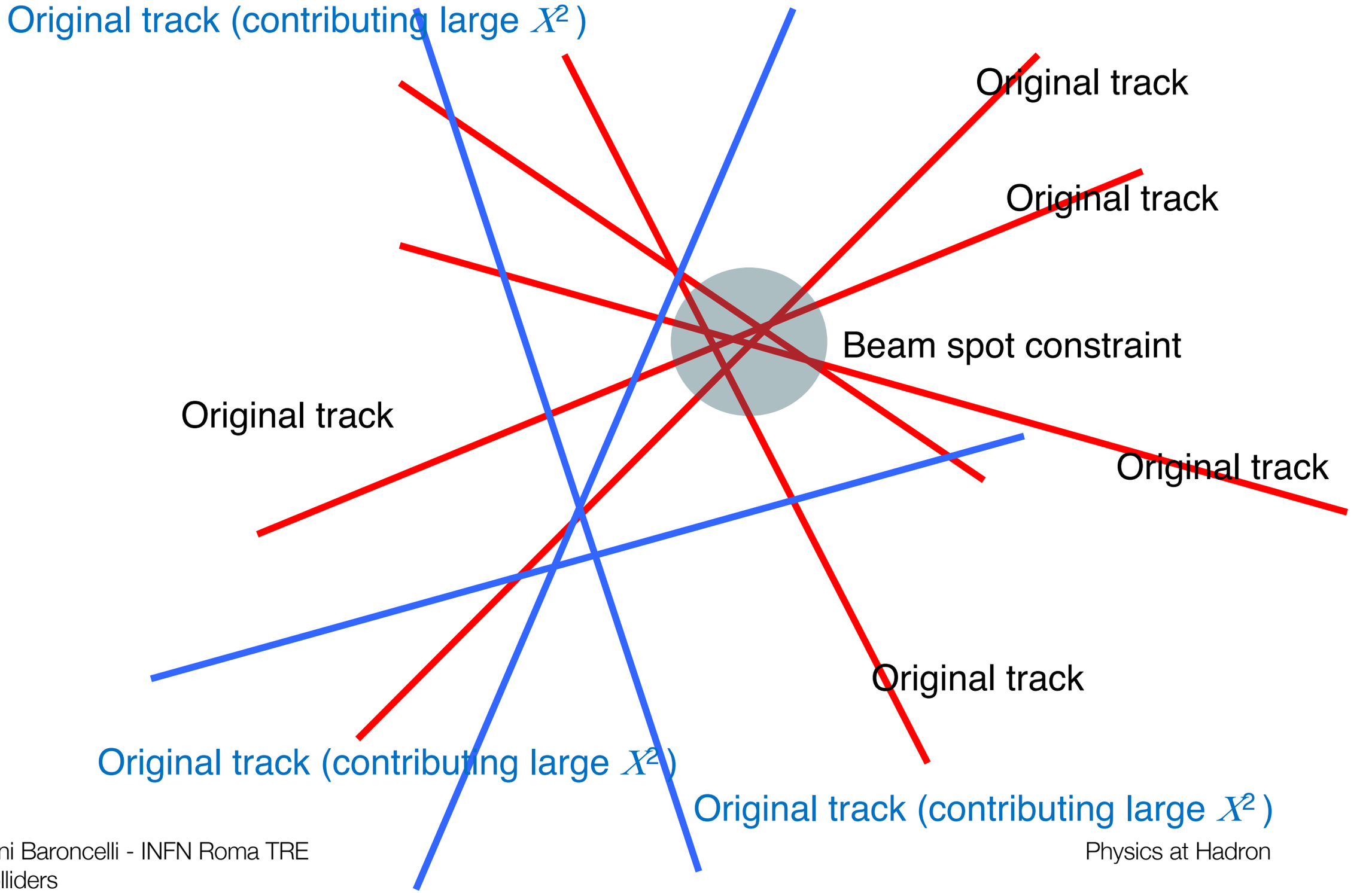

Vertex fitting - 1

Original track is modified imposing that it passes through V_p

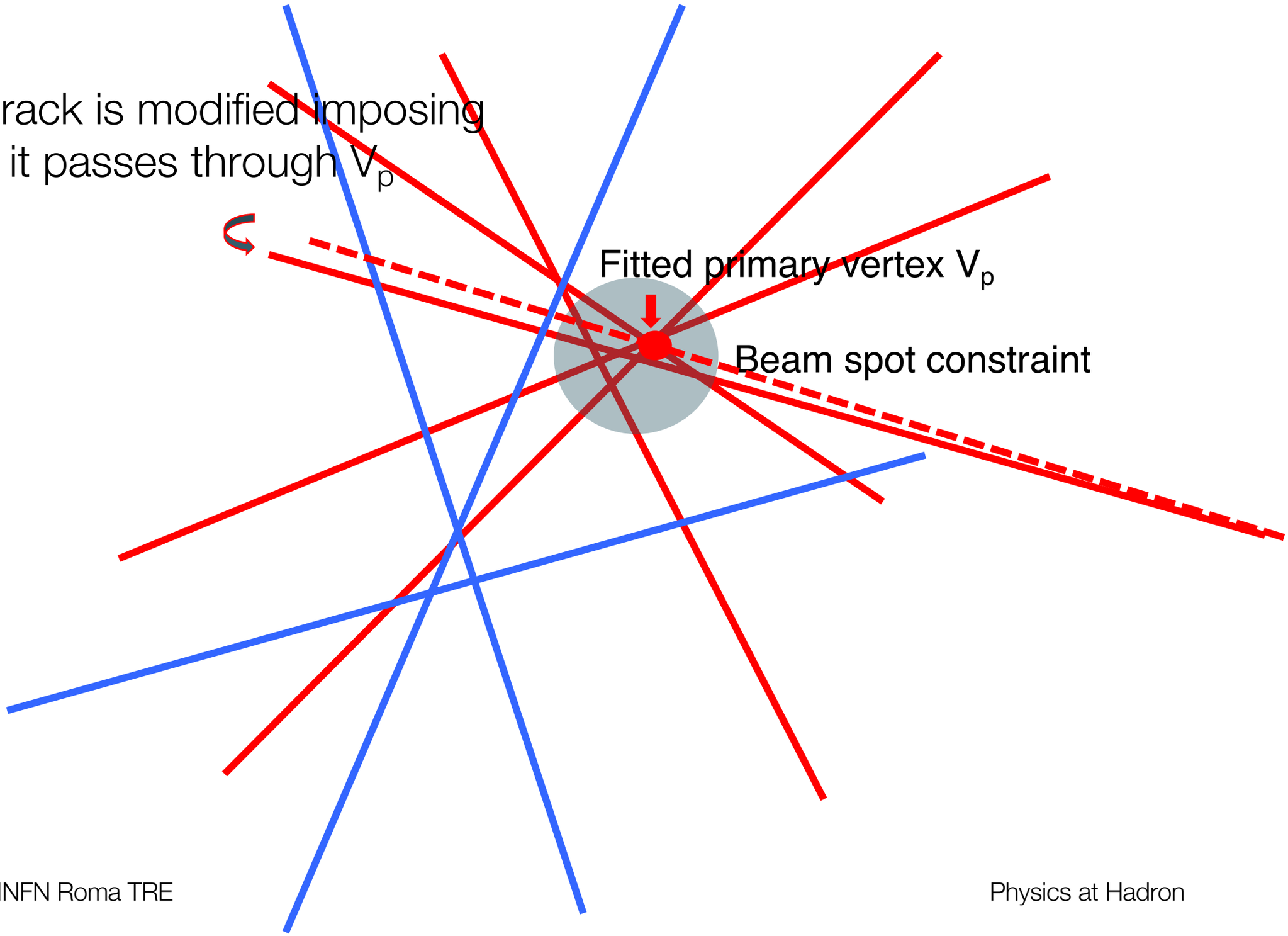

Vertex fitting - 2

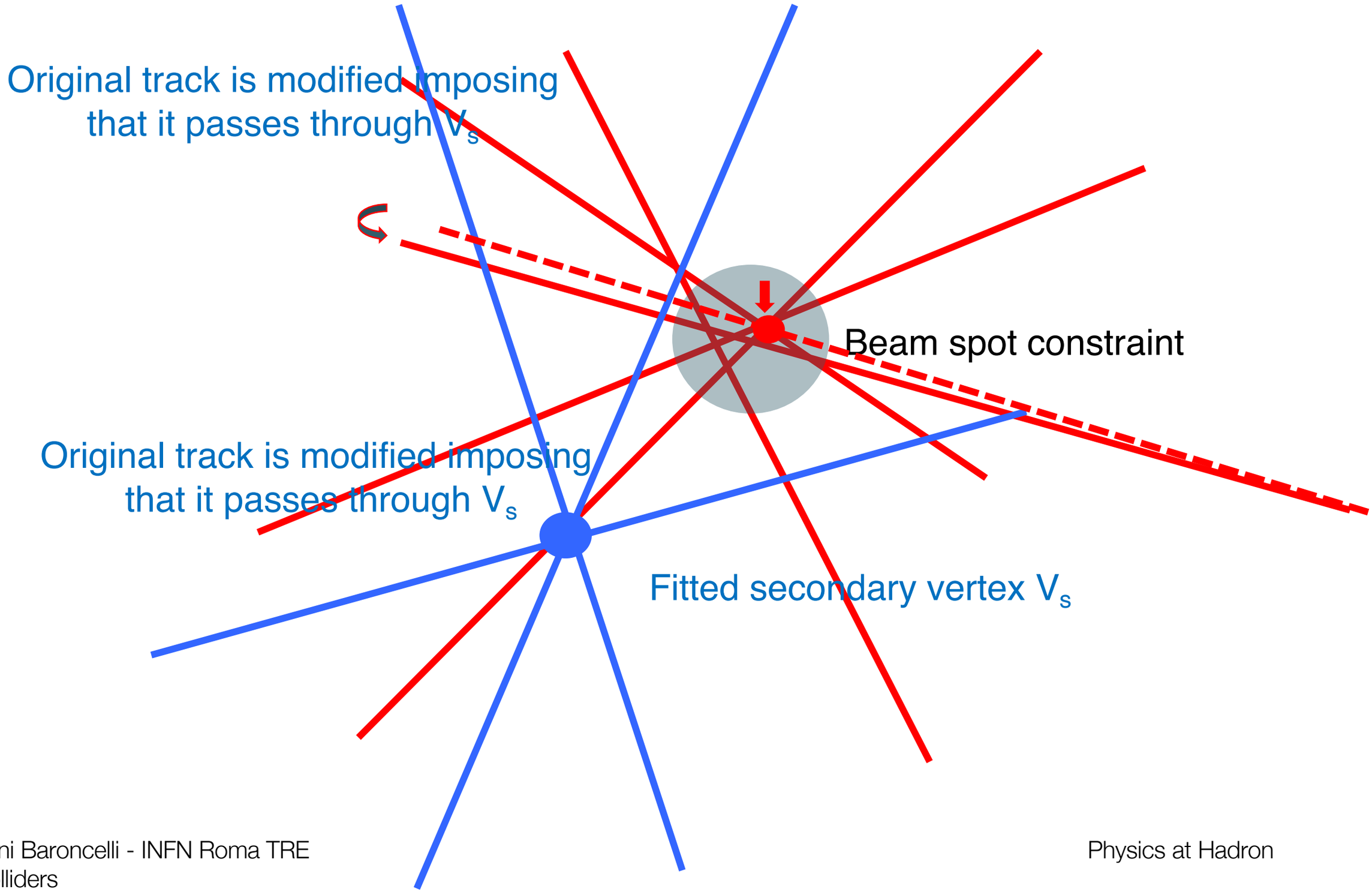

ATLAS vertexing

takes z-position of track at beam-line as seed
iterative Chi^2 fit of nearby tracks
new seed from tracks displaced by more than 7
beam-spot used as a constraint

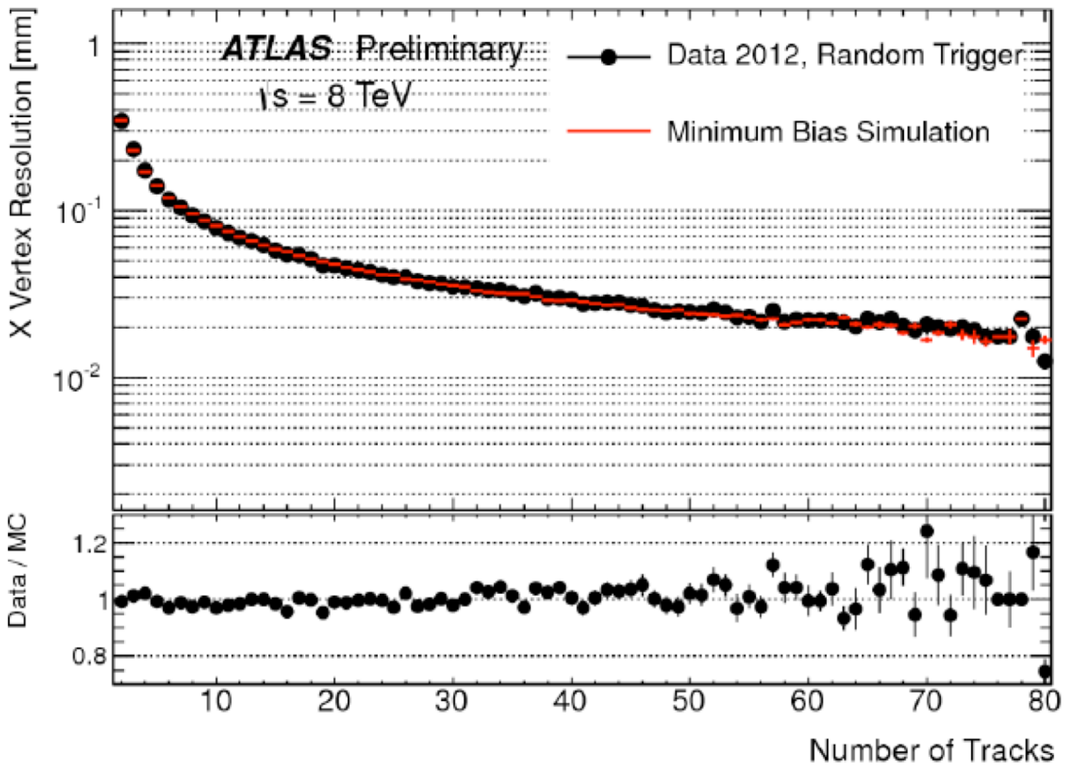

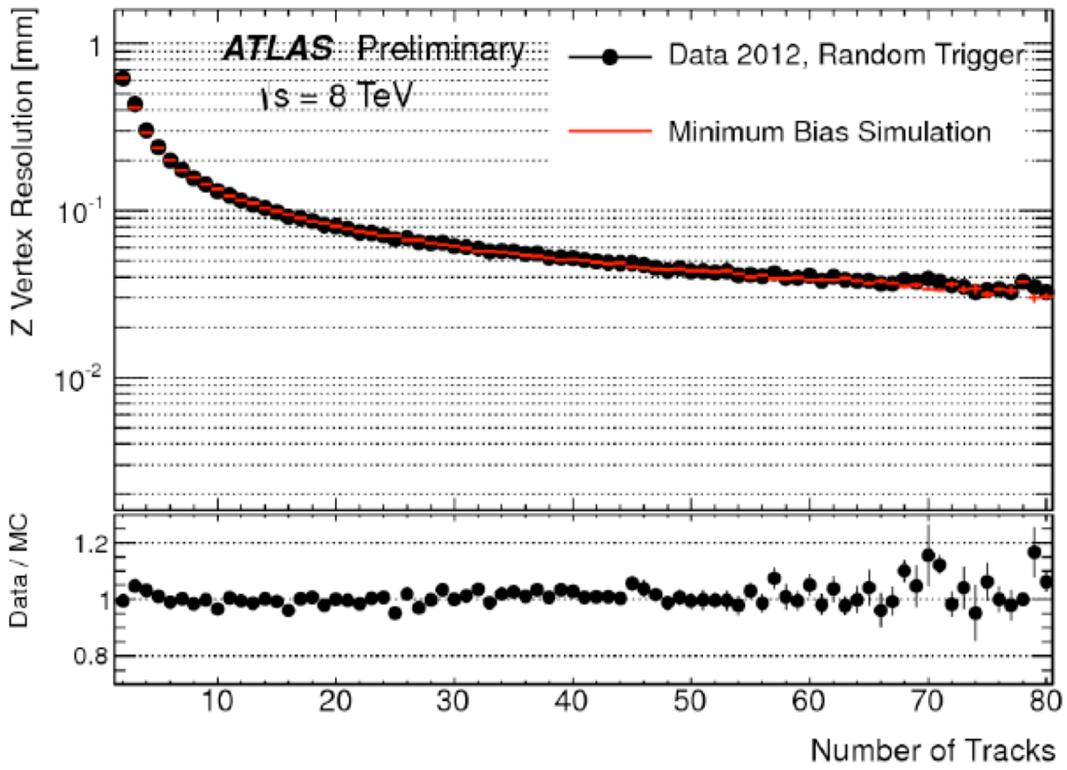

Vertex position resolution in data and MC for the transverse (left) and longitudinal coordinate as a function of number of tracks in vertex [2].

Crowded events → Pile Up!

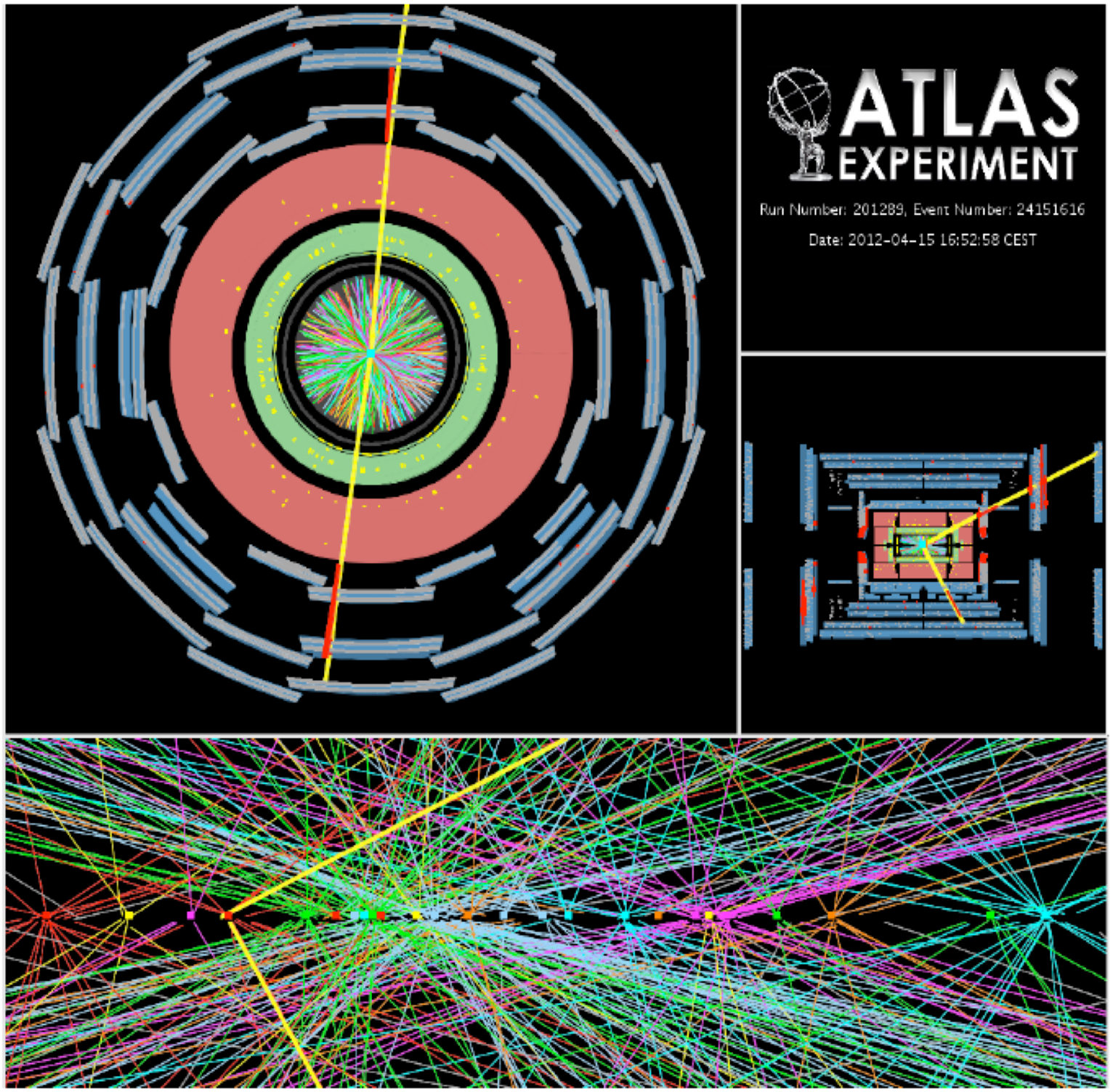

candidate $Z \to \mu^+\mu^-$ event with 25 reconstructed vertices.

High pile-up events: μ and N_{PV} (or N_{Vx})

The number of proton-proton interactions per bunch crossing follows a Poisson distribution with mean value μ. During a fill, μ decreases with decreasing beam intensity and increasing emittance, such that the quoted peak value, or μ^{peak}, is the highest value in a single bunch crossing at the start of the stable beam period of the fill. The number of interactions per bunch crossing also varies between bunches. The number of interactions averaged over all bunch crossings and averaged over the data analysed will be referred to as $\langle\mu\rangle$.

In data, μ is calculated using the following formula:

$$\mu = \frac{L \times \sigma_{\text{inel}}}{n_{\text{bunch}} f_{\text{r}}} \qquad \frac{L}{f_r} \sim \frac{N_1 N_2}{A} \tag{1}$$

where L is the luminosity, σ_{inel} is the total inelastic cross-section, n_{bunch} the number of colliding bunches and f_{r} the LHC revolution frequency. The uncertainty on μ depends on the uncertainties on the luminosity and the total inelastic cross-section. The luminosity measurement is performed with dedicated detectors and calibrated using special LHC fills. The uncertainty on the integrated luminosity is $\sim 3.9\%$ [5] for the 2011 physics data. The high-intensity runs studied have an additional 1% uncertainty to account for the extrapolation of direct luminosity measurements from lower intensity runs. The total inelastic cross-section used, $\sigma_{\text{inel}} = 71.5$ mb, is taken from Pythia [6]. The value is $\sim$3% lower than the measurement from TOTEM of 73.5 ± 1.9 mb [7]. The total cross-section has also been measured by ATLAS to be $69.1 \pm 2.4(\text{exp.}) \pm 6.9(\text{extr.})$ mb [8, 9] by extrapolating a measurement of the cross-section for events in the acceptance of scintillators in the forward region. The difference between the ATLAS and TOTEM measurements and the nominal value from Pythia is taken as a systematic uncertainty on μ of 3%.

$\langle n_{Vx} \rangle$ vs μ

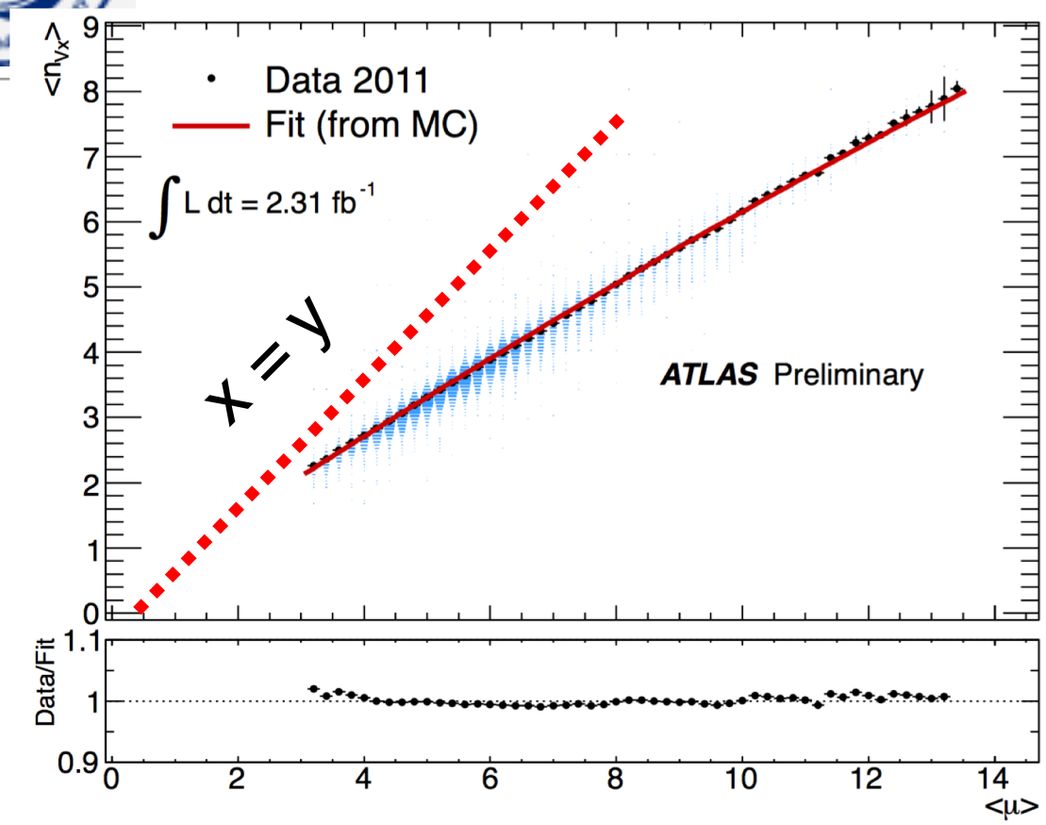

In an ideal detector with perfect resolution and acceptance you would expect to have

$\langle n_{Vx} \rangle \sim \mu$

ε is the vertex reconstruction efficiency
p_{mask} is the inability of resolving nearby vertices
$F(\varepsilon\mu, p_{mask})$ is a correction due to masking effects (two undistinguished close vertices)

The average number of reconstructed vertices is shown as a function of the average number of interactions μ. The red triangles show the simulation prediction for minimum-bias events without any trigger bias using the 2012 setup for beam and detector conditions. The simulation covers the μ range up to 22 and a higher interval which was observed in some special high-μ data taking runs.

The simulation has been fitted (orange line) with a function taking into account the vertex reconstruction efficiency ε and the inability of resolving nearby interactions in distinct vertices (vertex masking): $\langle n_{vertices} \rangle = \varepsilon\mu - F(\varepsilon\mu, p_{mask})$. $F(\varepsilon\mu, p_{mask})$ is a function that estimates the correction to the number of reconstructed vertices for masking effects. The probability of not resolving two interactions in distinct vertices, p_{mask}, depends on the detector and vertex reconstruction algorithm performance (assumed to be independent from pile-up) and on the density of the interactions (which depends on the beamspot longitudinal profile).The latter dependence is exploited to test the effect of a different beamspot longitudinal profile (approximately flat, called *Crab Kissing*); this is shown in the Figure as a blue line.

Fakes have been found to be negligible in the range covered by simulation and are assumed to be equally negligible in the extrapolated regions. The correction to the number of reconstructed vertices for masking effects $F(\varepsilon\mu, p_{mask})$ is show by the dotted lines for the two configurations.

High pile-up events

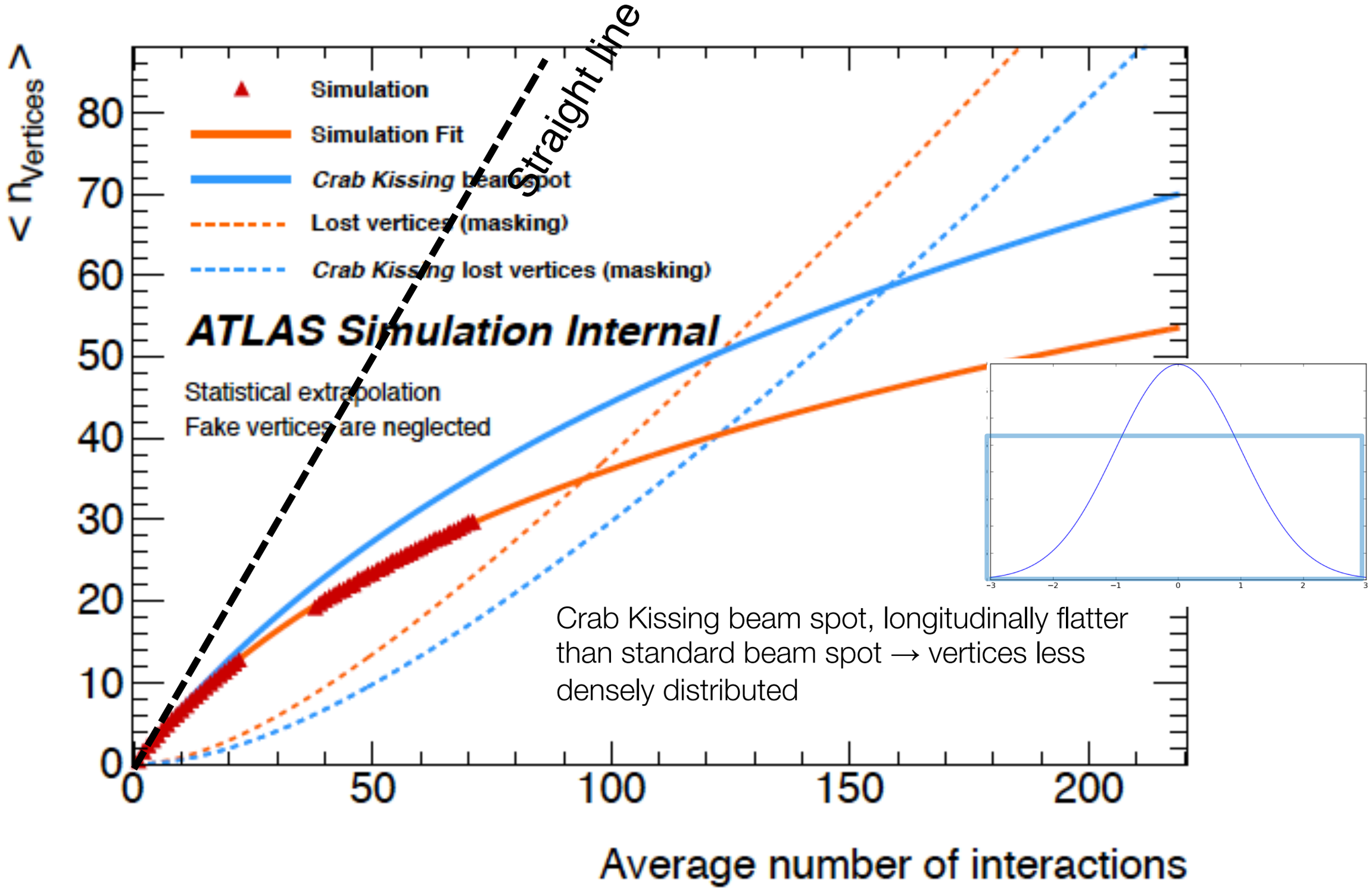

Crab Kissing beam spot, longitudinally flatter than standard beam spot → vertices less densely distributed

High pile-up events & robust reconstruction

non-primary = not pointing to a primary vertex

A special track selection allows the reconstruction of tracks with p_T>400 MeV in events with many superimposed vertices

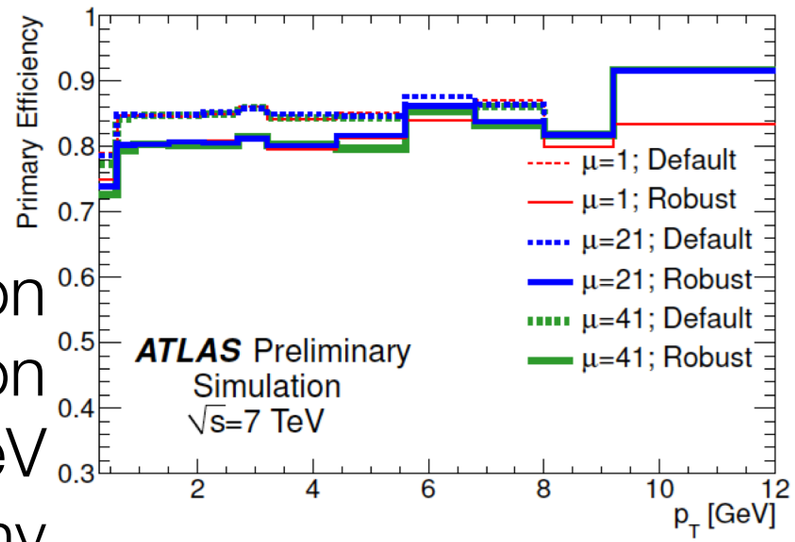

(a) Primary track reconstruction efficiency vs p_T

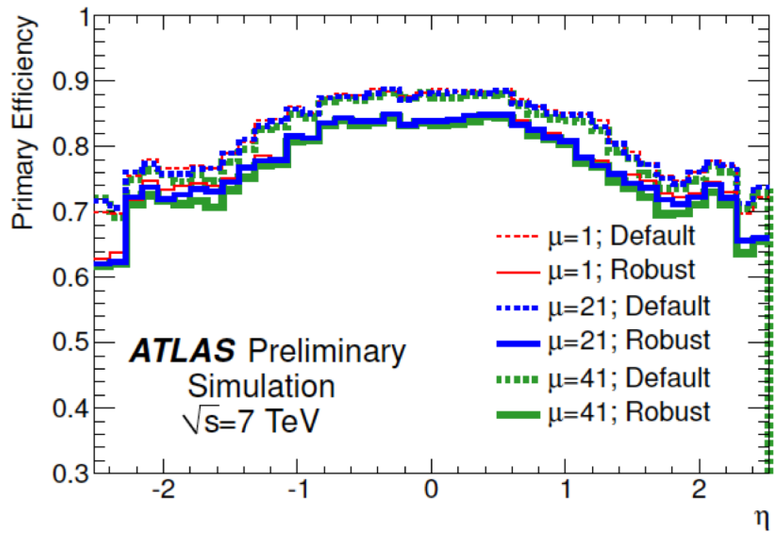

(b) Primary track reconstruction efficiency vs η

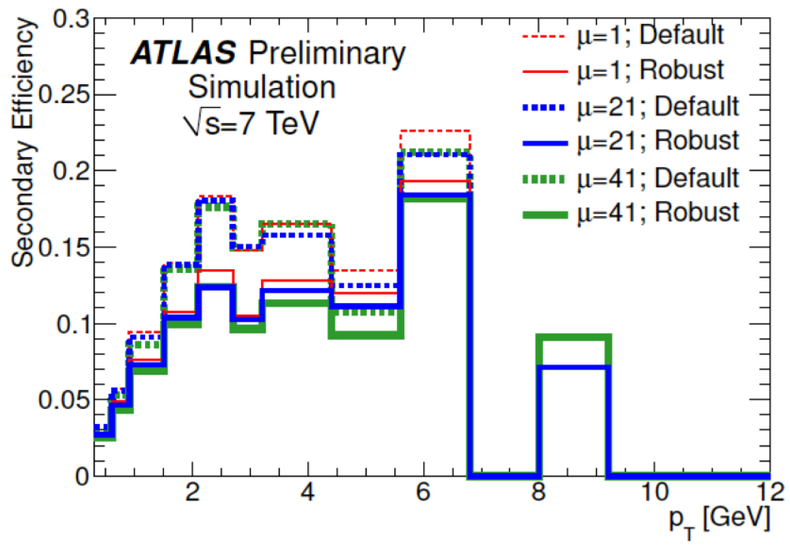

(c) Secondary efficiency vs p_T

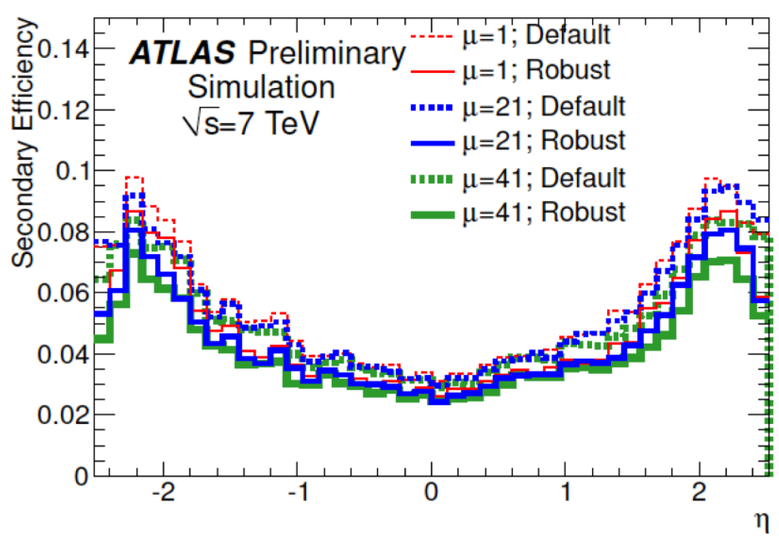

(d) Secondary efficiency vs η

Vertices in high pile-up events

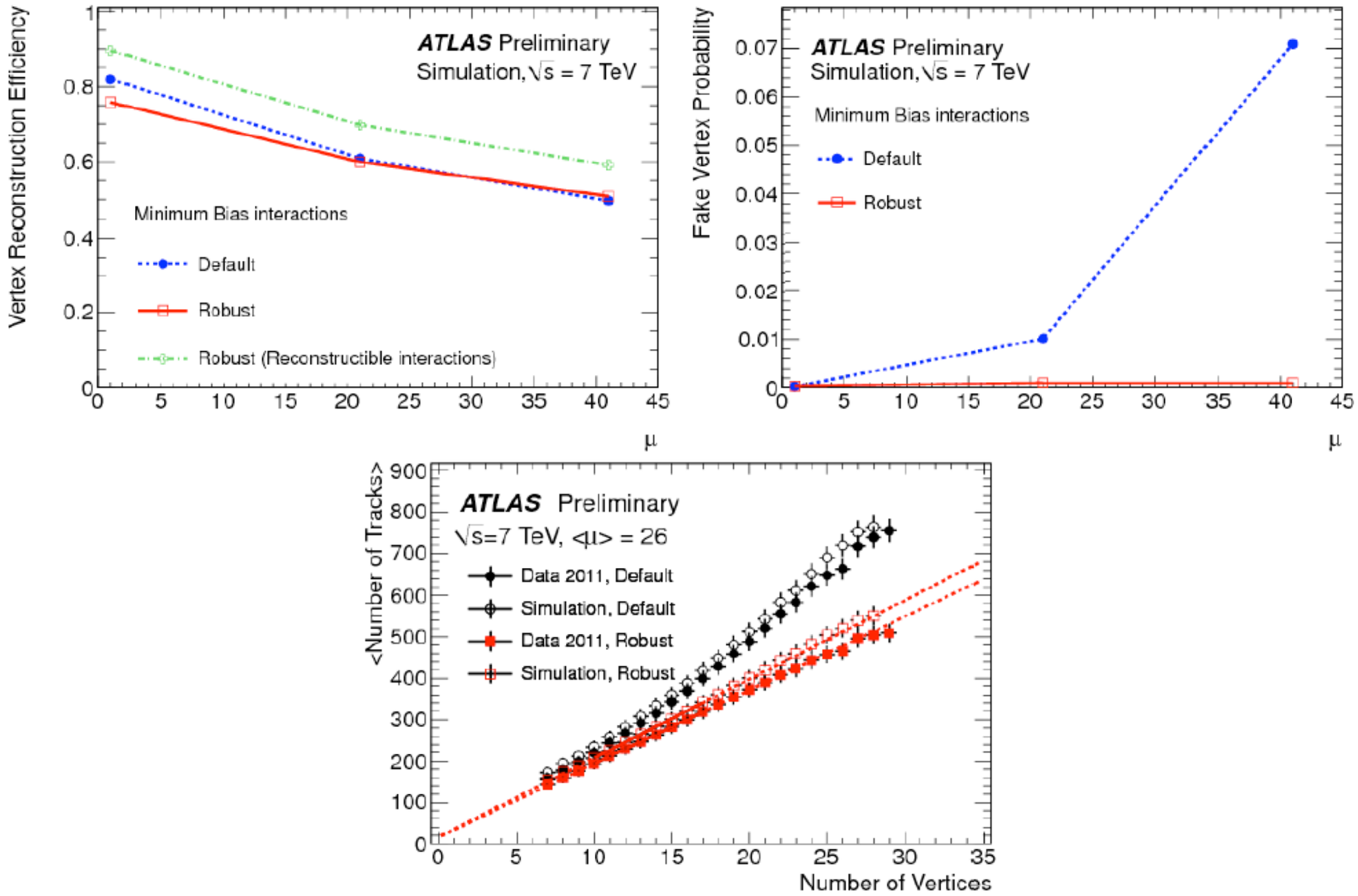

Vertex reconstruction efficiency (top left) and fake probability (top right) as a function of the average number of interactions in minimum bias MC and the average number of tracks per event as a function of the number of vertices for data and simulation (bottom) [4].

Fake vertices vs η

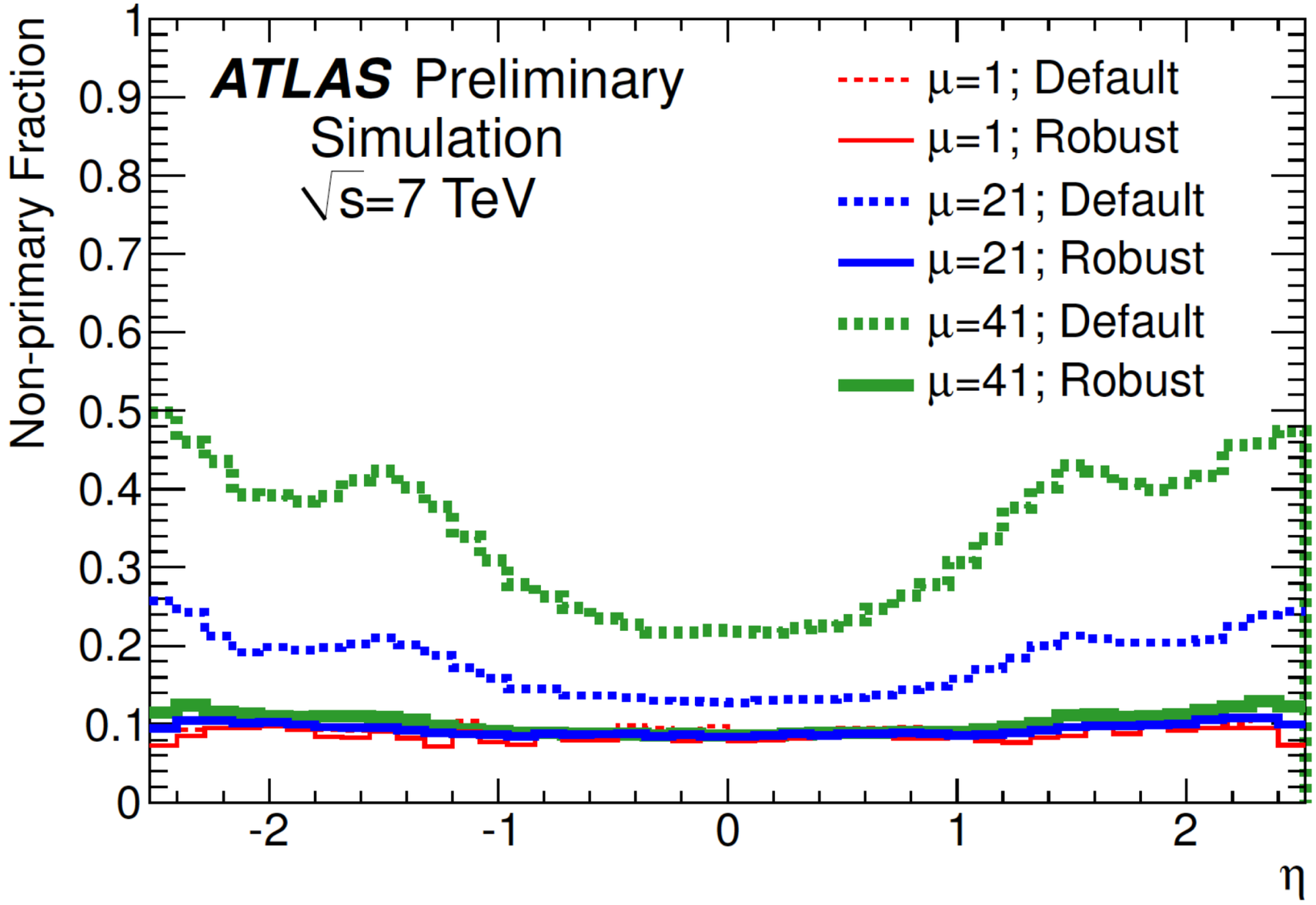

(a) Non-primary fraction vs η

Vertex resolution

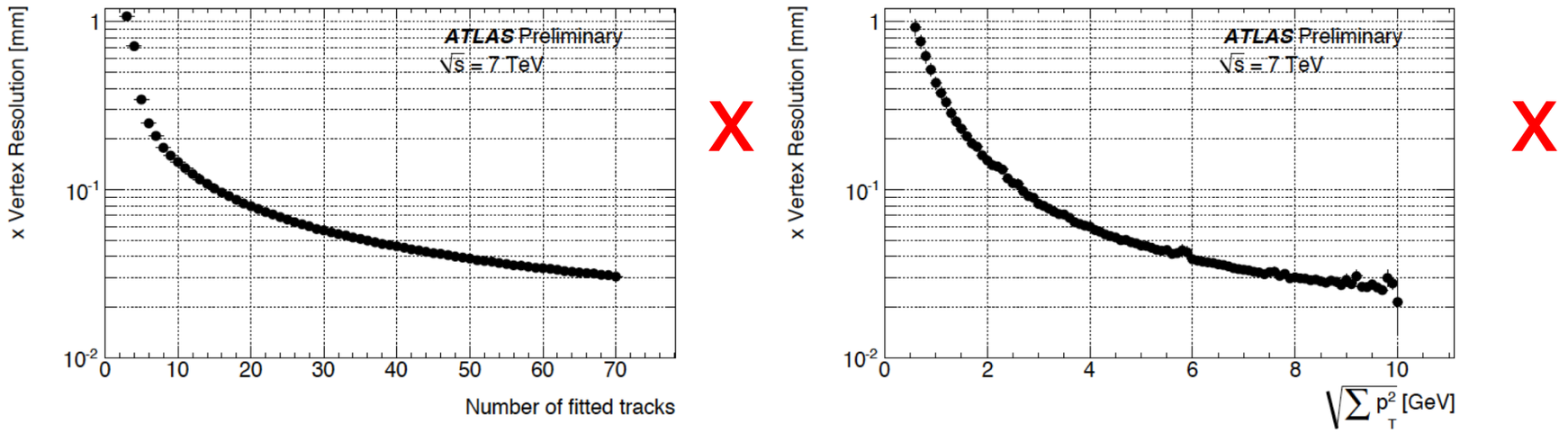

Figure 8: Estimated vertex resolution $\sigma_{x\mathrm{PV,true}}$ in 7 TeV data as a function of the number of tracks N_{trk} (left) or as a function of the value of $\sqrt{\sum_{\mathrm{trk}} p_{\mathrm{T}}^2}$ (right).

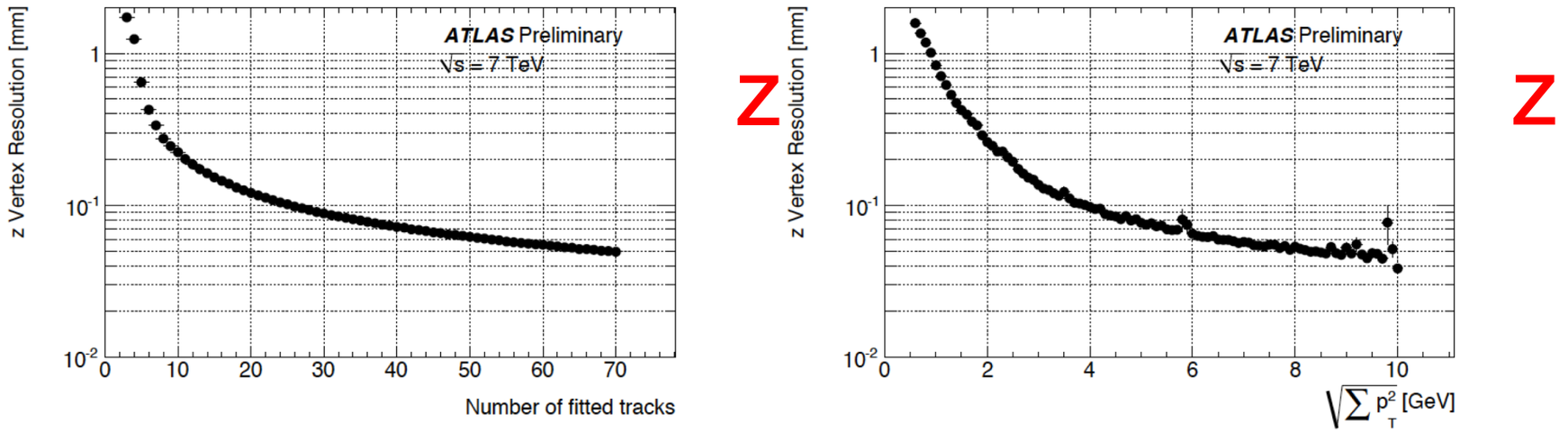

Figure 9: Estimated vertex resolution $\sigma_{z\mathrm{PV,true}}$ in 7 TeV data as a function of the number of tracks N_{trk} (left) or as a function of the value of $\sqrt{\sum_{\mathrm{trk}} p_{\mathrm{T}}^2}$ (right).

Summary

- Use of MC in data analysis
- Material budget using gamma conversions and secondary hadronic interactions → detector radiography
- Tracking using Inner Detectors → Kalman filter technique

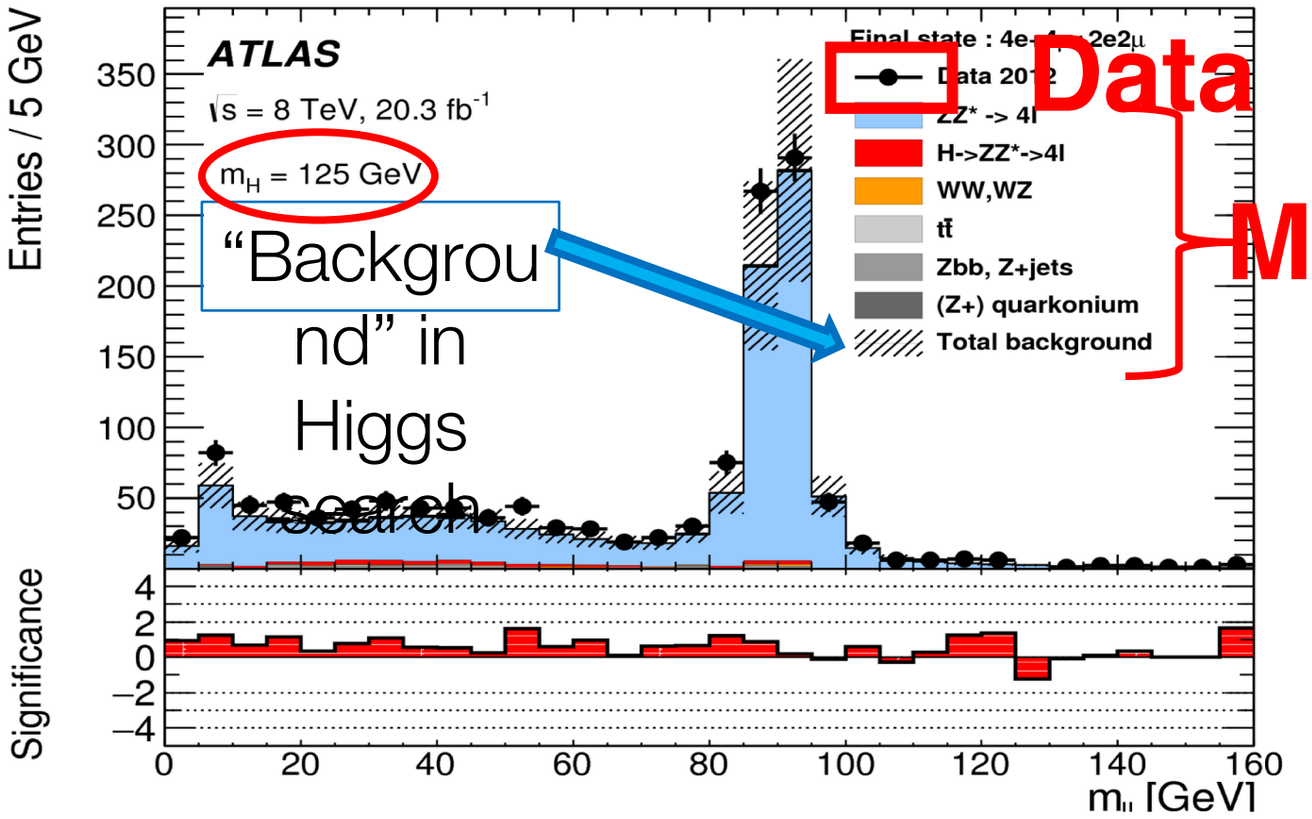

- Alignment and effect of mis-alignment → impact on resolution and efficiency
- Checking the momentum scale using invariant mass of known resonances (and 'half cosmics')
- Primary and secondary vertices
- Pile-up